Goethe Universität Frankfurt
Institut für Theoretische Physik

Coarse Graining Renormalization in an Effective Theory of Strong Coupling LQCD in 1+1D and 2+1D

Master Thesis

by Christoph Konrad

Supervisor and First Referee: Prof. Dr. Owe Philipsen
Second Referee: Prof. Dr. Marc Wagner

September 2020

Abstract

In this thesis coarse graining renormalization transformations are applied to an effective theory of LQCD in 1+1 and 2+1 dimensions. The theory is valid in the strong coupling and heavy quark regime. The tool of choice determines recursion relations for the couplings of the theory at varying length scales.
In 1+1 dimensions the method is introduced in the context of pure gauge theory. Step by step, parts of the quark determinant are included in the description of the model and the corresponding running couplings are obtained. Yielding the transfer matrix, the recursion relations are solved analytically. The thermodynamic limit is taken for some intensive observables. Afterwards, continuum extrapolation is performed numerically and results are discussed.
In 2+1 dimensions the coarse graining method is applied in the pure gauge and static quark limit. Running couplings are obtained and the fixed points of the transformations are discussed. Last, the critical coupling of the confinement-deconfinement transition is determined in both limits. Comparisons to literature values are drawn.

Contents

Chapter 1

Introduction

Quantum chromodynamics (QCD) describes the theory of strong interactions. It characterizes the behavior of quarks, the fermions of the theory, and gluons, its gauge bosons. The different kinds of quarks are called flavors, of which six are known: up, down, charm, strange, top and bottom. Next to the electromagnetic and weak interactions, the strong force is part of the standard model of today's particle physics. [1]
Additionally to the usual quantum numbers, e.g. electric charge and spin, the fundamental particles of QCD carry the color charge. It can have the values red, green and blue. In everyday life the particles can only be found in color neutral states. These are build either from three quarks occupying all the three values or a quark-antiquark pair, where the particles are in a color-anticolor combination [1].
Because the force between quarks increases with their distance, separating the particles results in pair production, which again leads to bound states. This phenomenon is called confinement. At high temperatures, however, the coupling of the quarks decreases. Then, the particles can transition into a deconfined state and appear in unbound states. This state is known as the quark gluon plasma [1, 2].
Due to the additional properties of QCD its phase diagram is expected to feature many interesting phenomena, which are still mostly hypothetical [3]. The current idea of the phase diagram of QCD is shown in figure 1.1.

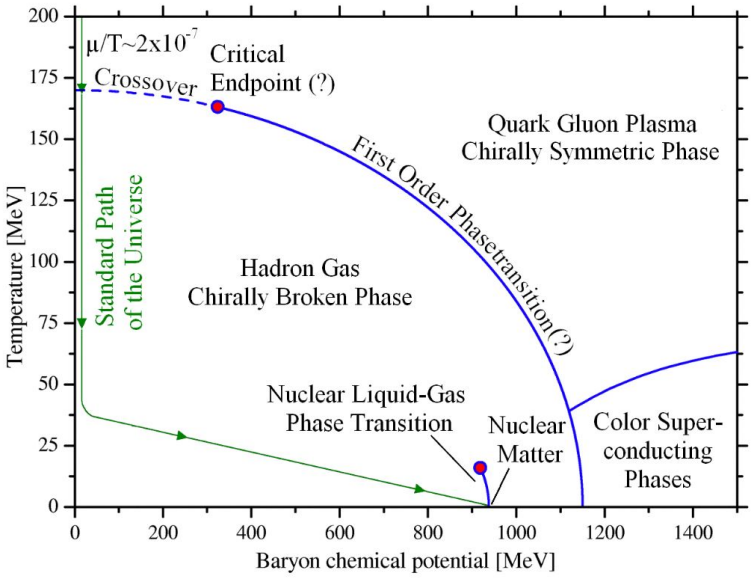

Figure 1.1: Current draft of the QCD phase diagram. The figure is taken from [4].

Next to the deconfinement transition, the nuclear liquid-gas transition will be of interest in this work. It describes the formation of droplets of nuclear matter at sufficiently high chemical potential. At zero temperature it is a first order transition. Away from this limit it changes into a crossover [5, 6].
Because of the high coupling between the particles QCD has to be treated non-perturbatively. The discretization of the theory has proven itself in this context and led to the development of lattice QCD (LQCD) [7].

In recent developments an effective theory of LQCD has been derived in 1+1 and 3+1 dimensions (1+1D and 3+1D) to study the model at finite chemical potential and temperature. This has been implemented by expanding around the vanishing inverse coupling β and the vanishing hopping parameter $\kappa \propto 1/m_q$ with m_q being the quark mass. Therefore, the theory is valid in the strong coupling and heavy quark regime [8–11].
The effective theory can be interpreted as a spin model, where the spins are the irreducible characters of the gauge group $\mathrm{SU}(N_c)$ and N_c is the amount of colors. The theory reproduced the deconfinement and nuclear liquid-gas transitions qualitatively [5, 6, 8].
The use of techniques on the effective theory that proved themselves in the context of Ising-type systems is suggested by the aforementioned interpretation. A prominent example of them are coarse graining renormalization transformations. They describe the process of iteratively reducing the spacial degrees of freedom. This leads to a description of the same theory on a coarser lattice. This is captured by scale dependent interaction strengths, the running couplings. In this thesis coarse graining renormalization transformations are applied on the effective theory in 1+1D and 2+1D [12, 13].
In chapter 2 renormalization group theory on the lattice is introduced and general features relevant to this thesis are discussed. Chapter 3 deals with pure gauge theory in 1+1D and its analytical solution is covered. Afterwards, in chapter 4 the derivation of the effective theory in 1+1D is summarized and comments regarding higher dimensions are made.
The application of coarse graining renormalization group transformations on the effective theory in 1+1D is studied in chapter 5. First, the tool of choice is tested on pure gauge theory. It reproduces the analytical solution that was previously discussed in chapter 3. Afterwards the static quark determinant is included in the effective action. The knowledge from this step is used to consider more and more parts of the quark determinant. Corrections to the heavy quark limit are incorporated up to $\mathcal{O}(\kappa^4)$ - the highest order the effective action is known to. This restriction is circumvented by assuming a general form of the effective action. All gauge integrals are performed analytically.
Regarding the effective theory in 2+1D coarse graining renormalization is applied in chapter 6 in the pure gauge and heavy quark limit, respectively. In contrast to the discussion regarding 1+1D, approximations have to be introduced to obtain the running couplings.
In chapter 7 the renormalization scheme is evaluated for 1+1D. First, it is observed that the running couplings are in all cases of a similar form. This insight allows us to solve the recursion relations analytically. Because of that, the partition function is obtained in terms of the transfer matrix and the thermodynamic limit is performed. In the last step the baryon density and the pressure are calculated on the lattice and after continuum extrapolation. The observables show the liquid-gas to nuclear matter transition paired with typical lattice artefacts.
The evaluation of the running couplings in 2+1D is covered in chapter 8. The fixed point of the renormalization transformation is determined analytically. This allows us to determine the critical inverse coupling β_c of the deconfinement transition in the pure gauge and the heavy quark limit, respectively. The results are compared to the literature.

Chapter 2

Renormalization Group Theory

The general idea of renormalization group transformations is to relate a physical system with a characteristic scale, e.g. the distance between two neighboring lattice sites of a discretized model, to the same model at a different scale. This process can be split into two steps, coarse graining and rescaling. The first corresponds to a reduction of degrees of freedom of the system, e.g. by integrating out appropriately chosen lattice sites. In the resulting expression the new scales of the theory are identified causing the new action to be of the same form as the previous one, except for altered coupling constants [12, 13].
In the following this will be discussed by considering the action

$$S[\psi] = \sum_n K_n \theta_n[\psi] \tag{2.1}$$

with the coupling constants K_n and functionals θ_n acting on the field configuration ψ. The latter is determined by each ψ_x corresponding to the field strength of ψ at lattice site x. Additionally, we collect the coupling constants K_n in a vector $\mathbf{K} = (K_1, \dots)$ [12].
The quantitiy of interest is the partition function [12]

$$Z(\mathbf{K}) = \int [\mathrm{d}\psi] e^{-S(\mathbf{K})[\psi]} \tag{2.2}$$

2.1 Coarse Graining and Rescaling

Let Λ be the lattice underlying our system of interest and a its length scale. To implement coarse graining we split Λ into two distinct sublattices Λ' and Λ'' with sites $\{x'\}$ and $\{x''\}$, respectively. We assume the distance between all nearest neighbors in Λ' to be increased by a factor $\Delta > 1$ compared to a, e.g. $a \to a\Delta$. Further, let ψ' and ψ'' denote the field configurations of the sublattices Λ' and Λ'' respectively. Now, the integration measure $[\mathrm{d}\psi]$ can be rewritten as [12, 14]

$$\int [\mathrm{d}\psi] = \int [\mathrm{d}\psi'][\mathrm{d}\psi''] = \int \left(\prod_{x' \in \Lambda'} \mathrm{d}\psi_{x'} \right) \left(\prod_{x'' \in \Lambda''} \mathrm{d}\psi_{x''} \right) \tag{2.3}$$

To reduce the degrees of freedom we integrate out the lattice sites of Λ'' and rewrite the resulting expression in terms of a new action S' [12]

$$\int [\mathrm{d}\psi''] e^{-S(\mathbf{K})[\psi', \psi'']} \stackrel{!}{=} e^{-S'[\psi']} \tag{2.4}$$

In general the new action S' is not of the same form as S. Often, however, by choosing the previously introduced lattice decomposition appropriately and introducing approximations, S' can be brought into the same form as S. Then the same functionals θ_n appear except for altered couplings $K_n \to K'_n$. Thus, (2.4) can be written as [12]

$$\int [\mathrm{d}\psi''] e^{-S(\mathbf{K})[\psi', \psi'']} = e^{-S(\mathbf{K}')[\psi']} + \text{corrections} \tag{2.5}$$

The details of this step depend on the particular system.
The model is now described on a coarser lattice with characteristic length $a' = a\Delta$ and the partition function (2.2) is left invariant under the scale transformation (except for possible correction terms) [12]

$$Z = \int [\mathrm{d}\psi] e^{-S(\mathbf{K})[\psi]} = \int [\mathrm{d}\psi'] e^{-S(\mathbf{K}')[\psi']} + \text{corrections} \tag{2.6}$$

2.2 Renormalization Group Transformations

2.2.1 General Properties

Renormalization group transformations are defined to relate the coupling constants at varying length scales. In the context of this discussion this implies that there exists a mapping R_Δ between the couplings $\mathbf{K}$ and $\mathbf{K}'$ [12]

$$\mathbf{K}' = R_\Delta(\mathbf{K}) \tag{2.7}$$

Imagine two successively applied coarse graining and rescaling iterations with factors Δ_1 and Δ_2 respectively. According to the previous discussion the system has length scale of $a' = a\Delta_1$ after the first iteration and $a'' = a'\Delta_2 = a\Delta_2\Delta_1$ after the second. This implies, that renormalization group transformations follow [12]

$$R_{\Delta_2\Delta_1}(\mathbf{K}) = \mathbf{K}'' = R_{\Delta_2}(\mathbf{K}') = R_{\Delta_2}(R_{\Delta_1}(\mathbf{K})) \tag{2.8}$$

In other words renormalization group transformations satisfy the closure relation $R_{\Delta_2\Delta_1} = R_{\Delta_2} \circ R_{\Delta_1}$ with the composition operator $\circ$. Because $\Delta_1, \Delta_2 > 1$, there is no inverse in the set of all renormalization group transformations $\{R_\Delta\}$. Thus, the tuple $(\{R_\Delta\}, \circ)$ forms a semi-group [12].
The couplings

$$\mathbf{K}^{(n)} = R_{\Delta_1 \dots \Delta_n}(\mathbf{K}^{(0)}) \tag{2.9}$$

now determine the interaction strengths at arbitrary scales and therefore correspond to the running couplings of the theory. The trajectories $\mathbf{K}^{(0)}, \dots, \mathbf{K}^{(n)}$ for all initial couplings $\mathbf{K}^{(0)}$ create a renormalization group flow on the coupling manifold [12].

2.2.2 The Renormalized Correlation Length

The correlation length of a system describes over which distances variations in the field ψ can be expected. If it is infinitely large, it implies, that the system undergoes a phase transition. Note, that the converse is not necessarily true, because not every phase transition implies a diverging correlation length. The interplay of renormalization group transformations and the correlation length will lead to important insights. [12]
For a lattice with scale a the physical correlation length ζ can be expressed in terms of its counterpart in lattice units ζ_1 by $\zeta = \zeta_1 a$. On the other hand, like any physical observable ζ is invariant under renormalization group transformations $\zeta = \zeta_\Delta \Delta a$. Therefore, the renormalized correlation length satisfies [12]

$$\zeta_\Delta = \frac{\zeta_1}{\Delta}. \tag{2.10}$$

2.2.3 Fixed Points

A particular choice of couplings $\mathbf{K}_c$ is called a fixed point, if [12]

$$\mathbf{K}_c = R_\Delta(\mathbf{K}_c) \tag{2.11}$$

If the system is at a fixed point $\mathbf{K}_c$, it shows scale invariance and we have

$$\zeta_\Delta(\mathbf{K}_c) = \zeta_1(R_\Delta(\mathbf{K}_c)) = \zeta_1(\mathbf{K}_c) \tag{2.12}$$

Then, following (2.10) the correlation length either vanishes or is infinitely large [12].
For $\zeta = \infty$ the fixed point is called critical as the system undergoes a phase transition. For $\zeta = 0$ the fixed point is called trivial and no critical behavior is implied. Further, for any non-fixed point (2.10) indicates, that the system is driven away from criticality by iterating the renormalization group transformation infinitely many

times [12]. A more detailed discussion of behavior away from fixed points is given in the next subsection.
The basin of attraction of a fixed point $\mathbf{K}_c$ corresponds to the set of all initial couplings $\{\mathbf{K}_0\}$ that converge to $\mathbf{K}_c$ by (repeated) application of the renormalization group transformation. Note that all points $\mathbf{K}_0$ in the basin of attraction of a critical point have the same correlation length. This can be quickly seen by considering the correlation length over the renormalization flow $\mathbf{K}^{(n)}$ of $\{\mathbf{K}_0\}$ [12]

$$\zeta_1(\mathbf{K}_0) = \Delta\zeta_1(\mathbf{K}^{(1)}) = \cdots = \Delta^n\zeta_1(\mathbf{K}^{(n)}) \tag{2.13}$$

In the limit $n \to \infty$ the running couplings flow towards the critical point, where the correlation length diverges. Because $\Delta > 1$, the same holds true for $\zeta_1(\mathbf{K}_0)$ [12].
The basin of attraction of a critical fixed point is called critical manifold [12].

2.2.4 Stability of Fixed Points

To gain information on the renormalization flow close to fixed points let us consider some coupling $\mathbf{K}$ with a small deviation $\delta\mathbf{K}$ from a critical point $\mathbf{K}_c$ [12]

$$\mathbf{K} = \mathbf{K}_c + \delta\mathbf{K} \tag{2.14}$$

We apply a renormalization group transformation on $\delta\mathbf{K}$ and expand it around the critical point

$$\mathbf{K}' = R_\Delta(\mathbf{K}) = \mathbf{K}_c + \left.\frac{\partial\mathbf{K}'}{\partial\mathbf{K}}\right|_{\mathbf{K}=\mathbf{K}_c} \delta\mathbf{K} + \mathcal{O}\left((\delta\mathbf{K})^2\right) \tag{2.15}$$

with the Jacobian $\mathbf{J}^{(\Delta)} := \left.\frac{\partial\mathbf{K}'}{\partial\mathbf{K}}\right|_{\mathbf{K}=\mathbf{K}_c} \delta\mathbf{K}$ [12]. This matrix now determines the behavior near the critical point at a given scale factor δ. For simplicity we assume $\mathbf{J}^{(\Delta)}$ to be symmetric and therefore diagonalizable with real eigenvalues [12].
The closure relation (2.8) transfers itself onto its linearization $\mathbf{J}^{(\Delta)}$ [12]

$$\mathbf{J}^{(\Delta_1)}\mathbf{J}^{(\Delta_2)} = \mathbf{J}^{(\Delta_1\Delta_2)} = \mathbf{J}^{(\Delta_2)}\mathbf{J}^{(\Delta_1)} \tag{2.16}$$

and the matrices commute with one another independent of the scale parameters. Consequently, the eigenvalues $j_{i,\Delta}$ of $\mathbf{J}^{(\Delta)}$ maintain the same behavior

$$j_i^{(\Delta_1)} j_i^{(\Delta_2)} = j_i^{(\Delta_1\Delta_2)} \tag{2.17}$$

Equation (2.17) is solved by the approach $j_i^{(\Delta)} = \Delta^{y_i}$ for some unknown and scale independent y_i [12].
The deviation $\delta\mathbf{K}'$ from the critical coupling compared to $\delta\mathbf{K}$ then determines the behavior we are interested in. Decomposing both in the eigenbasis $\{\mathbf{e}_i^{(\Delta)}\}$ of $\mathbf{J}^{(\Delta)}$ gives

$$\delta\mathbf{K}' = \sum_i a_i^{(\Delta)\prime}\mathbf{e}_i^{(\Delta)} = \mathbf{J}^{(\Delta)}\delta\mathbf{K} = \mathbf{J}^{(\Delta)}\sum_i a_i^{(\Delta)}\mathbf{e}_i^{(\Delta)} = \sum_i a_i^{(\Delta)} j_i^{(\Delta)}\mathbf{e}_i^{(\Delta)} \tag{2.18}$$

The eigenvalues $j_i^{(\Delta)}$ now dictate the renormalization flow [12].
For $y_i > 0$ the deviation in direction $e_i^{(\Delta)}$ increases. Contributions of this kind have been found to correspond to deviations from the critical manifold. By iterating the transformation infinitely many times the coupling is driven away from criticality. This corresponds to an unstable recursion relation. If all $y_i < 0$, contributions in all direction $e_i^{(\Delta)}$ decrease and cause deviations only inside the critical manifold. After an infinite number of iterations the system still shows critical behavior. For $y_i = 0$ the coefficients are not altered. They have been found to be important for logarithmic corrections to the scaling behavior of the system [12].

Chapter 3

Pure Lattice Gauge Theory in 1+1D

Pure lattice gauge theory in 1+1D can be solved analytically in dependence on single group integrals. This solution is discussed for periodic boundary conditions in both the temporal and spacial direction. Periodicity in the former direction is mandatory for describing systems at finite temperature [15, 16].
The studied system is described by the Wilson gauge action with a compact Lie group G [7, 15, 16]

$$S_G = \frac{\beta}{d_f} \sum_P \mathrm{Re}\,\mathrm{Tr}\,[\mathbb{1} - U_P] \tag{3.1}$$

Here β is the inverse coupling strength, P a plaquette, U_P a plaquette of link variables in the fundamental representation and d_f its dimension. Additionally, in this chapter Λ will denote the set of all sites on the 1+1D lattice. [7, 15, 16].
In this thesis we are interested in the case of special unitary groups $G = \mathrm{SU}(N_c)$, because they describe the gauge fields of LQCD [7].
Because the partition function can be used to obtain important thermodynamic observables, e.g. the pressure and density, it is our quantity of interest. In terms of the gauge action (3.1) it reads [7, 15]

$$Z = \int [\mathrm{d}U] e^{-S_G[U]} \tag{3.2}$$

The integration measure is given by

$$\int [\mathrm{d}U] = \prod_{n\in\Lambda} \int \mathrm{d}U_0(n) \int \mathrm{d}U_1(n) \tag{3.3}$$

where $U_0(n)$ is the temporal link variable at lattice site n and $U_1(n)$ is its spacial counterpart [7].
Like any class function[1] the integrand in (3.2) can be expressed in terms of a character expansion [15, 16]

$$Z = \int [\mathrm{d}U] \prod_P \sum_r c_r \chi_r(U_P) \tag{3.4}$$

The sum goes over all irreducible representations r of the group. The χ_r are the characters of the respective representation r and c_r the corresponding character coefficients [16]

$$c_r = \int \mathrm{d}U \chi_r(U^\dagger) \exp\left(-\frac{\beta}{d_f} \mathrm{Re}\,\mathrm{Tr}\,[\mathbb{1} - U]\right) \tag{3.5}$$

The irreducible characters follow the orthogonality, gluing and separation relation

$$\int \mathrm{d}U \chi_r(U) \chi_{r'}(U^\dagger) = \delta_{rr'} \tag{3.6}$$

$$\int \mathrm{d}\Omega \chi_r(U\Omega^\dagger) \chi_{r'}(\Omega V) = \frac{\delta_{rr'}}{d_r} \chi_r(UV) \tag{3.7}$$

$$\int \mathrm{d}\Omega \chi_r\left(\Omega U \Omega^\dagger V\right) = \frac{1}{d_r} \chi_r(U)\chi_r(V) \tag{3.8}$$

[1] A class function f has the property $f(\Omega U \Omega^{-1}) = f(U)$ for all elements of the gauge group $\Omega, U \in G$

with the dimension d_r of the representation r and some group elements $U, V \in G$ [7, 15, 17]. Further properties will be used later on in this thesis and can be found for example in the references [15], [17] and [18].
Another observable of interest will be the lattice string tension σ_L. It is related to the Wilson loop W_C, which describes the expectation value of a closed path C of link variables on the lattice

$$W(C) = \frac{1}{Z}\int [\mathrm{d}U]\chi_f \left(\mathcal{P}\prod_{(n,i)\in C} U_i(n)\right)\prod_P\sum_r c_r\chi_r(U_P) = d_f e^{-A_L\sigma_L} \tag{3.9}$$

Here we used the area of the loop in lattice units A_L and the path ordered product $\mathcal{P}\prod_{(n,i)\in C}$ along the closed contour C [15, 16].

3.1 Gluing of Plaquettes

To perform all gauge integrals Migdal proposed to use the gluing relation (3.7) [19].
Consider two neighboring plaquettes and their contribution of the character expansion, e.g.

$$\sum_r c_r\chi_r\left(U_0(x)U_1(x+e_0)U_0^\dagger(x+e_1)U_1^\dagger(x)\right) \text{ and } \sum_r c_r\chi_r\left(U_0(x+e_0)U_1(x+1e_0)U_0^\dagger(x+e_0+e_1)U_1^\dagger(x+e_0)\right)$$

Both share the link variable $U_1(x+e_1)$, which we integrate out using the gluing relation (3.7). This is illustrated in figure 3.1 and results in

$$\begin{aligned}
&\sum_r\sum_{r'} c_r c_{r'}\int \mathrm{d}U_1(x+e_0)\chi_r\left(U_0(x)U_1(x+e_0)U_0^\dagger(x+e_1)U_1^\dagger(x)\right)\\
&\chi_{r'}\left(U_0(x+e_0)U_1(x+2e_0)U_0^\dagger(x+e_0+e_1)U_1^\dagger(x+e_0)\right)\\
=&\sum_r \frac{c_r^2}{d_r}\chi_r\left(U_0^\dagger(x+e_1)U_1^\dagger(x)U_0(x)U_0(x+e_0)U_1(x+2e_0)U_0^\dagger(x+e_0+e_1)\right)
\end{aligned} \tag{3.10}$$

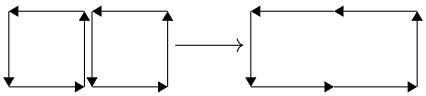

Figure 3.1: Gluing two plaquettes to form a larger contour. Figure based on [15].

The link variables in the characters in (3.10) now describe a path ordered product around both plaquettes and the exponent of the character coefficient resembles the amount of plaquettes enclosed by this path, its area in lattice units [15, 19].
This can be generalized to arbitrary closed contours that share a common edge. Because of the closure relation of the group, we can parameterize the paths as UV and $V^\dagger W$, where V is the shared edge and U as well as W are the residual parts of the respective contours. Due to the invariance of the Haar measure under multiplication with other group elements, e.g. $\mathrm{d}U = \mathrm{d}(UU')$, it is then sufficient to integrate only over V to perform the integration over the whole shared edge. Additionally, we assume that the loops enclose areas A_1 and A_2, respectively. Their contributions to the partition function then read [15, 19]

$$\sum_r d_r\left(\frac{c_r}{d_r}\right)^{A_1}\chi_r(UV) \text{ and } \sum_r d_r\left(\frac{c_r}{d_r}\right)^{A_2}\chi_r(V^\dagger W)$$

By performing the integration over V, one obtains [15, 19]

$$\int \mathrm{d}V\left(\sum_r d_r\left(\frac{c_r}{d_r}\right)^{A_1}\chi_r(UV)\right)\left(\sum_r d_r\left(\frac{c_r}{d_r}\right)^{A_2}\chi_r(V^\dagger W)\right) = \sum_r d_r\left(\frac{c_r}{d_r}\right)^{A_1+A_2}\chi_r(UW) \tag{3.11}$$

Because U and W are the parts of the two contours that are not directly next to each other, but were connected by the edge V, the character $\chi_r(UW)$ describes the combined path around the outer edges of the previous contours. This relation is also known as Migdal's recursion relation [15, 19].

3.2 The Partition Function

We assume that the lattice has N_x spacial, N_τ temporal sites and lattice spacing a. This corresponds to a system with spacial extend $V = N_x a$ and temperature $T = (N_\tau a)^{-1}$.
With Migdal's recursion relation the partition function can be obtained quickly by gluing all plaquettes in the lattice. The remaining path is then given by the outer edges of the lattice. Because of the periodic boundary conditions, the partition function reads [15]

$$Z = \int \mathrm{d}U \mathrm{d}V \sum_r d_r \left(\frac{c_r}{d_r}\right)^{N_x N_\tau} \chi_r\left(UVU^\dagger V^\dagger\right) \tag{3.12}$$

The gauge integration is then finished by first using the separation relation (3.8) and the orthogonality relation (3.6) afterwards [15]

$$Z = \sum_r \left(\frac{c_r}{d_r}\right)^{N_x N_\tau} = c_0^{N_x N_\tau} \sum_r \left(\frac{c_r}{d_r c_0}\right)^{N_x N_\tau} \tag{3.13}$$

This is an analytic function and thus the theory has no phase transitions at finite temperature and inverse coupling β [15, 16, 19].
Note that the coefficients are for finite β bound by $0 \leq \frac{c_r}{d_r c_0} < 1$ for $r \neq 0$ [10, 11]. Therefore, if the spacial or temporal extends are large, the only relevant term in the sum is the trivial character contribution [16]

$$Z \overset{N_x N_\tau \gg 1}{\approx} c_0^{N_x N_\tau} \tag{3.14}$$

The only gauge integrals left appear in the expression for the character coefficients (3.5). For $G = \mathrm{SU}(N_c)$ they can be solved in terms of an infinite series

$$c_r = \sum_{k=-\infty}^{\infty} \det_{1 \leq i,j \leq N_c} I_{l_j + i - j + k}\left(\frac{\beta}{N_c}\right) \tag{3.15}$$

where I is the modified Bessel function of the first kind [20]. The l_j are related to the $N_c - 1$ non-negative integers $(p_1, \ldots, p_{N_c - 1})$ labeling the irreducible representation r [18, 20]

$$l_j = \sum_{n=j}^{N_c - 1} p_n + N_c - j \tag{3.16}$$

For $j = N_c$ we have $l_{N_c} = 0$. The fundamental representation of $\mathrm{SU}(N_c)$ is labeled by $(1, 0, \ldots, 0)$ and the anti-fundamental representation by $(0, \ldots, 0, 1)$ [18, 20].

3.3 The Wilson Loop and String Tension

The string tension determines whether the potential energy between two static quarks increases with their distance. If the string tension is non-zero, at some distance between the quarks the potential energy becomes large enough for pair production. Thus, the quarks only appear in color screened states and are confined. If the string tension vanishes and the potential energy decreases sufficiently fast, pair production may not set in and the former consequences do not apply. Then they exist in a deconfined state [15]. In the following we calculate the Wilson loop and use (3.9) to obtain the string tension.
The gauge integrals that have to be performed to obtain the Wilson loop reside in (3.9). We assume the contour C in the Wilson loop to enclose an area A' and denote the path ordered product as V.
To apply Migdal's recursion relation (3.11) the lattice is divided into two regions, the one enclosed by C and the area outside of it. The contour of the ladder case can be parameterized by $WV^\dagger$, where W is the path ordered product of link variables, that do not appear in C. The contribution to the integration by the surrounding area is given by [15]

$$\sum_r d_r \left(\frac{c_r}{d_r}\right)^{N_x N_\tau - A'} \chi_r(WV^\dagger) = c_0^{N_x N_\tau - A'} \sum_r d_r \left(\frac{c_r}{d_r c_0}\right)^{N_x N_\tau - A'} \chi_r(WV^\dagger)$$

whereas the contribution by the enclosed area and the contour C is

$$\sum_r d_r \left(\frac{c_r}{d_r}\right)^{A'} \chi_r(V) \text{ and } \chi_f(V)$$

The contour C now appears in the integrand of (3.9) three times in various representations. Gauge integrals of this type depend strongly on the structure of the group and can be complicated to solve, if $N_c \geq 3$ [17, 18]. However, in the limit of large spacial extend we can use a similar argument as was used to obtain (3.14). In this case, the coefficients of any representation other than the trivial one is suppressed exponentially. Thus, we neglect these contributions and the Wilson loop reads [15, 16]

$$W(C) \overset{N_x \gg 1}{\approx} \frac{c_0^{N_x N_\tau - A'}}{Z} \sum_r d_r \left(\frac{c_r}{d_r}\right)^{A'} \int \mathrm{d}V \chi_r(V)\chi_f(V) = d_f \left(\frac{c_f}{d_f c_0}\right)^{A'} \tag{3.17}$$

Using (3.9) the string tension is obtained [15, 16]

$$\sigma_L = -\log \frac{c_f}{d_f c_0} \tag{3.18}$$

Because of the previously used inequality the string tension is non-zero for any finite β and the quarks are always confined. This result is not surprising, because switching from confined to deconfined quarks requires a phase transition, which was does not exist in this theory [15, 16]. However, the string tension will be of use in the evaluation of the 1+1D effective theory in chapter 7.

Chapter 4

On the Effective Theory

In this chapter the derivation of an effective theory of lattice QCD in 1+1D is summarized and some adjustments that are necessary in higher dimensions are discussed. The complete derivation can be found in [9] for 1+1D and in [10, 11, 21] for the 3+1D theory.
Until now only the Wilson gauge action (3.1) has been introduced. To fully describe QCD on the lattice, however, our system of interest has to be filled with (dynamical) quarks. In our case these are described by the Wilson fermion action [7]

$$S_F = \bar{\psi} Q[U] \psi \tag{4.1}$$

where $Q[U]$ is the Wilson-Dirac-Operator [7]

$$Q[U] = \mathbb{1} - \kappa \sum_{v=0}^{d} \left[e^{a\mu\delta_{v0}} (\mathbb{1} + \gamma_v) U_v(x) \delta_{y,x+\hat{v}} + e^{-a\mu\delta_{v0}} (\mathbb{1} - \gamma_v) U_v^\dagger(y) \delta_{y,x-\hat{v}} \right] \tag{4.2}$$

Here $\kappa = (2 + 2d + 2am)^{-1}$ is the hopping parameter, d the amount of spacial dimensions, γ_v the Dirac matrices for $d+1$ dimensional space time, μ the chemical potential and $\hat{v}$ the unit vector in direction v. For $d = 1$ the matrices are equivalent to the first two Pauli matrices [9]

$$\gamma_0 = \sigma_1 = \begin{pmatrix} 0 & 1 \\ 1 & 0 \end{pmatrix} \quad \text{and} \quad \gamma_1 = \sigma_2 = \begin{pmatrix} 0 & -i \\ i & 0 \end{pmatrix} \tag{4.3}$$

The action (4.1) is chosen instead of the naive discretization of the fermion action of QCD. The latter has been shown to imply additional particles, usually referred to as doublers, in the continuum limit, that do not exist in full QCD. This problem is solved by introducing a counter term, that shifts their mass by a term proportional to $1/a$. In the continuum limit $a \to 0$ their total mass diverges and the doublers become unphysical. A drawback of (4.1) is the explicit breaking of chiral symmetry even for vanishing quark masses [7].
The Wilson fermion action reproduces the continuum action of QCD to first order in the lattice spacing a. This choice, however, is not unique because different actions as well as corrections to (4.1) have been proposed to reduce certain side effects. These include for example the introduction of counter terms to (4.1) increasing the order at which discretization artefacts start to appear. Wilson actions including such terms are called improved Wilson actions [7]
The action and partition function of our description of lattice QCD read, respectively, [7]

$$S = S_G + S_F \tag{4.4}$$

$$Z = \int [\mathrm{d}U] \mathcal{D}[\bar{\psi}] \mathcal{D}[\psi] e^{-S[U,\bar{\psi},\psi]} \tag{4.5}$$

The fermionic contribution is a Gaussian integral over Grassmann fields and can be performed analytically [14]

$$Z = \int [\mathrm{d}U] \det Q[U] e^{-S_G[U]} \tag{4.6}$$

The description of the system of interest is shifted into an effective action by performing the integration over all spacial link variables

$$Z_{\text{eff}} = \int [\mathrm{d}U_0] e^{-S_{\text{eff}}} \quad \text{with} \quad S_{\text{eff}} = -\log \prod_{i=1}^{d} \int [\mathrm{d}U_i] \det Q e^{-S_G} \tag{4.7}$$

We will find, that the resulting action is dimensionally reduced from $d+1 \to d$, whereas the temporal evolution of the system is fully shifted into the path integral over the time-like gauge field [9–11, 21].
To determine the effective action the character expansion and a hopping parameter expansion around $\kappa = 0$ are our tools of choice [9–11, 21]. First, the pure gauge limit $\kappa = 0$ (section 4.1), then the strong coupling limit $\beta = 0$ (section 4.2) is discussed. Deviations from both limits imply corrections, which are covered afterwards (section 4.3).

4.1 The Gauge Field as an Effective Spin Model

To obtain the effective gauge action we turn back to the character expansion, which was already introduced in chapter 3.
In the 1+1D theory we can immediately use Migdal's recursion relation to perform the integration. This is achieved by ordering the plaquettes by their spacial position and gluing them together [8, 15, 19]. This is illustrated in figure 4.1.

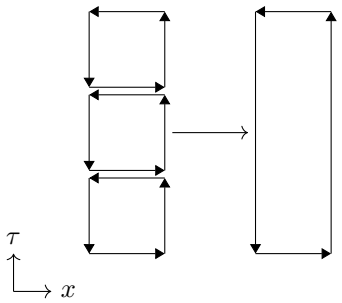

Figure 4.1: Gluing plaquettes in the temporal direction is the first step to obtain the effective gauge action in 1+1D. Figure based on [15].

The neighboring plaquettes on the left hand side of figure 4.1 share a common spacial link. Integrating them out leads according to Migdal's recursion relation to a rectangle expanding into the temporal direction [8, 19]. Applying this to all N_τ plaquettes for a given x and using the periodic boundary conditions leads to the effective action

$$\begin{aligned}
S_{\text{eff}} &= -\log c_0^{N_x N_\tau} \int [\mathrm{d}U_1] \prod_{x=1}^{N_x} \prod_{\tau=1}^{N_\tau} \sum_r \frac{c_r}{d_r c_0} \chi_r \Big(U_1(x,\tau) U_0(x+1,\tau) U_1^\dagger(x,\tau+1) U_0^\dagger(x,\tau) \Big) \\
&= -\log c_0^{N_x N_\tau} \prod_{x=1}^{N_x} \int \mathrm{d}U_1(x,1) \sum_r \left(\frac{c_r}{d_r c_0} \right)^{N_\tau} \\
&\quad \chi_r \Big(U_1(x,1) U_0(x+1,1) \dots U_0(x+1,N_\tau) U_1^\dagger(x,N_\tau+1) U_0^\dagger(x,N_\tau) \dots U_0^\dagger(x,1) \Big) \\
&= -\log c_0^{N_x N_\tau} \prod_{x=1}^{N_x} \sum_r \left(\frac{c_r}{d_r c_0} \right)^{N_\tau} \chi_r \Big(U_0(x+1,1) \dots U_0(x+1,N_\tau) \Big) \chi_r \Big(U_0^\dagger(x,N_\tau) \dots U_0^\dagger(x,1) \Big)
\end{aligned} \tag{4.8}$$

Using the invariance of the Haar measure for the remaining temporal link integrals then implies [8]

$$\begin{aligned}
S_{\text{eff}} &= -\log c_0^{N_x N_\tau} - \sum_{x=1}^{N_x} \log \sum_r \left(\frac{c_r}{d_r c_0} \right)^{N_\tau} \chi_r(U_x^\dagger) \chi_r(U_{x+1}) \\
\int [\mathrm{d}U_0] &\to \prod_{x=1}^{N_x} \int \mathrm{d}U_x =: \int [\mathrm{d}U]
\end{aligned} \tag{4.9}$$

Because only the sum over spacial positions is calculated the effective action is dimensionally reduced compared to our initial theory [8].
The description of the system at hand is shifted into effective nearest neighbor interactions between complex and continuous valued spins $\chi_r(U_x)$. They are often referred to as Polyakov loops in the representation r, as they describe windings of link variables in the temporal direction. In the fundamental representation they are usually denoted as $L_x := \chi_f(U_x)$ [10, 11, 21].
The effective partition function is given by

$$Z_{\text{eff}} = c_0^{N_x N_\tau} \int [\mathrm{d}U] \prod_{\langle x,y \rangle} \sum_r \lambda_r \chi_r(U_x) \chi_r(U_y^\dagger) \tag{4.10}$$

where we defined the coupling constants

$$\lambda_r := u_r^{N_\tau} := \left(\frac{c_r}{d_r c_0} \right)^{N_\tau} \tag{4.11}$$

As we will find in section 7.4.2, the trivial character coefficient is the vacuum contribution to the free energy density and cancels in expectation values of observables. The latter holds true in higher dimensions as well [10, 11, 21].
In higher dimensional pure gauge theory spacial plaquettes appear and approximations become necessary to derive the effective action. The additional steps include neglecting spacial plaquettes and aborting the sums over representations at the fundamental and anti-fundamental terms. Then the partition function is of the form [8]

$$Z_{\text{eff}} = \int [\mathrm{d}U] \prod_{\langle x,y \rangle} \left(1 + \lambda_f \left(L_x L_y^\dagger + L_x^\dagger L_y \right) \right) + \mathcal{O}(u_f^{N_\tau+4}) \tag{4.12}$$

Here the trivial character coefficient has already been disregarded.
Corrections to (4.12) can be obtained by including higher representations and spacial plaquettes in various combinations. This leads to

- Further characters in the interaction terms, e.g. in the adjoint representation

$$1 + \lambda_f \left(L_x L_y^\dagger + L_x^\dagger L_y \right) \to 1 + \lambda_f \left(L_x L_y^\dagger + L_x^\dagger L_y \right) + \lambda_a \chi_a(U_x) \chi_a(U_y^\dagger) \tag{4.13}$$

  In this case the correction is of order $\mathcal{O}(u_f^{2N_\tau})$. Other non-fundamental character contributions are of even higher orders [22].

- Additional interactions over distances beyond nearest neighbors, e.g. between lattice sites with $|x-y|/a = \sqrt{2}$ [8, 23]. This is implemented into the partition function by including

$$\prod_{[x,y]} \left(1 + \lambda_{2,f} \left(L_x L_y^\dagger + L_y L_x^\dagger \right) \right) \quad \text{with} \quad \lambda_{2,f} = N_\tau (N_\tau - 1) u_f^{2N_\tau+2} \tag{4.14}$$

  in the integrand of (4.12). This example causes corrections of order $\mathcal{O}\left(u^{2N_\tau+2}\right)$ [8]. Here $[x, y]$ refers to pairs of lattice sites at the distance mentioned above.

- Adjustments to the coupling strengths λ_r, $\lambda_{2,r}$, etc. For λ_f and $\lambda_{2,f}$ the corrections are of the order $\mathcal{O}(u_f^{N_\tau+4})$ and $\mathcal{O}(u_f^{2N_\tau+4})$, respectively. Because the overall N_τ dependence of the additional terms does not change, high order corrections can become necessary to accurately determine the coupling strengths, if $u_f \not\ll 1$ [8].

Note that (4.12) and (4.10) are explicitly center symmetric. In 3+1D the effective theory is able to reproduce its spontaneous breaking resulting in the confinement-deconfinement phase transition [8]. In chapter 8 we will find, that this holds true in 2+1D as well.

4.2 The Quark Determinant

The Wilson-Dirac-operator (4.2) describes the interaction of quarks between each pair of lattice sites x and y. For light quarks $\kappa \approx (2+2d)^{-1}$ its determinant is highly non-local because it allows interactions over long ranges. In the heavy quark regime $\kappa \ll 1$, however, only interactions over shorter ranges are important [9–11]. In the following the quark determinant is expanded around the latter limit for a single flavor of quarks $N_f = 1$ in 1+1D and spacial links are integrated out. Comments regarding higher N_f and higher dimensions are included at their given time.
First, it is useful to split the Wilson-Dirac-operator into its temporal T and spacial contributions S, respectively, [9]

$$T = \kappa e^{a\mu}(\mathbb{1}+\gamma_0)U_0(x)\delta_{y,x+\hat{0}} + \kappa e^{-a\mu}(\mathbb{1}-\gamma_0)U_0^\dagger(x)\delta_{y,x-\hat{0}} \tag{4.15}$$

$$S = \kappa(\mathbb{1}+\gamma_1)U_1(x)\delta_{y,x+\hat{1}} + \kappa(\mathbb{1}-\gamma_1)U_1^\dagger(x)\delta_{y,x-\hat{1}} \tag{4.16}$$

$$Q = \mathbb{1} - T - S \tag{4.17}$$

This lets us factorize the quark determinant into two contributions. One describes only a temporal evolution of quarks, which is called the static determinant. The other describes dynamical quarks and is called kinetic quark determinant. The latter will contain the long range interactions mentioned above. To be more specific the quantities read [9]

$$\det Q = \det(\mathbb{1}-T-S) = \det\left(\mathbb{1}-T\right)\det\left(\mathbb{1}-\frac{S}{\mathbb{1}-T}\right) \tag{4.18}$$

After applying multiple relations for the Dirac matrices to the static contribution in (4.18) one obtains [9]

$$\det(\mathbb{1}-T) = \prod_x \det\left(\mathbb{1}+h_1U_x\right)^2 \det\left(\mathbb{1}+\bar{h}_1U_x^\dagger\right)^2 =: \prod_x \det Q_{\text{stat}}^{\text{loc}}(U_x) =: \det Q_{\text{stat}} \tag{4.19}$$

where we defined the heavy quark couplings

$$h_1 = (2\kappa)^{N_\tau}e^{N_\tau a\mu} \tag{4.20}$$

$$\bar{h}_1 = (2\kappa)^{N_\tau}e^{-N_\tau a\mu} \tag{4.21}$$

The U_x are the same temporal windings as in section 4.1 and $\det Q_{\text{stat}}^{\text{loc}}(U_x)$ describes the evolution of static quarks at lattice site x. Note that the form (4.19) holds in higher dimensions as well [10, 11].
For SU(3) the static determinant can be expressed in terms of Polyakov loops [10, 11]

$$\det Q_{\text{stat}} = \prod_x \left(1+h_1L_x+h_1^2L_x^\dagger+h_1^3\right)\left(1+\bar{h}_1L_x^\dagger+\bar{h}_1^2L_x+\bar{h}_1^3\right) \tag{4.22}$$

whereas higher choices of N_c imply more complicated expressions [11].
To obtain the kinetic quark determinant the spacial contribution to the Wilson-Dirac-operator is further divided into the propagation in positive x direction P and negative x direction M. Using the trace-log identity results in [9]

$$\det Q_{\text{kin}} = \det\left(\mathbb{1}-\frac{S}{\mathbb{1}-T}\right) = \det(\mathbb{1}-P-M) = \exp\left(-\operatorname{Tr}\sum_{n=1}^{\infty}\frac{1}{n}(P+M)^n\right) \tag{4.23}$$

It can be shown that only closed loops of the propagators P and M are allowed. Therefore both have to appear in the same amount inside a trace. Otherwise the term immediately vanishes. Because each P and M carries a κ, only even orders in the hopping parameter appear in the expanded logarithm [9–11].
At a given n the longest loop extends from x to $x+n/2$. Because for low quark masses high order terms, e.g. with $n \gg 1$, are necessary, this captures the non-local behavior of the quark determinant [9–11].
The expression (4.23) is expanded around heavy quark limit $\kappa = 0$ and the Dirac matrices are evaluated. This has to be done order by order, after which the spacial links can be integrated out. To second order in κ this leads to [9]

$$\int [\mathrm{d}U_1]\det Q_{\text{kin}} = 1 - \frac{\kappa^2 N_\tau}{N_c}\sum_x \left(\operatorname{Tr}\frac{h_1U_x}{\mathbb{1}+h_1U_x} - \operatorname{Tr}\frac{\bar{h}_1U_x^\dagger}{\mathbb{1}+\bar{h}_1U_x^\dagger}\right)\left(\operatorname{Tr}\frac{h_1U_{x+1}}{\mathbb{1}+h_1U_{x+1}} - \operatorname{Tr}\frac{\bar{h}_1U_{x+1}^\dagger}{\mathbb{1}+\bar{h}_1U_{x+1}^\dagger}\right) + \mathcal{O}(\kappa^4) \tag{4.24}$$

The right hand side introduces a new type of nearest neighbor interaction with coupling constant $\kappa^2 N_\tau / N_c =: h_2$. The traced fractions represent one-point correlation functions, that will also appear in variations at higher orders in κ. Therefore, it is useful to define [9, 11]

$$W_{ab\bar{a}\bar{b}}(U) = \mathrm{Tr}\left(\frac{(h_1 U)^a}{(\mathbb{1} + h_1 U)^b}\frac{\left(\bar{h}_1 U^\dagger\right)^{\bar{a}}}{\left(\mathbb{1} + \bar{h}_1 U^\dagger\right)^{\bar{b}}}\right) \tag{4.25}$$

$$W^-_{ab\bar{a}\bar{b}}(U) = W_{ab00} - W_{00\bar{a}\bar{b}} \tag{4.26}$$

$$W^+_{ab\bar{a}\bar{b}}(U) = W_{ab00} + W_{00\bar{a}\bar{b}} \tag{4.27}$$

These correlation functions are referred to as node functions. With those definitions the kinetic quark determinant to leading order reads [9]

$$\det Q_{\mathrm{kin}} = 1 - h_2 \sum_{\langle x,y\rangle} W^-_{1111}(U_x) W^-_{1111}(U_y) + \mathcal{O}(\kappa^4) \tag{4.28}$$

In higher dimensions (4.28) holds as well [10, 11].
For general chemical potential the kinetic determinant has been derived in 1+1D [9] and 3+1D [10] to $\mathcal{O}(\kappa^4)$, whereas the expression in the heavy and dense regime is known to $\mathcal{O}(\kappa^8)$ [11].
To obtain the effective action, it is common to rewrite the kinetic determinant as an exponential. If expanded, it reproduces $\det Q_{\mathrm{kin}}$ to the given order. To leading order this results in [9, 11]

$$\det Q_{\mathrm{kin}} \to \exp\left(-h_2 \sum_{\langle x,y\rangle} W^-_{1111}(U_x) W^-_{1111}(U_y)\right) + \mathcal{O}(\kappa^4) \tag{4.29}$$

At higher orders, however, counter terms have to be included in the exponential. This process is known as resummation and improves the convergence of the theory, because an infinite number of terms is included in the quark determinant. Afterwards, the argument of the exponential corresponds to the kinetic quark contribution to the effective action [9–11]. To fourth order in κ for 1+1D it can be found in [9].
Note that there are methods to rewrite the node functions in terms of Polyakov loops in the fundamental representation. Therefore, the interpretation of the effective theory as a spin model holds in this limit as well [10, 11].
For N_f degenerate flavors it can be shown that only the following simple substitutions have to be made [9–11]

$$\det Q_{\mathrm{stat}} \to \det Q^{N_f}_{\mathrm{stat}}, \quad h_2 \to N_f h_2, \quad h_{3_1} \to N_f h_{3_1}, \quad h_{3_2} \to N_f h_{3_1} \tag{4.30}$$

4.3 Gauge Corrections to the Fermion Couplings

To describe deviations from the strong coupling and heavy quark limits corrections to the effective action become necessary. These can be shifted into the couplings, which then become a function of both κ and β, e.g. $h_1(\kappa) \to h_1(\kappa, \beta)$. By inserting plaquettes to the spacial link integration in section 4.2 the corrections are obtained [10, 11].
In 1+1D they have been derived to order $\mathcal{O}(\kappa^n u_f^m)$ with $n + m \leq 7$ [9]

$$h_1 = (2\kappa)^{N_\tau} e^{N_\tau a\mu} \exp\left(2N_\tau \kappa^2 \frac{u_f - u_f^{N_\tau}}{1 - u_f} + \kappa^4 N_\tau \left(-8u_f + 6u_f^2 + 4u_f^3 N_\tau\right)\right) \tag{4.31}$$

$$h_2 = \frac{\kappa^2 N_\tau}{N_c}\left(1 + 2\frac{u_f - u_f^{N_\tau}}{1 - u_f}\right) \tag{4.32}$$

$$h_{3_1} = \frac{\kappa^4 N_\tau}{n_c^2}\left(1 + 4\frac{u_f - u_f^{N_\tau}}{1 - u_f}\right) \tag{4.33}$$

$$h_{3_2} = \frac{\kappa^4 N_\tau (N_\tau - 1)}{N_c^2}\left(1 + 4\sum_{n=1}^{N_\tau - 2} n u_f^n \frac{N_\tau - (n+1)}{N_\tau - 1}\right) \tag{4.34}$$

Chapter 5

1+1D: Coarse Graining Renormalization in the Effective Theory

In this chapter we will apply renormalization group transformations to the effective theory of 1+1D heavy quark QCD.
We start with pure gauge theory, where the running couplings result in the exact expression for the partition function, which was already discussed in chapter 3. In the next step the static quark determinant is included. Still, the scheme will be valid to arbitrary order in β. Subsequently, corrections to the heavy quark limit up to $\mathcal{O}(\kappa^4)$ are implemented. Finally, assuming a certain form of the effective action the recursion relations are generalized to arbitrary order in both κ and β.
All running couplings are expressed in terms of single integrals over the gauge group, which are solved analytically.

5.1 Pure Gauge Theory

Pure gauge theory in two dimensions is commonly deemed to be trivial, as its analytical solution is well known from literature and the theory governs no physical degrees of freedom [15, 16]. Here it is used as a test bed for our recursion scheme. The partition function for 1+1D pure gauge theory was already given in (4.10).
Periodic boundary conditions in space are assumed. Because our effective theory can be interpreted as a 1D spin model, it is natural to apply similar techniques as have been applied to the 1D Ising model. Thus, the recursion scheme will be obtained by integrating every second site of the lattice. This corresponds to a renormalization group transformation with scale factor 2. [10–12, 15]
To capture the renormalization group transformation we substitute $[\mathrm{d}U] \to [\mathrm{d}U]^{(n)}$, $N_x \to N_x^{(n)}$ and $\lambda_r \to \lambda_r^{(n)}$ in (4.10). These quantities describe the interaction measure and the amount of lattice sites remaining after n coarse graining iterations as well as the couplings between them, respectively [12]. The pure gauge partition function then reads

$$Z_{\mathrm{pg}} = c_0^{N_x N_\tau} \int [\mathrm{d}U]^{(n)} \prod_{x=1}^{N_x^{(n)}} \sum_r \lambda_r^{(n)} \chi_r(U_x) \chi_r(U_{x+1}^\dagger) \tag{5.1}$$

with the boundary conditions

$$\lambda_r^{(0)} = \lambda_r = \left(\frac{c_r}{d_r c_0} \right)^{N_\tau} \tag{5.2}$$

$$[\mathrm{d}U]^{(0)} = [\mathrm{d}U] \tag{5.3}$$

$$N_x^{(0)} = N_x \tag{5.4}$$

To obtain a recursion scheme the interaction terms are grouped into pairs of two and the product is expanded

$$\begin{aligned} Z_{\mathrm{pg}} =& c_0^{N_x N_\tau} \int [\mathrm{d}U]^{(n)} \prod_{\substack{x=1 \\ x \bmod 2=0}}^{N_x^{(n)}} \left(\sum_r \lambda_r^{(n)} \chi_r(U_x) \chi_r(U_{x+1}^\dagger) \right) \left(\sum_r \lambda_r^{(n)} \chi_r(U_{x+1}) \chi_r(U_{x+2}^\dagger) \right) \\ =& c_0^{N_x N_\tau} \int [\mathrm{d}U]^{(n)} \prod_{\substack{x=1 \\ x \bmod 2=0}}^{N_x^{(n)}} \sum_{rr'} \lambda_r^{(n)} \lambda_{r'}^{(n)} \chi_r(U_x) \chi_r(U_{x+1}^\dagger) \chi_{r'}(U_{x+1}) \chi_{r'}(U_{x+2}^\dagger) \end{aligned} \tag{5.5}$$

Now the integration over the link variable U_{x+1} can be performed. Thus, the integration measure transforms as

$$[\mathrm{d}U]^n = \prod_{x=1}^{N_x^{(n)}} \mathrm{d}U_x \to \prod_{\substack{x=1 \\ x \bmod 2=0}}^{N_x^{(n)}} \mathrm{d}U_x \stackrel{!}{=} [\mathrm{d}U]^{(n+1)} \tag{5.6}$$

The gauge integral is performed with the orthogonality relation for irreducible characters (3.6), which collapses one of the sums

$$Z_{\mathrm{pg}} = c_0^{N_x N_\tau} \int [\mathrm{d}U]^{(n+1)} \prod_{\substack{x=1 \\ x \bmod 2=0}}^{N_x^{(n)}} \sum_{rr'} \lambda_r^{(n)} \lambda_{r'}^{(n)} \chi_r(U_x) \chi_{r'}(U_{x+2}^\dagger) \int \mathrm{d}U_{x+1} \chi_r(U_{x+1}^\dagger) \chi_{r'}(U_{x+1}) \tag{5.7}$$

$$= c_0^{N_x N_\tau} \int [\mathrm{d}U]^{(n+1)} \prod_{\substack{x=1 \\ x \bmod 2=0}}^{N_x^{(n)}} \sum_r \lambda_r^{(n)2} \chi_r(U_x) \chi_r(U_{x+2}^\dagger) \tag{5.8}$$

After renaming the lattice sites and identifying the renormalized quantities one obtains the recursion relations [12]

$$\lambda_r^{(n+1)} = \lambda_r^{(n)2} \tag{5.9}$$

$$N_x^{(n+1)} = \frac{N_x^{(n)}}{2} \tag{5.10}$$

The relations are quickly solved by $\lambda_r^{(n)} = \lambda_r^{2^n}$ and $N_x^{(n)} = 2^{-n} N_x$, respectively.
If the amount of spacial sites is a power of two, e.g. $N_x = 2^{n_x}$, the recursion scheme can be iterated n_x times to perform all gauge integrals and solve the theory [12]. Due to the periodic boundary conditions this leads to

$$Z_{\mathrm{pq}} = c_0^{N_x N_\tau} \sum_r \lambda_r^{(n_x)} = c_0^{N_x N_\tau} \sum_r \left(\frac{c_r}{d_r c_0} \right)^{N_x N_\tau} \tag{5.11}$$

Thus, our procedure reproduces the expression (3.13) obtained with Migdal's recursion relation.

5.2 The Static Quark Limit at Finite Density

5.2.1 From Pure Gauge to Static Quarks

Because the static determinant depends only on temporal links, the partition function for heavy quarks is simply determined by including $\det Q_{\mathrm{stat}}$ into the gauge integrals [9–11]

$$Z_{\mathrm{sq}} = c_0^{N_x N_\tau} \int [\mathrm{d}U] \det Q_{\mathrm{stat}} \prod_{\langle x,y \rangle} \sum_r \lambda_r \chi_r(U_x) \chi_r(U_y^\dagger) = c_0^{N_x N_\tau} \int [\mathrm{d}U] \prod_x \sum_r \lambda_r \chi_r(U_x) \chi_r(U_{x+1}^\dagger) \det Q_{\mathrm{stat}}^{\mathrm{loc}}(U_x) \tag{5.12}$$

To gain an intuition how the recursion relation is going to look like, it is instructive to notice that we can get from pure gauge theory to static quarks by substituting the Haar measure $\mathrm{d}U_x$ for all lattice sites

$$\mathrm{d}U_x \to \mathrm{d}U_x \det Q_{\mathrm{stat}}^{\mathrm{loc}}(U_x) \tag{5.13}$$

In context of (5.7), this corresponds to

$$\int \mathrm{d}U_{x+1}\chi_r(U_{x+1}^\dagger)\chi_{r'}(U_{x+1}) \to \int \mathrm{d}U_{x+1}\det Q_{\mathrm{stat}}^{\mathrm{loc}}(U_{x+1})\chi_r(U_{x+1}^\dagger)\chi_{r'}(U_{x+1}) \tag{5.14}$$

The static determinant induces deviations from the orthogonality relation (3.6) and thus creates dependencies on the intrinsic structure of the gauge group. Because this can be complicated especially for $N_c \geq 3$, mixed terms between all different representations will be allowed [17, 18].
The appearance of combinations of all possible interaction terms is a typical feature of renormalization group transformations and the simplicity of the pure gauge limit is ascribed to the triviality of the theory [12, 15, 16]. Contrary to higher dimensions renormalization group transformations in 1D usually do not increase the range of interactions. Thus, no further approximations are expected to be necessary in this chapter and allowing all possible mixed terms of interactions can be expected to occur in the remaining cases of this chapter as well. [12, 15].

5.2.2 The Renormalization Scheme

Based on the previous subsection we formulate our recursion approach to be

$$Z = c_0^{N_x N_\tau}\int [\mathrm{d}U]^{(n)}\det Q_{\mathrm{stat}}^{(n)}\prod_{x=1}^{N_x^{(n)}}\sum_{r,r'}\lambda_{rr'}^{(n)}\chi_r(U_x)\chi_{r'}(U_{x+1}^\dagger) \tag{5.15}$$

where $[\mathrm{d}U]^{(n)}$, $\det Q_{\mathrm{stat}}^{(n)}$ and $N_x^{(n)}$ contain only the integration measure, local static determinant and lattice sites after n coarse graining iterations, respectively. The two indices of the couplings $\lambda_{rr'}^{(n)}$ allow interactions involving distinct irreducible representations.
With the following boundary conditions the initial expression for the partition function (5.12) is reproduced by (5.15)

$$\lambda_{rr'}^{(0)} = \lambda_r\delta_{rr'} = \left(\frac{c_r}{d_r c_0}\right)^{N_\tau}\delta_{rr'} \tag{5.16}$$

$$\det Q_{\mathrm{stat}}^{(0)} = \det Q_{\mathrm{stat}} \tag{5.17}$$

To obtain the running couplings the same integration scheme as in section 5.1 is used. We start by grouping the interaction terms into pairs of two and pull every second gauge integral into the product [12]

$$\begin{aligned}
Z_{\mathrm{sq}} &= c_0^{N_x N_\tau}\int [\mathrm{d}U]^{(n)}\det Q_{\mathrm{stat}}^{(n)}\prod_{\substack{x=1\\ x \bmod 2=0}}^{N_x^{(n)}}\left(\sum_{r_1,r_1'}\lambda_{r_1r_1'}^{(n)}\chi_{r_1}(U_{x-1})\chi_{r_1'}(U_x^\dagger)\right)\left(\sum_{r_2,r_2'}\lambda_{r_2'r_2}^{(n)}\chi_{r_2'}(U_x)\chi_{r_2}(U_{x+1}^\dagger)\right)\\
&= c_0^{N_x N_\tau}\int [\mathrm{d}U]^{(n+1)}\det Q_{\mathrm{stat}}^{(n+1)}\prod_{x=1}^{N_x^{(n)}/2}\sum_{r_1,r_2}\chi_{r_1}(U_x)\chi_{r_2}(U_{x+1}^\dagger)\sum_{r_1',r_2'}\lambda_{r_1r_1'}^{(n)}\lambda_{r_2'r_2}^{(n)}\int \mathrm{d}U\det Q_{\mathrm{stat}}^{\mathrm{loc}}(U)\chi_{r_1'}(U^\dagger)\chi_{r_2'}(U)\\
&\overset{!}{=} c_0^{N_x N_\tau}\int [\mathrm{d}U]^{(n+1)}\det Q_{\mathrm{stat}}^{(n+1)}\prod_{x=1}^{N_x^{(n+1)}}\sum_{r_1,r_2}\lambda_{r_1r_2}^{(n+1)}\chi_{r_1}(U_x)\chi_{r_2}(U_{x+1}^\dagger)
\end{aligned} \tag{5.18}$$

From the first to the second line we renamed the sites on the coarse grained lattice as well as the variable in the gauge integral.
The recursion relation for the running couplings can be simply read of from (5.18) [12, 15]

$$\lambda_{r_1r_2}^{(n+1)} = \sum_{r_1',r_2'}\lambda_{r_1r_1'}^{(n)}\lambda_{r_2'r_2}^{(n)}\int \mathrm{d}U\det Q_{\mathrm{stat}}^{\mathrm{loc}}(U)\chi_{r_1'}(U^\dagger)\chi_{r_2'}(U) \tag{5.19}$$

The gauge integral is solved in section 5.2.3. The expression shows the complex behavior we expected in section 5.2.1.
In the limit $h_1, \bar{h}_1 \to 0$ the static determinant approaches $\det Q_{\mathrm{stat}}^{\mathrm{loc}}(U) \to 1$ and the gauge integral can be performed with the orthogonality relation for irreducible characters (3.6) [9–11]. Thus, the pure gauge recursion relation (5.9) is recovered.

5.2.3 The Static Quark Gauge Integral

To solve the recursion relations for static quarks it is necessary to perform the gauge integral

$$f_{\mathrm{sq}}(r,r') = \int \mathrm{d}U \det Q^{\mathrm{loc}}_{\mathrm{stat}}(U)\chi_r(U^\dagger)\chi_{r'}(U) \tag{5.20}$$

As both the irreducible characters and the static determinant are class functions, the integrand in (5.20) depends only on the eigenvalues $y_1,\dots,y_{N_c}$ of the group element $U \in \mathrm{SU}(N_c)$ [24].
Here we follow the approach by Nishida that can be used to solve integrals over some class function f with [24,25]

$$\int \mathrm{d}U f(U) = \int \mathrm{d}U \sum_{t=1}^{N_c} \tilde{f}_{1,t}(y_1)\dots\tilde{f}_{N_c,t}(y_{N_c}) \tag{5.21}$$

This procedure has been applied in previous discussions of the 3+1D effective theory [24, 26].
The approach consists of re-writing the $\mathrm{SU}(N_c)$ Haar measure in the Polyakov gauge by [25]

$$\int \mathrm{d}U \to \frac{1}{(2\pi)^{N_c}} \prod_{t=1}^{N_c} \left(\int_{-\pi}^{\pi} \mathrm{d}\phi_t\right) |\Delta|^2 2\pi\delta\left(\sum_{t=1}^{N_c}\phi_t \mod 2\pi\right) \tag{5.22}$$

where Δ is the Vandermonde determinant [18, 25]

$$\Delta = \begin{vmatrix} z_1^{N_c-1} & \dots & z_{N_c}^{N_c-1} \\ \vdots & & \vdots \\ z_1^{N_c-N_c} & \dots & z_{N_c}^{N_c-N_c} \end{vmatrix} \text{ and } z_j = e^{i\phi_j} \tag{5.23}$$

The delta function in (5.22) can be expressed by its Fourier series [25]

$$2\pi\delta\left(\sum_{t=1}^{N_c}\phi_t \mod 2\pi\right) = \sum_{k=-\infty}^{\infty} \exp\left(-ik\sum_{t=1}^{N_c}\phi_t\right) = \sum_{k=-\infty}^{\infty} z_1^{-k}\dots z_{N_c}^{-k} \tag{5.24}$$

The irreducible characters can be expressed with Weyl's character formula [18]

$$\chi_r(U) = \frac{1}{\Delta}\begin{vmatrix} z_1^{l_1} & \dots & z_{N_c}^{l_1} \\ \vdots & & \vdots \\ z_1^{l_{N_c}} & \dots & z_{N_c}^{l_{N_c}} \end{vmatrix} \tag{5.25}$$

The $l_1,\dots,l_{N_c}$ have already been discussed in section 3.2 and are given by (3.16).
Inserting (5.22)-(5.25) in (5.20) yields [25]

$$f_{\mathrm{sq}} = \frac{1}{(2\pi)^{N_c}} \sum_{k=-\infty}^{\infty} \sum_{i_1,\dots,i_{N_c}} \sum_{j_1,\dots,j_{N_c}} \epsilon_{i_1,\dots,i_{N_c}}\epsilon_{j_1,\dots,j_{N_c}} \prod_{t=1}^{N_c} \int_{-\phi}^{\phi} \mathrm{d}\phi_t z_t^{l'_j-l_i-k} \left(1+h_1 z_t\right)^{2N_f} \left(1+\bar{h}_1\frac{1}{z_t}\right)^{2N_f} \tag{5.26}$$

The sums over indices $i_1,\dots,i_{N_c}$ and $j_1,\dots,j_{N_c}$ can be summed up to the determinant of a matrix $\mathbf{M}_{\mathrm{sq}}$ with dimension N_c [25]

$$f_{\mathrm{sq}} = \sum_{k=-\infty}^{\infty} \det_{1\le i,j\le N_c} M_{\mathrm{sq},l'_j-l_i-k} \tag{5.27}$$

whereas each matrix element is given by [25]

$$M_{\mathrm{sq},l'_j-l_i-k} = \frac{1}{2\pi i}\oint \mathrm{d}z z^{l'_j-l_i-k}(1+h_1 z)^{2N_f}(z+\bar{h}_1)^{2N_f} \tag{5.28}$$

Additionally, we shifted $k \to k-2N_f-1$, brought the integrand into rational form and transformed the integration to a contour integral over the complex unit circle.

The integral (5.28) can be solved by application of Cauchy's residue theorem. The only pole of the integrand lies at $z = 0$ and exists if and only if $l'_j - l_i - k < 0$. Then it is equivalent to the residue at $z = 0$ [27]

$$M_{\mathrm{sq},l'_j-l_i-k} = \frac{1}{(k+l_i-l'_j-1)!}\,\frac{\partial^{k+l_i-l'_j-1}}{\partial z^{k+l_i-l'_j-1}}(1+h_1 z)^{2N_f}(z+\bar{h}_1)^{2N_f}\bigg|_{z=0} \tag{5.29}$$

The derivative can be distributed to each factor with the general product rule and gives

$$M_{\mathrm{sq},l'_j-l_i-k} = \frac{1}{(k+l_i-l'_j-1)!}\sum_{t=0}^{k+l_i-l'_j-1}\binom{k+l_i-l'_j-1}{t}\frac{(2N_f)!}{(2N_f-t)!}\frac{(2N_f)!}{(2N_f-k-l_i+l'_j+1+t)!} \\ h_1^t\,\bar{h}_1^{2N_f-k-l_i+l'_j+1+t} \tag{5.30}$$

If the previous condition is not met, the integral vanishes. Thus, the lower limit of the sum over k in (5.27) becomes finite, as the order of the pole becomes non-positive for each matrix element. To be more precise, due to the l_i's and l'_j's being subsequently decreasing non-negative integers $l_1 > \cdots > l_{N_c} = 0$, $l'_1 > \cdots > l'_{N_c} = 0$ each summand is guaranteed to vanish for $k \leq -l_1$ [18].
Additionally, there exists an upper limit of k, beyond which all summands vanish. Because the derivatives in (5.29) are taken of a polynomial of order $4N_f$, the matrix $\mathbf{M}_{\mathrm{sq}}$ at a given k has only zero entries, if for all choices of i and j the inequality $k + l_i - l'_j - 1 > 4N_f$ holds true. Thus, the sum (5.27) terminates at $k = 4N_f + l'_1 + 1$ and has in total only a finite amount of terms.
All in all, the static quark gauge integral gives

$$f_{\mathrm{sq}} = \sum_{k=-l_1+1}^{4N_f+l'_1+1}\det_{1\leq i,j\leq N_c}\begin{cases} M_{\mathrm{sq},l'_j-l_i-k} & \text{if } k > l'_j - l_i \\ 0 & \text{otherwise}\end{cases} \tag{5.31}$$

Figure 5.1 shows a plot of matrices, where each pair of indices (i, j) corresponds to the static quark gauge integral of the respective representations $f_{\mathrm{sq}}(r_i, r'_j)$ for $N_c = 3$, $N_f = 1$ and $\bar{h}_1 = 0$ at varying values of h_1. The values of the indices correspond to the first 36 representations of SU(3), satisfying $0 \leq p_1, p_2 \leq 5$. Representations are enumerated according to the bijection $i \leftrightarrow 6p_1(r_i) + p_2(r_i) + 1$.

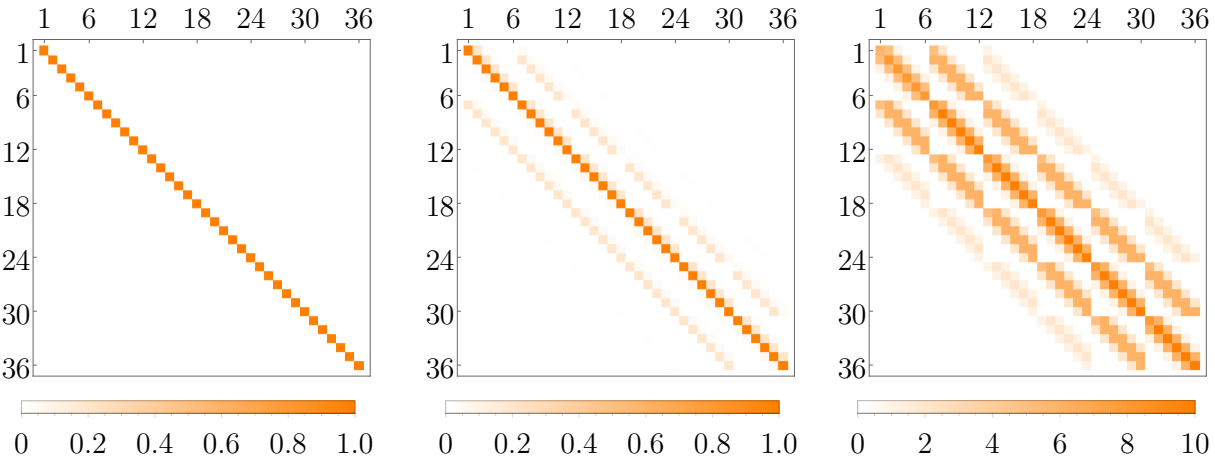

(a) $h_1 = 0$ (b) $h_1 = 1/10$ (c) $h_1 = 1$

Figure 5.1: The heavy quark gauge integral matrix for $N_c = 3$, $N_f = 1$ and $\bar{h}_1 = 0$ for the first 36 representations at varying values of h_1

Figure 5.1 shows the deviation of (5.31) from the pure gauge limit. For vanishing heavy quark couplings ($h_1 = 0$, Figure 5.1a) the heavy quark integral reproduces the orthogonality relation for irreducible characters. At small couplings ($h_1 = 1/10$, Figure 5.1b) deviations from the pure gauge case become apparent, as matrix elements away from the diagonal assume non-zero values. Still, the diagonal is the most protruding feature of the matrix. At high couplings ($h_1 = 1$, Figure 5.1c) many off-diagonal elements are comparable to on-diagonal ones and the matrix has a band structure. Additionally, the matrix elements can become noticeably larger than 1. Here the dynamics of the system can be expected to differ from pure gauge theory [15, 16].

5.3 Leading Order Corrections

5.3.1 The Running Couplings

Considering the leading order corrections in κ to the effective action is the next natural step.
As discussed in the section 4.3, including both the gauge field and kinetic quarks to the theory implies modifications to the coupling constants, e.g. $h_1(\kappa) \to h_1(\kappa, \beta)$ and $h_2(\kappa) \to h_2(\kappa, \beta)$. Even though the corrections have only been derived for lower dimensional representations, e.g. fundamental and anti-fundamental, we include all irreducible representations in the effective gauge action. Deriving similar corrections originating from higher representations is, however, beyond the scope of this thesis [9–11, 21].
We start by using the leading order effective action of kinetic quarks [9]

$$S_2 = h_2 \sum_{\langle x,y \rangle} W^-_{1111}(U_x) W^-_{1111}(U_y), \tag{5.32}$$

split the exponential into product form and expand it to be able to perform the gauge integrals [9–11]

$$\begin{aligned} Z &= c_0^{N_x N_\tau} \int [\mathrm{d}U] \det Q_{\mathrm{stat}} e^{-S_2} \prod_{\langle x,y \rangle} \sum_r \lambda_r \chi_r(U_x) \chi_r(U_y^\dagger) \\ &= c_0^{N_x N_\tau} \int [\mathrm{d}U] \det Q_{\mathrm{stat}} \prod_{x=1}^{N_x} \sum_{r,\alpha} \frac{(-h_2)^\alpha}{\alpha!} \lambda_r \chi_r(U_x) \chi_r(U_{x+1}^\dagger) W^{-,\alpha}_{1111}(U_x) W^{-,\alpha}_{1111}(U_{x+1}) + \mathcal{O}(\kappa^4) \end{aligned} \tag{5.33}$$

Building on the static quark discussion 5.2.1 one can again expect mixed terms between different contributions of the interaction terms. Here, however, this may not only impact the gauge and kinetic quark contributions separately, but may induce a loss of the factorization of both as well [12].
The approach consists of writing the running couplings as a tensor $h^{\alpha\alpha'(n)}_{rr'}$ [12]. The indices correspond to the representations of the gauge interaction and the powers of the node function, respectively,

$$Z_2 = c_0^{N_x N_\tau} \int [\mathrm{d}U]^{(n)} \det Q^{(n)}_{\mathrm{stat}} \prod_{x=1}^{N_x^{(n)}} \sum_{\substack{r,r' \\ \alpha,\alpha'}} h^{\alpha\alpha'(n)}_{rr'} \chi_r(U_x) \chi_{r'}(U_{x+1}^\dagger) W^{-,\alpha}_{1111}(U_x) W^{-,\alpha'}_{1111}(U_{x+1}) \tag{5.34}$$

With (5.3), (5.17) and (5.4) the partition function (5.33) is reproduced to leading order in κ by the boundary condition

$$h^{\alpha\alpha'(0)}_{rr'} = \frac{(-h_2)^\alpha}{\alpha!} \lambda_r \delta_{rr'} \delta_{\alpha\alpha'} \tag{5.35}$$

It implies both the initial factorization of the effective action and the gauge action as well as the resummation to an exponential.
The coarse graining iteration can be performed analogously to the heavy quark discussion 5.2.2 [12]

$$\begin{aligned} Z =& c_0^{N_x N_\tau} \int [\mathrm{d}U]^{(n+1)} \det Q^{(n+1)}_{\mathrm{stat}} \prod_{x=1}^{N_x^{(n)}/2} \sum_{\substack{r_1,r_2 \\ \alpha_1,\alpha_2}} \chi_{r_1}(U_{x-1}) \chi_{r_2}(U_{x+1}^\dagger) W^{-,\alpha_1}_{1111}(U_{x-1}) W^{-,\alpha_2}_{1111}(U_{x+1}) \\ & \sum_{\substack{r_1',r_2' \\ \alpha_1',\alpha_2'}} h^{\alpha_1\alpha_1'(n)}_{r_1 r_1'} h^{\alpha_2'\alpha_2(n)}_{r_2' r 2} \int \mathrm{d}U \det Q^{\mathrm{loc}}_{\mathrm{stat}}(U) \chi_{r_1'}(U^\dagger) \chi_{r_2'}(U) W^{-,\alpha_1'+\alpha_2'}_{1111}(U) \\ \overset{!}{=}& c_0^{N_x N_\tau} \int [\mathrm{d}U]^{(n+1)} \det Q^{(n+1)}_{\mathrm{stat}} \prod_{x=1}^{N_x^{(n+1)}} \sum_{\substack{r_1,r_2 \\ \alpha_1,\alpha_2}} h^{\alpha_1\alpha_2(n+1)}_{r_1 r_2} \chi_{r_1}(U_x) \chi_{r_2}(U_{x+1}^\dagger) W^{-,\alpha_1}_{1111}(U_x) W^{-,\alpha_2}_{1111}(U_{x+1}) \end{aligned} \tag{5.36}$$

Reading of the running couplings from (5.36) we obtain [12]

$$h^{\alpha_1\alpha_2(n+1)}_{r_1 r_2} = \sum_{\substack{r_1',r_2' \\ \alpha_1',\alpha_2'}} h^{\alpha_1\alpha_1'(n)}_{r_1 r_1'} h^{\alpha_2'\alpha_2(n)}_{r_2' r 2} \int \mathrm{d}U \det Q^{\mathrm{loc}}_{\mathrm{stat}}(U) \chi_{r_1'}(U^\dagger) \chi_{r_2'}(U) W^{-,\alpha_1'+\alpha_2'}_{1111}(U) \tag{5.37}$$

The gauge integral induces the occurring coupling between powers of node functions and the gauge action.

5.3.2 The Leading Order Gauge Integral

To solve the gauge integral from (5.37)

$$f_2(r,r',\alpha) = \int \mathrm{d}U \det Q^{\mathrm{loc}}_{\mathrm{stat}}(U)\chi_r(U^\dagger)\chi_{r'}(U)W^{-,\alpha}_{1111}(U) \tag{5.38}$$

steps analogously to section 5.2.3 are performed. Additionally, the node function has to be expressed in terms of the $z_1,\dots,z_{N_c}$ [24]

$$W^{-}_{1111} = \sum_{t=1}^{N_c}\left(\frac{h_1 z_t}{1+h_1 z_t} - \frac{\bar{h}_1 z_t^{-1}}{1+\bar{h}_1 z_t^{-1}}\right) \tag{5.39}$$

$$W^{-,\alpha}_{1111} = \sum_{m_1\dots m_{N_c}} \delta\left(\sum_{t=1}^{N_c} m_t,\alpha\right)\binom{\alpha}{m_1,\dots,m_{N_c}}\prod_{t=1}^{N_c}\left(\frac{h_1 z_t}{1+h_1 z_t} - \frac{\bar{h}_1 z_t^{-1}}{1+\bar{h}_1 z_t^{-1}}\right)^{m_t} \tag{5.40}$$

whereas powers of the node function are obtained with the multinomial theorem.
To bring (5.40) into factorizing form the Kronecker delta is substituted with

$$\delta\left(\sum_{t=1}^{N_c} m_t,\alpha\right) = \frac{1}{K}\sum_{u=1}^{K} e^{2\pi i(\sum_{t=1}^{N_c} m_t-\alpha)u/K} \tag{5.41}$$

Choosing K, however, is not arbitrary, because the right hand side of (5.58) does not vanish, if and only if $\sum_{t=1}^{N_c} m_t-\alpha_n$ is divisible by K instead of just $\sum_{t=1}^{N_c} m_t-\alpha=0$. As this sum is bounded by $0\le|\sum_{t=1}^{N_c} m_t-\alpha|\le(N_c-1)\alpha$, the smallest sufficient choice of K is given by $K=(N_c-1)\alpha+1$.
With (5.22)-(5.25) and (5.40) the leading order gauge integral (5.38) reads after shifting $k\to k-2N_f$ [25]

$$f_2 = \frac{\alpha!}{K}\sum_{k=-\infty}^{\infty}\sum_{u=1}^{K}\exp\left(-2\pi i\frac{\alpha u}{K}\right)\det_{1\le i,j\le N_c} M_{2,l'_j-l_i-k}(\alpha) \tag{5.42}$$

$$\begin{aligned} M_{2,l'_j-l_i-k}(\alpha) = &\sum_{m=0}^{\alpha}\frac{1}{m!}\exp\left(2\pi i\frac{mu}{K}\right)\frac{1}{2\pi i}\oint \mathrm{d}z z^{l'_j-l_i-k}\left(1+h_1 z\right)^{2N_f-m}\left(z+\bar{h}_1\right)^{2N_f-m} \\ &\left(h_1 z(z+\bar{h}_1)-\bar{h}_1(1+h_1 z)\right)^m \end{aligned} \tag{5.43}$$

The complex integration is performed again with Cauchy's residue theorem [27]. Because the effective kinetic quark action is valid to leading order in the hopping parameter, we assume that the expansion of the exponential in section 5.3 was done to the same accuracy. Thus, the highest possible value of α is $2\le 2N_f$ and, likewise to the static quark limit, a pole exists only at $z=0$. The general case will be of interest in section 5.4.
The calculation of the residue is simplified by expanding the last factor in (5.43). Then, because of the equivalent pole structure to the static quark limit the result from section 5.2.3 can be reused [27]

$$\begin{aligned} M_{2,l'_j-l_i-k}(\alpha) = &\sum_{m=0}^{\alpha}\frac{1}{m!}\exp\left(2\pi i\frac{mu}{K}\right)\sum_{v=0}^{m}\binom{m}{v}h_1^v(-\bar{h}_1)^{m-v} \\ &\frac{1}{2\pi i}\oint \mathrm{d}z z^{l'_j-l_i-k+m-v}\left(1+h_1 z\right)^{2N_f+v}\left(z+\bar{h}_1\right)^{2N_f+m-v} \\ = &\sum_{m=0}^{\alpha}\frac{1}{m!}\exp\left(2\pi i\frac{mu}{K}\right)\sum_{v=0}^{m}\binom{m}{v}h_1^v(-\bar{h}_1)^{m-v}\sum_{t=0}^{k+l_i-l'_j-m+v-1}\frac{1}{(k+l_i-l'_j-m+v-1)!} \\ &\binom{k+l_i-l'_j-m+v-1}{t}(2N_f+v)_t\,(2N_f+m-v)_{k+l_i-l'_j-m+v-1-t}\,h_1^t\bar{h}_1^{2N_f+v-k-l_i+l'_j+1+t} \end{aligned} \tag{5.44}$$

For brevity we exploit the convention, that the sum over t vanishes if its upper limit is smaller than the lower limit, even if its terms are mathematically ill-defined.
In case all terms of the m-summation are zero, the matrix element is zero as well. Because the order of the pole is reduced for increasing m, the lower limit of the k-summation receives no adjustments compared to section

5.2.3. In the integrand of (5.43) varying m does not lead to a change of the order of the polynomial. Thus, the upper limit of the k-summation remains unchanged as well.
The leading order gauge integral reads together with (5.44)

$$f_2 = \frac{\alpha!}{K} \sum_{k=-l_1+1}^{4N_f+l_1'+1} \sum_{u=1}^{K} \exp\left(-2\pi i \frac{\alpha u}{K}\right) \det_{1\le i,j\le N_c} M_{2,l_j'-l_i-k}(\alpha) \tag{5.45}$$

The low amount of adjustments necessary from the heavy quark integral (5.31) is due to the fact that the static determinant enters in the denominator of the node function, but cancels with the determinant from the effective action. At powers $\alpha \geq 2N_f$, e.g. when expanding the effective action to higher order than $\mathcal{O}(\kappa^2)$,this is not guaranteed anymore if the amount of flavors N_f is not chosen appropriately [10, 11]. This may lead to further contributions in the gauge integral. However, this is subject in section 5.4.3 in context of a more general gauge integral.

5.4 Next to Leading Order Corrections

Fourth order corrections in κ to the effective action provide the next increase in accuracy of the theory. To this order the effective kinetic quark action can be found in [9]. For brevity we write it as

$$S_4 =: \sum_x S_4^{\text{loc}}(U_x, U_{x+1}, U_{x+2}) \tag{5.46}$$

To prepare the corresponding partition function we start with the same steps in section 5.3 by bringing the exponential into product form and expanding it [9–11]

$$\begin{aligned} Z &= c_0^{N_x N_\tau} \int [\mathrm{d}U] \det Q_{\text{stat}} e^{-S_4} \prod_{\langle x,y\rangle} \sum_r \lambda_r \chi_r(U_x)\chi_r(U_y^\dagger) + \mathcal{O}(\kappa^6) \\ &= c_0^{N_x N_\tau} \int [\mathrm{d}U] \det Q_{\text{stat}} \prod_{x=1}^{N_x} \sum_r \lambda_r \chi_r(U_x)\chi_r(U_{x+1}^\dagger) \left(1 - S_4^{\text{loc}}(U_x, U_{x+1}, U_{x+2}) + \frac{h_2^2}{2} W_{1111}^{-,2}(U_x) W_{1111}^{-,2}(U_{x+1})\right) \\ &\quad + \mathcal{O}(\kappa^6) \end{aligned} \tag{5.47}$$

Here, however, the discussion is restricted to an expansion to $\mathcal{O}(\kappa^4)$, because of both the high amount of terms appearing at higher orders and the accuracy of the action being equivalent to that order. Higher orders of the resummed action can be implemented analogously.

5.4.1 Modifications to the Integration Scheme

Including the kinetic determinant to this order implies more node functions and next to nearest neighbor interactions. In the context of the 1D Ising model long range couplings have been found to create complications with the integration scheme previously used. Simply summing up every second spin does not lead to a recursion scheme anymore. Instead the form of the action is lost after the first iteration [15].
As generating recursion schemes was possible for nearest neighbor interactions, we transform long range couplings to effectively short range by considering the interactions between two neighboring pairs of lattice sites [15]

$$\begin{aligned} Z =& c_0^{N_x N_\tau} \int [\mathrm{d}U] \det Q_{\text{stat}} \prod_{\substack{x=1 \\ x \bmod 2 = 0}}^{N_x} \sum_{r_{x-1}} \lambda_{r_{x-1}} \chi_{r_{x-1}}(U_{x-1}) \chi_r(U_x^\dagger) \sum_{r_x} \lambda_{r_x} \chi_{r_x}(U_x) \chi_r(U_{x+1}^\dagger) \\ & \left(1 - S_{\text{eff},\kappa^4}^{\text{loc}}(U_{x-1}, U_x, U_{x+1}) + \frac{h_2^2}{2} W_{1111}^-(U_{x-1}) W_{1111}^-(U_x)\right) \\ & \left(1 - S_{\text{eff},\kappa^4}^{\text{loc}}(U_x, U_{x+1}, U_{x+2}) + \frac{h_2^2}{2} W_{1111}^-(U_x) W_{1111}^-(U_{x+1})\right) + \mathcal{O}(\kappa^6) \\ =:& c_0^{N_x N_\tau} \int [\mathrm{d}U] \det Q_{\text{stat}} \prod_{\substack{x=1 \\ x \bmod 2 = 0}}^{N_x} A(U_{x-1}, U_x, U_{x+1}, U_{x+2}) + \mathcal{O}(\kappa^6) \end{aligned} \tag{5.48}$$

The quantity A now describes the interaction between the pairs (U_{x-1}, U_x) and (U_{x+1}, U_{x+2}) and only nearest neighbor interactions occur between them. Therefore, the interaction length is reduced effectively. The integration scheme is then given by integrating over every second pair instead of every second lattice site [15].
As we noticed in the previous sections, the recursion schemes generate all possible mixtures between different parts of the action in a non-trivial way. Here this leads to a loss of the factorization between the two constituents of the pairs and thus to a large amount of terms in the interaction [12].

5.4.2 Obtaining the Running Couplings

Analogously to the previous sections we will express the renormalization scheme in terms of a coupling tensor $h^{r_1 r_2 r_3 r_4 (n)}_{a_1 a_2 a_3 a_4}$ that realizes the mixture of all possible terms, e.g. it describes mixed terms between different representations, the node functions and combinations thereof [12].
To characterize all possible couplings we need to investigate the effective pair interaction A. Because it is a product of expanded parts of the effective kinetic quark action, products of node functions depending on the same gauge variable appear [15]. We denote those contributions by $W_v(U)$, where v is a set of node functions and their respective powers

$$W_v(U) = \prod_{(ab\bar{a}\bar{b},\alpha)\in v} W^{\alpha}_{ab\bar{a}\bar{b}}(U) \tag{5.49}$$

Examples to this are $v = \{(0000, 0)\}$, which describes a constant and $v = \{(1100, 3), (0011, 2)\}$ corresponding to $W_v = W^3_{1100} W^2_{0011}$. Hereinafter, the W_v's are referred to as compound node functions.
With the newly introduced entity we can express the pair interaction A in terms of some to be specified coupling tensor $h_{v_1 v_2 v_3 v_4}$ [15]

$$A(U_{x-1}, U_x, U_{x+1}, U_{x+2}) \overset{!}{=} \sum_{v_1,v_2,v_3,v_4} h_{v_1 v_2 v_3 v_4} W_{v_1}(U_{x-1}) W_{v_1}(U_x) W_{v_2}(U_{x+1}) W_{v_3}(U_{x+2}) \tag{5.50}$$

To fully reproduce the partition function to next to leading order (5.48) all compound node functions appearing in A have to be identified for each gauge variable $U_{x-1}, \ldots, U_{x+2}$, respectively. In appendix B the possible values for each index $v_1, \ldots, v_4$ are listed and the respective amounts of compound node functions are given in table 5.1.

Index	v_1	v_2	v_3	v_4
Number of compound node functions	12	72	28	4

Table 5.1: The amount of compound node functions needed for each index $v_1, \ldots, v_4$ to reproduce the next to leading order partition function (5.48)

Because renormalization typically realizes all possible combinations of interactions, a total of $12 \cdot 72 \cdot 28 \cdot 4 = 96768$ terms has to be allowed by the running couplings, even though most of the $h_{v_1 v_2 v_3 v_4}$ vanish. By including N_{g} representations of the gauge action this number is increased to $96768 N_g^4$ [12].
To capture the coupling between the gauge action and kinetic quark action the approach reads [12]

$$\begin{aligned} Z_4 =& c_0^{N_x N_\tau} \int [\mathrm{d}U]^{(n)} \det Q^{(n)}_{\mathrm{stat}} \prod_{\substack{x=1 \\ x \bmod 2 = 0}}^{N_x^{(n)}} \sum_{\substack{v_1,v_2,v_3,v_4 \\ r_1,r_2,r_3,r_4}} h^{r_1 r_2 r_3 r_4 (n)}_{v_1 v_2 v_3 v_4} \chi_{r_1}(U_{x-1}) \chi_{r_2}(U_x^\dagger) \chi_{r_3}(U_x) \chi_{r_4}(U_{x+1}^\dagger) \\ & W_{v_1}(U_{x-1}) W_{v_2}(U_x) W_{v_3}(U_{x+1}) W_{v_4}(U_{x+2}) \end{aligned} \tag{5.51}$$

The boundary condition reads

$$h^{r_1 r_2 r_3 r_4 (0)}_{v_1 v_2 v_3 v_4} = h_{v_1 v_2 v_3 v_4} \lambda_{r_1} \delta_{r_1 r_2} \lambda_{r_3} \delta_{r_3 r_4} \tag{5.52}$$

The values of $h_{v_1 v_2 v_3 v_4}$ can be obtained by using (5.50) with the list of compound node functions in appendix B.

Now the coarse graining iteration can be performed to obtain the running couplings analogously to the previous sections

$$\begin{aligned}
Z_4 =& c_0^{N_x N_\tau} \int [\mathrm{d}U]^{(n)} \det Q_{\mathrm{stat}}^{(n)} \prod_{\substack{x=1 \\ x \bmod 4=0}}^{N_x^{(n)}} \Bigg(\sum_{\substack{v_1,v_2,v_3',v_4' \\ r_1,r_2,r_3,r_4'}} h_{v_1 v_2 v_3' v_4'}^{r_1 r_2 r_3 r_4'(n)} \chi_{r_1}(U_{x-1}) \chi_{r_2}(U_x^\dagger) \chi_{r_3}(U_x) \chi_{r_4'}(U_{x+1}^\dagger) \\
& W_{v_1}(U_{x-1}) W_{v_2}(U_x) W_{v_3'}(U_{x+1}) W_{v_4'}(U_{x+2}) \Bigg) \Bigg(\sum_{\substack{v_1',v_2',v_3,v_4 \\ r_1',r_2',r_3',r_4}} h_{v_1' v_2' v_3 v_4}^{r_1' r_2' r_3' r_4(n)} \chi_{r_1'}(U_{x+1}) \chi_{r_2'}(U_{x+2}^\dagger) \chi_{r_3'}(U_{x+2}) \chi_{r_4}(U_{x+3}^\dagger) \\
& W_{v_1'}(U_{x+1}) W_{v_2'}(U_{x+2}) W_{v_3}(U_{x+3}) W_{v_4}(U_{x+4}) \Bigg) \\
=& c_0^{N_x N_\tau} \int [\mathrm{d}U]^{(n+1)} \det Q_{\mathrm{stat}}^{(n+1)} \prod_{\substack{x=1 \\ x \bmod 2=0}}^{N_x^{(n)}/2} \sum_{\substack{v_1,v_2,v_3,v_4 \\ r_1,r_2,r_3,r_4}} \chi_{r_1}(U_{x-1}) \chi_{r_2}(U_x^\dagger) \chi_{r_3}(U_x) \chi_{r_4}(U_{x+1}^\dagger) W_{v_1}(U_{x-1}) W_{v_2}(U_x) \\
& W_{v_3}(U_{x+1}) W_{v_4}(U_{x+2}) \sum_{\substack{v_1',v_2',v_3',v_4' \\ r_1',r_2',r_3',r_4'}} h_{v_1 v_2 v_3' v_4'}^{r_1 r_2 r_3 r_4'(n)} h_{v_1' v_2' v_3 v_4}^{r_1' r_2' r_3' r_4(n)} \left(\int \mathrm{d}U \det Q_{\mathrm{stat}}^{\mathrm{loc}} W_{v_1'}(U) W_{v_3'}(U) \chi_{r_4'}(U^\dagger) \chi_{r_1'}(U) \right) \\
& \left(\int \mathrm{d}U \det Q_{\mathrm{stat}}^{\mathrm{loc}} W_{v_2'}(U) W_{v_4'}(U) \chi_{r_2'}(U^\dagger) \chi_{r_3'}(U) \right) \\
\overset{!}{=}& c_0^{N_x N_\tau} \int [\mathrm{d}U]^{(n+1)} \det Q_{\mathrm{stat}}^{(n+1)} \prod_{\substack{x=1 \\ x \bmod 2=0}}^{N_x^{(n+1)}} \sum_{\substack{v_1,v_2,v_3,v_4 \\ r_1,r_2,r_3,r_4}} h_{v_1 v_2 v_3 v_4}^{r_1 r_2 r_3 r_4(n+1)} \chi_{r_1}(U_{x-1}) \chi_{r_2}(U_x^\dagger) \chi_{r_3}(U_x) \chi_{r_4}(U_{x+1}^\dagger) \\
& W_{v_1}(U_{x-1}) W_{v_2}(U_x) W_{v_3}(U_{x+1}) W_{v_4}(U_{x+2}) \qquad (5.53)
\end{aligned}$$

The running couplings now read

$$\begin{aligned}
h_{v_1 v_2 v_3 v_4}^{r_1 r_2 r_3 r_4(n+1)} = & \sum_{\substack{v_1',v_2',v_3',v_4' \\ r_1',r_2',r_3',r_4'}} h_{v_1 v_2 v_3' v_4'}^{r_1 r_2 r_3 r_4'(n)} h_{v_1' v_2' v_3 v_4}^{r_1' r_2' r_3' r_4(n)} \left(\int \mathrm{d}U \det Q_{\mathrm{stat}}^{\mathrm{loc}}(U) W_{v_1'}(U) W_{v_3'}(U) \chi_{r_4'}(U^\dagger) \chi_{r_1'}(U) \right) \\
& \left(\int \mathrm{d}U \det Q_{\mathrm{stat}}^{\mathrm{loc}}(U) W_{v_2'}(U) W_{v_4'}(U) \chi_{r_2'}(U^\dagger) \chi_{r_3'}(U) \right) \qquad (5.54)
\end{aligned}$$

Together both gauge integrals couple the interactions between pairs of lattice sites.

5.4.3 The Gauge Node Integral

By using the appearing compound node functions listed in appendix B one can find 188 distinct gauge integrals appearing in (5.54), if the gauge action is disregarded. By using the commutativity of the characters this number increases to $188 N_g(N_g+1)/2$, if N_g irreducible representations are included.
At this order of the effective action one can find integrals, that involve high powers of node functions, e.g. over $\det Q_{\mathrm{stat}}^{\mathrm{loc}} W_{1100}^5$, from appendix B. In contrast to section 5.3.2 we are therefore not able to exclude additional residues for arbitrary N_f [10, 11].
To cope with the large amount of integrals and to provide a general solution to them in hindsight of section 5.5 we consider the function [24]

$$f_{\kappa^4}\left(r, r', \begin{pmatrix} \alpha_1 \\ \vdots \\ \alpha_N \end{pmatrix}, \begin{pmatrix} a_1 \\ \vdots \\ a_N \end{pmatrix}, \begin{pmatrix} b_1 \\ \vdots \\ b_N \end{pmatrix}, \begin{pmatrix} \bar{a}_1 \\ \vdots \\ \bar{a}_N \end{pmatrix}, \begin{pmatrix} \bar{b}_1 \\ \vdots \\ \bar{b}_N \end{pmatrix} \right) = \int \mathrm{d}U \det Q_{\mathrm{stat}}^{\mathrm{loc}} \chi_r^\dagger(U) \chi_{r'}(U) \prod_{i=1}^{N} W_{a_i b_i \bar{a}_i \bar{b}_i}^{\alpha_i}(U) \qquad (5.55)$$

Performing the steps from the previous cases analogously one obtains [18, 24, 25]

$$\begin{aligned} f_4 =& \frac{1}{(2\pi i)^{N_c}} \sum_{k=-\infty}^{\infty} \int \mathrm{d}z_1 \dots \mathrm{d}z_{N_c} z_1^{k-1} \dots z_{N_c}^{k-1} \begin{vmatrix} z_1^{-l_1} & \dots & z_{N_c}^{-l_1} \\ \vdots & & \vdots \\ z_1^{-l_{N_c}} & \dots & z_{N_c}^{-l_{N_c}} \end{vmatrix} \begin{vmatrix} z_1^{l'_1} & \dots & z_{N_c}^{l'_1} \\ \vdots & & \vdots \\ z_1^{l'_{N_c}} & \dots & z_{N_c}^{l'_{N_c}} \end{vmatrix} \\ & \left(1 + h_1 z_1\right)^{2N_f} \left(1 + \bar{h}_1 \frac{1}{z_1}\right)^{2N_f} \dots \left(1 + h_1 z_{N_c}\right)^{2N_f} \left(1 + \bar{h}_1 \frac{1}{z_{N_c}}\right)^{2N_f} \\ & \prod_{n=1}^{N} \left[\sum_{m=1}^{N_c} h_1^{a_n} \bar{h}_1^{\bar{a}_n} \frac{z_m^{a_n - \bar{a}_n}}{\left(1 + h_1 z_m\right)^{b_n} \left(1 + \bar{h}_1 \frac{1}{z_m}\right)^{\bar{b}_n}} \right]^{\alpha_n} \end{aligned} \tag{5.56}$$

To obtain a similar expression of the integral as in the previous cases the last product has to be brought into a form factorizing with regards to the integration variables. Again this can be done using the multinomial theorem [24, 25]

$$\begin{aligned} \left[\sum_{m=1}^{N_c} h_1^{a_n} \bar{h}_1^{\bar{a}_n} \frac{z_m^{a_n - \bar{a}_n}}{\left(1 + h_1 z_m\right)^{b_n} \left(1 + \bar{h}_1 \frac{1}{z_m}\right)^{\bar{b}_n}} \right]^{\alpha_n} =& \sum_{m_{1n}=0}^{\alpha_n} \dots \sum_{m_{N_c n}=0}^{\alpha_n} \binom{\alpha_n}{m_{1n}, \dots, m_{N_c n}} \delta\left(\sum_{t=1}^{N_c} m_{tn}, \alpha_n \right) \\ & \prod_{t=1}^{N_c} h_1^{a_n m_{tn}} \bar{h}_1^{\bar{a}_n m_{tn}} \left(1 + h_1 z_t\right)^{-b_n m_{tn}} \left(1 + \bar{h}_1 \frac{1}{z_t}\right)^{-\bar{b}_n m_{tn}} \end{aligned} \tag{5.57}$$

Likewise to the leading order discussion section section 5.3.2 to decouple the summations over the $m_{1n}, \dots, m_{N_c n}$ the Kronecker delta is substituted with

$$\delta\left(\sum_{t=1}^{N_c} m_{tn}, \alpha_n \right) = \frac{1}{K_n} \sum_{u_n=1}^{K_n} e^{2\pi i (\sum_{t=1}^{N_c} m_{tn} - \alpha_n) u_n / K_n} \tag{5.58}$$

Choosing K_n now depends on each power α_n, respectively. Following the same arguments from section 5.3.2 yields $K_n = (N_c - 1)\alpha_n + 1$.
By plugging (5.57) and (5.58) into (5.56) and re-expressing the determinants, the integrals are decoupled [25]

$$\begin{aligned} f_4 =& \frac{\alpha_1! \dots \alpha_N!}{K_1 \dots K_N} \sum_{k=-\infty}^{\infty} \sum_{u_1=1}^{K_1} \dots \sum_{u_N=1}^{K_N} \sum_{i_1,\dots,i_{N_c}} \sum_{j_1,\dots,j_{N_c}} \exp\left(-2\pi i \sum_{n=1}^{N} \alpha_n u_n / K_n \right) \epsilon_{i_1,\dots,i_{N_c}} \epsilon_{j_1,\dots,j_{N_c}} \prod_{t=1}^{N_c} \\ & \sum_{m_{t1}=0}^{\alpha_1} \dots \sum_{m_{tN}=0}^{\alpha_N} \frac{1}{m_{t1}! \dots m_{tN}!} \exp\left(2\pi i \sum_{n=1}^{N} m_{tn} u_n / K_n \right) h_1^{\sum_{n=1}^{N} a_n m_{tn}} \bar{h}_1^{\sum_{n=1}^{N} \bar{a}_n m_{tn}} \\ & \frac{1}{2\pi i} \int \mathrm{d}z_t z_t^{l'_{j_t} - l_{i_t} + k - 1 - 2N_f + \sum_{n=1}^{N} (a_n - \bar{a}_n) m_{tn}} \left(1 + h_1 z_t\right)^{-\left(\sum_{n=1}^{N} b_n m_{tn} - 2N_f\right)} \left(1 + \bar{h}_1 \frac{1}{z_t}\right)^{-\left(\sum_{n=1}^{N} \bar{b}_n m_{tn} - 2N_f\right)} \end{aligned} \tag{5.59}$$

Again the sums over $i_1 \dots i_{N_c}$ and $j_1 \dots j_{N_c}$ can be collected as the determinant of a matrix $\mathbf{M_4}$ [25]

$$f_4 = \frac{\alpha_1! \dots \alpha_N!}{K_1 \dots K_N} \sum_{k=-\infty}^{\infty} \sum_{u_1=1}^{K_1} \dots \sum_{u_N=1}^{K_N} \exp\left(-2\pi i \sum_{n=1}^{N} \alpha_n u_n / K_n \right) \det_{1 \le i,j \le N_c} M_{4, l'_j - l_i + k} \tag{5.60}$$

with $M_{4,l'_j - l_i + k}$ in rational form given as

$$\begin{aligned} M_{4,l'_j - l_i + k} =& \sum_{m_1=0}^{\alpha_1} \dots \sum_{m_N=0}^{\alpha_N} \frac{1}{m_1! \dots m_N!} \exp\left(2\pi i \sum_{n=1}^{N} m_n u_n / K_n \right) h_1^{\sum_{n=1}^{N} (a_n - b_n) m_n + 2} \bar{h}_1^{\sum_{n=1}^{N} \bar{a}_n m_n} \\ & \frac{1}{2\pi i} \oint \mathrm{d}z z^{l'_j - l_i + k - 1 - 2N_f + \sum_{n=1}^{N} (a_n - \bar{a}_n + \bar{b}_n) m_n} \left(z + \frac{1}{h_1}\right)^{-\left(\sum_{n=1}^{N} b_n m_n - 2N_f\right)} \left(z + \bar{h}_1\right)^{-\left(\sum_{n=1}^{N} \bar{b}_n m_n - 2N_f\right)} \end{aligned} \tag{5.61}$$

Application of Cauchy's residue theorem then leads to the final result for the matrix $\mathbf{M_4}$. Since the integrand is already in rational form, both the poles and their respective order can be readily read of and are listed in table 5.2 [27].

Pole at z =	Order
0	$-(l'_j - l_i + k - 1 - 2N_f + \sum_{n=1}^{N}(a_n - \bar{a}_n + \bar{b}_n)m_n)$
$-\frac{1}{h_1}$	$\sum_{n=1}^{N} b_n m_n - 2N_f$
$-\bar{h}_1$	$\sum_{n=1}^{N} \bar{b}_n m_n - 2N_f$

Table 5.2: Poles and their respective orders in the gauge node integral

Note that the poles only contribute if their position lies inside the complex unit circle and their order is positive. The last two poles show a competition between the static determinant and the node functions. This results in a piecewise expression for $\mathbf{M_4}$. To shorten the notation this behavior is captured by introducing a piecewise operator $B\big(g(x)\big)$, taking a Boolean condition $g(x)$ and acting on some function $f(x)$ as [27]

$$B\big(g(x)\big)f(x) := \begin{cases} f(x) & \text{if } g(x) \text{ is true} \\ 0 & \text{if } g(x) \text{ is false} \end{cases} \tag{5.62}$$

As an example the expression $B(n > 0)\frac{1}{(n-1)!}$ is well defined for all integers n.
The procedure is illustrated on calculating the residue at $z = -\frac{1}{h_1}$. In the following, the integrand in (5.61) is denoted as $f(z)$, whereas the order of the pole is denoted as g. Its residue at this pole can be calculated as [27]

$$\mathrm{Res}_{-\frac{1}{h_1}} f = B\left(g > 0 \wedge h_1 > 1\right) \frac{1}{(g-1)!} \frac{\partial^{g-1}}{\partial z^{g-1}} \left(z + \frac{1}{h_1}\right)^g f(z)\bigg|_{z=-\frac{1}{h_1}} \tag{5.63}$$

The derivatives of the product can be distributed to each factor quickly with the general product rule

$$\begin{aligned} \mathrm{Res}_{-\frac{1}{h_1}} f =& B\left(g > 0 \wedge h_1 > 1\right) \frac{1}{(g-1)!} \sum_{t=1}^{g-1} \binom{g-1}{t} \left[\frac{\partial^t}{\partial z^t} z^{l'_j - l_i + k - 1 - 2N_f + \sum_{n=1}^{N}(a_n - \bar{a}_n + \bar{b}_n)m_n}\right] \\ & \left[\frac{\partial^{g-1-t}}{\partial z^{g-1-t}} \left(z + \bar{h}_1\right)^{-\left(\sum_{n=1}^{N} \bar{b}_n m_n - 2N_f\right)}\right] \Bigg|_{z=-\frac{1}{h_1}} \end{aligned} \tag{5.64}$$

For each factor the derivative can be expressed by falling factorials $(x)_y = x \cdot (x-1) \cdot \ldots \cdot (x-y+1)$. Afterwards, $z = -\frac{1}{h_1}$ is applied [27]

$$\begin{aligned} \mathrm{Res}_{-\frac{1}{h_1}} f =& B\left(g > 0 \wedge h_1 > 1\right) \frac{1}{(g-1)!} \sum_{t=0}^{g-1} \binom{g-1}{t} \left(l'_j - l_i + k - 1 - 2N_f + \sum_{n=1}^{N}(a_n - \bar{a}_n + \bar{b}_n)m_n\right)_t \\ & \left(-\frac{1}{h_1}\right)^{l'_j - l_i + k - 1 - 2N_f + \sum_{n=1}^{N}(a_n - \bar{a}_n + \bar{b}_n)m_n - t} \left(-\sum_{n=1}^{N} \bar{b}_n m_n + 2\right)_{g-1-t} \left(\bar{h}_1 - \frac{1}{h_1}\right)^{-\left(\sum_{n=1}^{N} \bar{b}_n m_n - 2 + g - 1 - t\right)} \end{aligned} \tag{5.65}$$

Due to its length the final expression for $M_{4,l'_j - l_i + k}$ is given in appendix A.
Note that the order of the pole at $z = 0$ depends on k. Because this index runs from $-\infty$ to ∞, having another sum depend on it may render computations inefficient. Analogously to the previous cases, this can be restricted by exploiting a symmetry of $\mathbf{M_4}$. Substituting the contour of the integral from counterclockwise to clockwise integration and back [27]

$$\oint \mathrm{d}z f(z) \to i \int_{-\pi}^{\pi} \mathrm{d}\phi e^{i\phi} f(e^{i\phi}) \to -i \int_{\pi}^{-\pi} \mathrm{d}\phi e^{-i\phi} f(e^{-i\phi}) \to \oint \mathrm{d}z z^{-2} f\left(\frac{1}{z}\right) \tag{5.66}$$

as well as transforming the integrand back into rational form gives

$$M_{4,l'_j-l_i+k} = \sum_{m_1=0}^{\alpha_1} \cdots \sum_{m_N=0}^{\alpha_N} \frac{1}{m_1! \dots m_N!} \exp\left(2\pi i \sum_{n=1}^{N} m_n u_n / K_n\right) \bar{h}_1^{\sum_{n=1}^{N}(\bar{a}_n - \bar{b}_n)m_n + 2} h_1^{\sum_{n=1}^{N} a_n m_n}$$
$$\frac{1}{2\pi i} \oint \mathrm{d}z z^{-l'_j + l_i - k - 1 - 2N_f + \sum_{n=1}^{N}(\bar{a}_n - a_n + b_n)m_n} \left(z + \frac{1}{\bar{h}_1}\right)^{-\left(\sum_{n=1}^{N} \bar{b}_n m_n - 2N_f\right)} \left(z + h_1\right)^{-\left(\sum_{n=1}^{N} b_n m_n - 2N_f\right)} \tag{5.67}$$

Comparing (5.61) to (5.67) $\mathbf{M_4}$ is found to be symmetric under the simultaneous exchange of

$$l'_j - l_i + k \leftrightarrow -(l'_j - l_i + k), \begin{pmatrix} a \\ \vdots \\ a_N \end{pmatrix} \leftrightarrow \begin{pmatrix} \bar{a} \\ \vdots \\ \bar{a}_N \end{pmatrix}, \begin{pmatrix} b \\ \vdots \\ b_N \end{pmatrix} \leftrightarrow \begin{pmatrix} \bar{b} \\ \vdots \\ \bar{b}_N \end{pmatrix}, h_1 \leftrightarrow \bar{h}_1 \tag{5.68}$$

This then leads to an altered pole structure as shown in table 5.3 [27].

Pole at z =	Order
0	$l'_j - l_i + k + 1 + 2N_f - \sum_{n=1}^{N}(\bar{a}_n - a_n + b_n)m_n$
$-\frac{1}{\bar{h}_1}$	$\sum_{n=1}^{N} \bar{b}_n m_n - 2N_f$
$-h_1$	$\sum_{n=1}^{N} b_n m_n - 2N_f$

Table 5.3: Poles and their respective orders after applying the symmetry transformation

For any node function in the effective action the indices satisfy $a_n \leq b_n$ and $\bar{a}_n \leq \bar{b}_n$. Therefore, the order of the $z = 0$ pole is in both cases (table 5.2 and 5.3) reduced by compound node functions. Further, in a single matrix element M_{4,l'_j-l_i+k} this pole may not contribute, if [9–11]

$$l'_j - l_i + k \geq 2N_f + 1 \qquad \text{in equation (5.61)}, \tag{5.69}$$
$$l'_j - l_i + k \leq -2N_f - 1 \qquad \text{in equation (5.67)} \tag{5.70}$$

Therefore, the interval of k containing poles at $z = 0$ in (5.61) can be reduced to $-2N_f \leq l'_j - l_i + k \leq 2N_f$ by exploiting the symmetry (5.68) if (5.69) is not met.
In contrast to the integrals from section 5.2.3 and 5.3 the existence of two more poles in (5.61) interferes with the termination of the infinite sum.
Because of the symmetry relation (5.68), considering only the limit $k \to \infty$ is sufficient to determine how fast the sum converges. For this case only the residues at $z \neq 0$ contribute and all terms in the matrix elements are proportional to $\bar{h}_1^k$ if $\bar{h}_1 < 1$ or to h_1^{-k}, if $h_1 > 1$. Therefore the elements of $\mathbf{M_4}$ are suppressed exponentially in k.

5.5 Renormalization Beyond Next to Leading Order Corrections

The pattern observed when going from leading to next to leading order can be generalized to arbitrary order $\mathcal{O}(\kappa^{2N_\kappa})$ by assuming that the effective kinetic quark action can be written in general as

$$S_{2N_\kappa} = \sum_{n_\kappa=1}^{N_\kappa} \sum_{x} S^{\mathrm{loc}}_{n_\kappa}(U_x, \dots, U_{x+n_\kappa}) = \sum_{n_\kappa=1}^{N_\kappa} \sum_{x} \sum_{q_0,\dots,q_{n_\kappa}} s_{q_0,\dots,q_{n_\kappa}} \prod_{i=0}^{n_\kappa} W_{q_i}(U_{x+i}) \tag{5.71}$$

This pattern appears because only closed loops with a length of at most $2N_\kappa$[1] are allowed in the kinetic quark determinant [9–11].
Together with the occurring node functions $W_{q_i}(U_{x+i})$ the $s_{q_0\dots,q_{n_\kappa}}$ have to be determined from the derivation of the effective action. In three dimensions it is known up to $\mathcal{O}(\kappa^8)$ [11]. But in our one dimensional system corrections higher than $\mathcal{O}(\kappa^4)$ are yet to be derived. Thus, we are not able to determine the boundary conditions

[1] At most N_κ steps in one direction and N_κ steps back to close the loop

in terms of the quark couplings h_2, h_{3_1}, h_{3_2}, etc. [9]
In discussions of the 3+1D effective theory the number of terms in the effective action has been shown to increase exponentially with its order in κ. Therefore, beyond next to leading order the amount of terms in the compound interaction (5.74) can be expected to increase even further compared to section 5.4.2.
With (5.71) the partition function reads [9–11]

$$Z = c_0^{N_x N_\tau} \int [\mathrm{d}U] \det Q_{\mathrm{stat}} \prod_{x=1}^{N_x} \exp\left(- \sum_{n_\kappa=1}^{N_\kappa} S_{\mathrm{eff},n_\kappa}(U_x, \dots, U_{x+n_\kappa}) \right) \sum_r \lambda_r \chi_r(U_x) \chi_r(U_{x+1}^\dagger) + \mathcal{O}\left(\kappa^{2(N_\kappa+1)}\right) \tag{5.72}$$

Expanding the exponential in κ to order $2N_\kappa$ brings the integrand in the general form

$$Z = c_0^{N_x N_\tau} \int [\mathrm{d}U] \det Q_{\mathrm{stat}} \prod_{x=1}^{N_x} \sum_{v_0,\dots,v_{N_\kappa}} h'_{v_0,\dots,v_{N_\kappa}} \prod_{i=0}^{N_\kappa} W_{v_i}(U_{x+i}) \sum_r \lambda_r \chi_r(U_x) \chi_r(U_{x+1}) + \mathcal{O}\left(\kappa^{2(N_\kappa+1)}\right) \tag{5.73}$$

To reduce the interaction length to effective nearest neighbor interactions the lattice sites are grouped into tuples governing the interaction terms originating from N_κ sites. As each of those terms includes interactions of range N_κ as well, the tuple contains $2N_\kappa$ link variables $A(U_x, \dots, U_{x+2N_\kappa-1})$ with [15]

$$A(U_x, \dots, U_{x+2N_\kappa-1}) = \sum_{v_0,\dots,v_{2N_\kappa-1}} h_{v_0,\dots,v_{2N_\kappa-1}} \left(\prod_{i=0}^{2N_\kappa-1} W_{v_i}(U_{x+i}) \right) \prod_{i=0}^{N_\kappa-1} \sum_r \lambda_r \chi_r(U_{x+i}) \chi_r(U_{x+i+1}^\dagger) \tag{5.74}$$

Using the effective lattice sites A the $\mathcal{O}(\kappa^{2N_\kappa})$ partition function is given by [15]

$$Z_{2N_\kappa} = c_0^{N_x N_\tau} \int [\mathrm{d}U] \det Q_{\mathrm{stat}} \prod_{\substack{x=1 \\ x \bmod N_\kappa = 0}}^{N_x} A(U_x, \dots, U_{x+2N_\kappa-1}) \tag{5.75}$$

The link variables of A can be split into a pair consisting of two sets of N_κ links $(U_x, \dots, U_{x+N_\kappa-1})$ and $(U_{x+N_\kappa}, \dots, U_{x+2N_\kappa-1})$. Between those only nearest neighbor interactions occur effectively [15].
Finding a renormalization scheme now corresponds to finding a recursion relation of the compound interaction $A \to A^{(n)}$. With the intuition from the previous section we want to allow different couplings for all possible combinations of node functions and characters. Thus, we set [12]

$$A^{(n)} = \sum_{\substack{v_0,\dots,v_{2N_\kappa-1} \\ r_0^2, r_1^1, r_1^2, \dots, r_{N_\kappa-1}^1, r_{N_\kappa-1}^2, r_{N_\kappa}^1}} h_{v_0,\dots,v_{2N_\kappa-1}}^{r_0^2, r_1^1, r_1^2, \dots, r_{N_\kappa-1}^1, r_{N_\kappa-1}^2, r_{N_\kappa}^1, (n)} \left(\prod_{i=0}^{2N_\kappa-1} W_{v_i}(U_{x+i}) \right) \prod_{i=0}^{N_\kappa-1} \chi_{r_i^2}(U_{x+i}) \chi_{r_{i+1}^1}(U_{x+i+1}^\dagger) \tag{5.76}$$

With this boundary condition the partition function to order $2N_\kappa$ (5.75) is reproduced

$$h_{v_0,\dots,v_{2N_\kappa-1}}^{r_0^2, r_1^1, r_1^2, \dots, r_{N_\kappa-1}^1, r_{N_\kappa-1}^2, r_{N_\kappa}^1, (0)} = h_{v_0,\dots,v_{2N_\kappa-1}} \prod_{i=0}^{N_\kappa-1} \lambda_{r_i^2} \delta_{r_i^2, r_{i+1}^1} \tag{5.77}$$

The compound interactions now follow the recursion relation [15]

$$\begin{aligned} A^{(n+1)}\Big((U_{x-N_\kappa}, \dots, U_{x-1}), (U_{x+N_\kappa}, \dots, U_{x+2N_\kappa-1}) \Big) = \int \mathrm{d}U_x \dots \mathrm{d}U_{x+N_\kappa-1} \det Q_{\mathrm{stat}}^{\mathrm{loc}}(U_x) \dots \det Q_{\mathrm{stat}}^{\mathrm{loc}}(U_{x+N_\kappa-1}) \\ A^{(n)}\Big((U_{x-N_\kappa}, \dots, U_{x-1}), (U_x, \dots, U_{x+N_\kappa-1}) \Big) A^{(n)}\Big((U_x, \dots, U_{x+N_\kappa-1}), (U_{x+N_\kappa}, \dots, U_{x+2N_\kappa-1}) \Big) \end{aligned} \tag{5.78}$$

from which the running couplings are found to be

$$h^{r_0^2,r_1^1,r_1^2,\ldots,r_{N_\kappa-1}^1,r_{N_\kappa-1}^2,r_{N_\kappa}^1,(n+1)}_{v_0,\ldots,v_{2N_\kappa-1}} = \sum_{\substack{a'_0,\ldots,a'_{2N_\kappa-1} \\ r_0^{'2},r_1^{'1},r_1^{'2},\ldots,r_{N_\kappa-1}^{'1},r_{N_\kappa-1}^{'2},r_{N_\kappa}^{'1}}} h^{r_0^2,r_1^1,r_1^2,\ldots,r_{N_\kappa-1}^1,r_{N_\kappa-1}^2,r_0^{'1},(n)}_{v_0,\ldots,v_{N_\kappa-1},v'_{N_\kappa},\ldots,a'_{2N_\kappa-1}} \left[\prod_{i=0}^{N_\kappa-1}\int \mathrm{d}U \det Q \;\mathrm{stat}\chi_{r_i^1}(U^\dagger)\chi_{r_i^2}(U)W_{v_i}(U)W_{v_{i+N_\kappa}}(U)\right] h^{r_0^{'2},r_1^{'1},r_1^{'2},\ldots,r_{N_\kappa-1}^{'1},r_{N_\kappa-1}^{'2},r_{N_\kappa}^1,(n)}_{a'_0,\ldots,a'_{N_\kappa-1},v_{N_\kappa},\ldots,v_{2N_\kappa-1}} \tag{5.79}$$

For $N_\kappa = 2$ the next to leading order running couplings (5.54) and for $N_\kappa = 1$ the leading order recursion relations are recovered, respectively. Furthermore, for $N_\kappa = 1$ the heavy quark running couplings are obtained by setting $h_2 = 0$, because all relevant compound node functions are constant [9–11].

Chapter 6

2+1D: Coarse Graining Renormalization and the Running Couplings

In this chapter we apply coarse graining renormalization transformations to the 2+1D effective theory in the pure gauge limit and the limit of static quarks at finite density. For both cases our knowledge from chapter 5 will be used. In contrast to the theory in 1+1D, however, further approximations will become necessary to obtain the running couplings.
Because we are interested in the thermodynamic limit, finite size effects will be neglected [12, 15].

6.1 Pure Gauge Theory

6.1.1 The Transformation Scheme

In 2+1D renormalization group transformations are known to typically cause new interactions on the coarser lattice over longer ranges than the starting system. To capture this behavior to order $\mathcal{O}(u^{2N_\tau+2})$ we allow interactions at distances $|x-y| = \sqrt{2}a$ and in the adjoint representation. The partition function then reads as discussed in section 4.1 [12, 15]

$$Z = \int [\mathrm{d}U] \prod_{\langle x,y\rangle} \left(1 + \lambda_f \left(L_x L_y^\dagger + L_y L_x^\dagger\right) + \lambda_a \chi_a(U_x)\chi_a(U_y^\dagger)\right) \prod_{[x,y]} \left(1 + \lambda_{2,f} \left(L_x L_y^\dagger + L_y L_x^\dagger\right)\right) + \mathcal{O}(u^{2N_\tau+4}) \tag{6.1}$$

The interpretation of the effective theory suggests to apply a similar transformation as it is typically done to the 2D Ising model in the literature. We therefore integrate out every second lattice site in a checkerboard pattern. This is illustrated in figure 6.1a. We choose to integrate out every red colored lattice site. Because of the interactions over diagonals, once more we divide the sublattice that we want to integrate over. This is depicted in figure 6.1b. An iteration of the renormalization group transformation is then given by first integrating out the red filled lattice sites and the red hollow sites afterwards [12, 15].

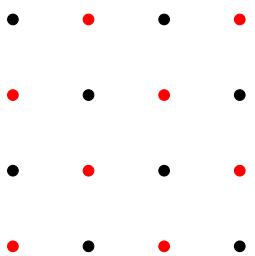

(a) Integrating out lattice sites in the 2+1D effective theory. Figure based on [15].

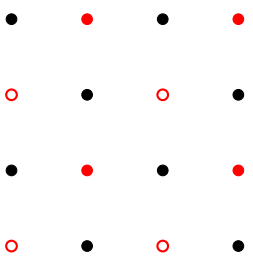

(b) Further dividing the lattice to control for diagonal interactions. Figure based on [15].

6.1.2 Determining the Running Couplings

Analogously to pure gauge theory in 1+1D, section 5.1, we substitute the couplings $\lambda_f \to \lambda_f^{(n)}$, $\lambda_a \to \lambda_a^{(n)}$ and $\lambda_{2,f} \to \lambda_{2,f}^{(n)}$. Further, we denote with $\langle x,y\rangle^{(n)}$ and $[x,y]^{(n)}$ nearest neighbors and next to nearest neighbors on the coarse grained lattice after n iterations. The partition function then reads [12, 15]

$$Z = \int [\mathrm{d}U]^{(n)} \prod_{\langle x,y\rangle^{(n)}} \left(1 + \lambda_f^{(n)} \left(L_x L_y^\dagger + L_y L_x^\dagger\right) + \lambda_a^{(n)} \chi_a(U_x)\chi_a(U_y^\dagger)\right) \prod_{[x,y]^{(n)}} \left(1 + \lambda_{2,f}^{(n)} \left(L_x L_y^\dagger + L_y L_x^\dagger\right)\right) + \mathcal{O}(u^{2N_\tau+4}) \tag{6.2}$$

with the boundary conditions

$$\lambda_f^{(0)} = \lambda_f, \quad \lambda_a^{(0)} = \lambda_a, \quad \lambda_{2,f}^{(0)} = \lambda_{2,f}, \quad \prod_{\langle x,y\rangle^{(0)}} = \prod_{\langle x,y\rangle}, \quad \prod_{[x,y]^{(0)}} = \prod_{[x,y]}, \quad \int [\mathrm{d}U]^{(0)} = \int [\mathrm{d}U] \tag{6.3}$$

To obtain the running couplings we consider a specific lattice site, say x, that we want to integrate out in the first integration step of the transformation (full red circles in figure 6.1b). Here we denote the product of all eight interaction terms between x and its neighbors with $A(U_x)$. All terms of order $\mathcal{O}(u_f^{2N_\tau+4})$ in $A(U_x)$ are neglected. Then at most two non-trivial characters of U_x appear in a given term and the integration can be performed with the orthogonality relation (3.6) [12, 15]

$$\begin{aligned}\int \mathrm{d}U_x A(U_x) = 1 + \lambda_f^{(n)2}\Big(&L^\dagger_{x-e_1}L_{x-e_2} + L^\dagger_{x-e_1}L_{e_2+x} + L^\dagger_{e_1+x}L_{x-e_2} + L^\dagger_{e_1+x}L_{e_2+x} + L_{x-e_1}L^\dagger_{x-e_2} \\ &+ L_{e_1+x}L^\dagger_{x-e_2} + L_{x-e_1}L^\dagger_{e_2+x} + L_{e_1+x}L^\dagger_{e_2+x} + L_{e_1+x}L^\dagger_{x-e_1} + L_{x-e_1}L^\dagger_{e_1+x} \\ &+ L_{e_2+x}L^\dagger_{x-e_2} + L_{x-e_2}L^\dagger_{e_2+x}\Big) + \mathcal{O}(u_f^{3N_\tau})\end{aligned} \tag{6.4}$$

Because of the approximation the contributions of both $\lambda_{2,f}^{(n)}$ and $\lambda_a^{(n)}$ do not appear anymore in (6.4). As there are diagonal interactions between non-integrated lattice sites (black dots in figure 6.1b), $\lambda_{2,f}^{(n)}$ still contributes to the partition function. Additionally, because the diagonal couplings drop out from (6.4), the integration over the second sublattice (red hollow circles in figure 6.1b) can be performed and yields expressions of the same form. Contributions involving the adjoint coupling thus drop out completely.
To the given order (6.4) can be rewritten into a product form [15]

$$\begin{aligned}\int \mathrm{d}U_x A(U_x) = &\left(1 + \lambda_f^{(n)2}(L_{x+e_1}L^\dagger_{x-e_1} + L_{x-e_1}L^\dagger_{x+e_1})\right)\left(1 + \lambda_f^{(n)2}(L_{x-e_1}L^\dagger_{x-e_2} + L_{x-e_2}L^\dagger_{x-e_1})\right) \\ &\left(1 + \lambda_f^{(n)2}(L_{x+e_2}L^\dagger_{x-e_1} + L_{x-e_1}L^\dagger_{x+e_2})\right)\left(1 + \lambda_f^{(n)2}(L_{x+e_2}L^\dagger_{x-e_2} + L_{x-e_2}L^\dagger_{x+e_2})\right) \\ &\left(1 + \lambda_f^{(n)2}(L_{x+e_1}L^\dagger_{x+e_2} + L_{x+e_2}L^\dagger_{x+e_1})\right)\left(1 + \lambda_f^{(n)2}(L_{x+e_1}L^\dagger_{x-e_2} + L_{x-e_2}L^\dagger_{x+e_1})\right) + \mathcal{O}(u_f^{3N_\tau})\end{aligned} \tag{6.5}$$

After putting this product back into the partition function, the factors describe interactions between the non-integrated lattice sites at distances $|x-y| = 2a$ and $|x-y| = \sqrt{2}a$. The coupling strength of the former is given by $\lambda_f^{(n)2}$. For the latter the symmetry of the system implies that the interaction terms appear twice. An additional contribution originates from the initial diagonal interactions between non-integrated lattice sites. The total interaction between two diagonal lattice sites x and y is denoted as $E(U_x, U_y)$ and reads [15]

$$E(U_x,U_y) = \left(1 + \lambda_f^{(n)2}(L_xL_y^\dagger + L_yL_x^\dagger)\right)^2 \left(1 + \lambda_{2,f}^{(n)}(L_xL_y^\dagger + L_yL_x^\dagger)\right) \tag{6.6}$$

To bring (6.6) into the same form as the initial interactions in (6.2) terms of order $\mathcal{O}(u_f^{2N_\tau+4})$ are neglected

$$E(U_x,U_y) = 1 + \left(2\lambda_f^{(n)2} + \lambda_{2,f}^{(n)}\right)(L_xL_y^\dagger + L_yL_x^\dagger) + \mathcal{O}(u_f^{2N_\tau+4}) \tag{6.7}$$

By rotating the lattice by $\pi/4$ the diagonal contribution (6.7) becomes the new nearest neighbor interaction, whereas the interactions at distance $|x-y| = 2a$ become the new diagonal ones [15]. Thus, the running couplings

read

$$\lambda_f^{(n+1)} = 2\lambda_f^{(n)2} + \lambda_{2,f}^{(n)} \tag{6.8}$$

$$\lambda_{2,f}^{(n+1)} = \lambda_f^{(n)2} \tag{6.9}$$

6.2 Static Quarks at Finite Density

In the last system of interest in this thesis the static quark determinant is included into our description of the 2+1D effective theory. Like in the previous section we allow diagonal interactions. The renormalization scheme will be accurate to the order $\mathcal{O}(u_f^{vN_\tau}\kappa^{wN_\tau})$ with $v+w=2$. By following the calculation including the adjoint representation its contributions can be found to exceed this condition and are therefore neglected. This is analogous to the previous section.
The partition function reads [8]

$$Z = \int [\mathrm{d}U] \det Q_{\mathrm{stat}} \prod_{\langle x,y\rangle} \left(1 + \lambda_f \left(L_x L_y^\dagger + L_y L_x^\dagger\right)\right) \prod_{[x,y]} \left(1 + \lambda_{2,f} \left(L_x L_y^\dagger + L_y L_x^\dagger\right)\right) + \mathcal{O}(u^{2N_\tau+4}) \tag{6.10}$$

In the static quark discussion in 1+1D in section 5.2, it was found that including the static determinant into the partition function implies mixed terms between the different representations after renormalization. Here this is applied to both the nearest neighbor and next to nearest neighbor interactions, respectively. This leads to the approach [15]

$$\begin{aligned} Z = \int [\mathrm{d}U]^{(n)} \det Q_{\mathrm{stat}}^{(n)} \prod_{\langle x,y\rangle^{(n)}} \Big(&1 + \lambda_{1,1}^{(n)}(L_x + L_y) + \lambda_{1,2}^{(n)}(L_x^\dagger + L_y^\dagger) + \lambda_{1,3}^{(n)} L_x L_y + \lambda_{1,4}^{(n)} L_x^\dagger L_y^\dagger \\ &+ \lambda_{1,5}^{(n)}(L_x L_y^\dagger + L_y L_x^\dagger)\Big) \prod_{[x,y]^{(n)}} \Big(1 + \lambda_{2,1}^{(n)}(L_x + L_y) + \lambda_{2,2}^{(n)}(L_x^\dagger + L_y^\dagger) + \lambda_{2,3}^{(n)} L_x L_y + \lambda_{2,4}^{(n)} L_x^\dagger L_y^\dagger \\ &+ \lambda_{2,5}^{(n)}(L_x L_y^\dagger + L_y L_x^\dagger)\Big) + \mathcal{O}(u^{2N_\tau+4}) \end{aligned} \tag{6.11}$$

The boundary conditions that have not been stated in the previous section read

$$0 = \lambda_{1,1}^{(0)} = \lambda_{1,2}^{(0)} = \lambda_{1,3}^{(0)} = \lambda_{1,4}^{(0)} = \lambda_{2,1}^{(0)} = \lambda_{2,2}^{(0)} = \lambda_{2,3}^{(0)} = \lambda_{2,4}^{(0)}, \quad \lambda_{1,5}^{(0)} = \lambda_f, \quad \lambda_{2,5}^{(0)} = \lambda_{2,f} \tag{6.12}$$

Like in the previous section we integrate out the lattice sites in a checkerboard pattern, first over red filled sites in figure 6.1b and red hollow sites afterwards. Before we do this, it turns out to be useful to define the gauge integral [28]

$$\int \mathrm{d}U \det Q_{\mathrm{stat}}^{\mathrm{loc}} L^j L^{\dagger k} =: o(j,k) = \int \mathrm{d}U L^j L^{\dagger k} + \mathcal{O}(\kappa^{N_\tau}) = \delta(j-k \bmod N_c, 0) + \mathcal{O}(\kappa^{N_\tau}) \tag{6.13}$$

It will capture the influence of the static determinant when integrating out a lattice site. Additionally, two statements have to be made regarding the following calculation

1. Because we expect coarse graining to increase the order of the couplings at least once, we assume all interaction strengths to be at least of order $\mathcal{O}(u_f^{vN_\tau}\kappa^{wN_\tau})$ with $v+w=2$. However, λ_f is of $\mathcal{O}(u_f^{N_\tau})$, so $\lambda_{1,5}^{(n)}$ is the only exception to this and counts as $v+w=1$.

2. We assume $N_c \geq 3$. Thus, all $o(j,k)$ with $|j-k|=1$ or $|j-k|=2$ count as an additional factor of κ^{N_τ}.

Again we choose a lattice site x of the red colored sites and denote with $A(U_x)$ the product of its eight interaction factors. Performing the gauge integration over U_x results in a large term, which is truncated at

order $\mathcal{O}(u_f^{vN_\tau}\kappa^{wN_\tau})$ with $v+w=3$ [12,15].

$$\begin{aligned}\int \mathrm{d}U_x A(U_x) =& \lambda_{1,5}^{(n)2}\Big(o(1,1)L_{e_1+x}L^\dagger_{x-e_2} + o(1,1)L_{e_1+x}L^\dagger_{e_2+x} + o(1,1)L^\dagger_{x-e_1}L_{x-e_2} + o(1,1)L^\dagger_{x-e_1}L_{e_2+x}\\ &+ o(1,1)L^\dagger_{e_1+x}L_{x-e_2} + o(1,1)L^\dagger_{e_1+x}L_{e_2+x} + o(1,1)L_{x-e_1}L^\dagger_{x-e_2} + o(1,1)L_{x-e_1}L^\dagger_{e_2+x}\\ &+ o(1,1)L^\dagger_{x-e_1}L_{e_1+x} + o(1,1)L_{x-e_1}L^\dagger_{e_1+x} + o(1,1)L_{e_2+x}L^\dagger_{x-e_2} + o(1,1)L_{x-e_2}L^\dagger_{e_2+x}\Big)\\ &+ \lambda_{1,5}^{(n)}\Big(o(0,1)L_{x-e_1} + o(0,1)L_{e_1+x} + o(1,0)L^\dagger_{x-e_1} + o(1,0)L^\dagger_{e_1+x} + o(0,1)L_{x-e_2}\\ &+ o(0,1)L_{e_2+x} + o(1,0)L^\dagger_{x-e_2} + o(1,0)L^\dagger_{e_2+x}\Big)\\ &+ \lambda_{1,1}^{(n)}\Big(o(0,0)L_{x-e_1} + o(0,0)L_{e_1+x} + o(0,0)L_{x-e_2} + o(0,0)L_{e_2+x}\Big)\\ &+ \lambda_{2,1}^{(n)}\Big(o(0,0)L_{-e_1-e_2+x} + o(0,0)L_{e_1-e_2+x} + o(0,0)L_{-e_1+e_2+x} + o(0,0)L_{e_1+e_2+x}\Big)\\ &+ \lambda_{1,2}^{(n)}\Big(o(0,0)L^\dagger_{x-e_1} + o(0,0)L^\dagger_{e_1+x} + o(0,0)L^\dagger_{x-e_2} + o(0,0)L^\dagger_{e_2+x}\Big)\\ &+ \lambda_{2,2}^{(n)}\Big(o(0,0)L^\dagger_{-e_1-e_2+x} + o(0,0)L^\dagger_{e_1-e_2+x} + o(0,0)L^\dagger_{-e_1+e_2+x} + o(0,0)L^\dagger_{e_1+e_2+x}\Big)\\ &+ o(0,0) + \mathcal{O}(u_f^{vN_\tau}\kappa^{wN_\tau}) \quad \text{with} \quad v+w=3 \end{aligned} \tag{6.14}$$

In contrast to the pure gauge limit some of the diagonal couplings still appear and terms including Polyakov loops of red hollow sites from figure 6.1b remain. Because in the interaction factors in (6.11) the terms are either equal to 1 or proportional to some coupling, there are two possible scenarios that have to be distinguished when integrating out the red hollow sites from figure 6.1b. Both are explained based on the term proportional to $\lambda_{2,1}^{(n)}L_{e_1+e_2+x}$ in (6.14)

1. We integrate over the product of $\lambda_{2,1}^{(n)}L_{e_1+e_2+x}$ with one of the constant terms. This leads to a contribution proportional to

$$\lambda_{2,1}^{(n)}\int \mathrm{d}U_{e_1+e_2+x}L_{e_1+e_2+x} = \lambda_{2,1}^{(n)}o(1,0) \tag{6.15}$$

   Based on the previous assumption this term is of higher order than $\mathcal{O}(u_f^{vN_\tau}\kappa^{wN_\tau})$ with $v+w=2$ and is therefore neglected.

2. We integrate over the product of $\lambda_{2,1}^{(n)}L_{e_1+e_2+x}$ and some other term proportional to $\lambda L_{e_1+e_2+x}$ or $\lambda L^\dagger_{e_1+e_2+x}$ with some coupling λ. This results in

$$\lambda_{2,1}^{(n)}\lambda\int \mathrm{d}U_{e_1+e_2+x}L_{e_1+e_2+x}L_{e_1+e_2+x} \quad \text{or} \quad \lambda_{2,1}^{(n)}\lambda\int \mathrm{d}U_{e_1+e_2+x}L_{e_1+e_2+x}L^\dagger_{e_1+e_2+x} \tag{6.16}$$

   which is again of higher order than $\mathcal{O}(u_f^{vN_\tau}\kappa^{wN_\tau})$ with $v+w=2$ and is therefore neglected. Terms of higher powers in the Polyakov loop are of even higher orders in $u_f^{N_\tau}$ and κ^{N_τ}.

Because the integration over the red hollow sites in figure 6.1b results in an additional factor of order $\mathcal{O}(u_f^{vN_\tau}\kappa^{wN_\tau})$ with $n+m\geq 1$, the overall order of terms involving the diagonal couplings in (6.14) exceed $\mathcal{O}(u_f^{vN_\tau}\kappa^{wN_\tau})$ with $v+w=2$ and are neglected. This decouples the red filled and hollow lattice sites and both give contributions

of the same form. For any integrated lattice site x this means

$$\begin{aligned}\int \mathrm{d}U_x A(U_x) =&\lambda_{1,5}^{(n)2}\Big(o(1,1)L_{e_1+x}L^\dagger_{x-e_2} + o(1,1)L_{e_1+x}L^\dagger_{e_2+x} + o(1,1)L^\dagger_{x-e_1}L_{x-e_2} + o(1,1)L^\dagger_{x-e_1}L_{e_2+x}\\ &+ o(1,1)L^\dagger_{e_1+x}L_{x-e_2} + o(1,1)L^\dagger_{e_1+x}L_{e_2+x} + o(1,1)L_{x-e_1}L^\dagger_{x-e_2} + o(1,1)L_{x-e_1}L^\dagger_{e_2+x}\\ &+ o(1,1)L^\dagger_{x-e_1}L_{e_1+x} + o(1,1)L_{x-e_1}L^\dagger_{e_1+x} + o(1,1)L_{e_2+x}L^\dagger_{x-e_2} + o(1,1)L_{x-e_2}L^\dagger_{e_2+x}\Big)\\ &+ \lambda_{1,5}^{(n)}\Big(o(0,1)L_{x-e_1} + o(0,1)L_{e_1+x} + o(1,0)L^\dagger_{x-e_1} + o(1,0)L^\dagger_{e_1+x} + o(0,1)L_{x-e_2}\\ &+ o(0,1)L_{e_2+x} + o(1,0)L^\dagger_{x-e_2} + o(1,0)L^\dagger_{e_2+x}\Big)\\ &+ \lambda_{1,1}^{(n)}\Big(o(0,0)L_{x-e_1} + o(0,0)L_{e_1+x} + o(0,0)L_{x-e_2} + o(0,0)L_{e_2+x}\Big)\\ &+ \lambda_{1,2}^{(n)}\Big(o(0,0)L^\dagger_{x-e_1} + o(0,0)L^\dagger_{e_1+x} + o(0,0)L^\dagger_{x-e_2} + o(0,0)L^\dagger_{e_2+x}\Big)\\ &+ o(0,0) + \quad \text{terms leading to contributions of order} \quad \mathcal{O}(u_f^{vN_\tau}\kappa^{wN_\tau}) \quad \text{with} \quad v+w>2\end{aligned} \tag{6.17}$$

Equation (6.17) now describes the interactions between the four lattice sites $x-e_1$, $x+e_1$, $x+e_2$ and $x-e_2$. Like in the pure gauge limit (6.17) ought to be brought into a factorizing form. For brevity we define the set of appearing interactions [15]

$$C := \{(x+e_1, x-e_1), (x+e_1, x-e_2), (x+e_1, x+e_2), (x-e_1, x+e_2), (x-e_1, x-e_2), (x+e_2, x-e_2)\} \tag{6.18}$$

To the given order of accuracy one finds the factorization

$$\begin{aligned}\int \mathrm{d}U_x A(U_x) =&o(0,0)\prod_{(a,b)\in C}\left(1 + \frac{1}{3}\left(\lambda_{1,1} + \frac{o(0,1)}{o(0,0)}\lambda_{1,5}^{(n)}\right)(L_a + L_b) + \frac{1}{3}\left(\lambda_{1,2} + \frac{o(1,0)}{o(0,0)}\lambda_{1,5}^{(n)}\right)(L_a^\dagger + L_b^\dagger)\right.\\ &\left. + \frac{o(1,1)}{o(0,0)}\lambda_{1,5}^{(n)2}(L_aL_b^\dagger + L_bL_a^\dagger)\right)\\ &+ \quad \text{terms leading to contributions of order} \quad \mathcal{O}(u_f^{vN_\tau}\kappa^{wN_\tau}) \quad \text{with} \quad v+w>2\end{aligned} \tag{6.19}$$

The factors now describe the interaction between the four lattice sites over the distances $\sqrt{2}a$ and $2a$. The overall factor of $o(0,0)$ is irrelevant to the running couplings. Additionally, because terms proportional to L_xL_y and $L_x^\dagger L_y^\dagger$ do not appear, the couplings $\lambda_{1,3}^{(n)}$, $\lambda_{1,4}^{(n)}$, $\lambda_{2,3}^{(n)}$ and $\lambda_{2,4}^{(n)}$ are disregarded completely [15].
As in section 6.1 after plugging (6.19) back into the partition function (6.2) the interactions over $\sqrt{2}a$ are found to appear twice. An additional contribution to them comes from the diagonal interactions between non-integrated lattice sites [15].
Let $E(x,y)$ denote the total interaction between two diagonal, non-integrated lattice sites. $E(x,y)$ can be approximated as

$$\begin{aligned}E(x,y) =&\left(1 + \frac{1}{3}\left(\lambda_{1,1} + \frac{o(0,1)}{o(0,0)}\lambda_{1,5}^{(n)}\right)(L_x + L_y) + \frac{1}{3}\left(\lambda_{1,2} + \frac{o(1,0)}{o(0,0)}\lambda_{1,5}^{(n)}\right)(L_x^\dagger + L_y^\dagger)\right.\\ &\left. + \frac{o(1,1)}{o(0,0)}\lambda_{1,5}^{(n)2}(L_xL_y^\dagger + L_yL_x^\dagger)\right)^2\left(1 + \lambda_{2,1}^{(n)}(L_x + L_y) + \lambda_{2,2}^{(n)}(L_x^\dagger + L_y^\dagger) + \lambda_{2,5}^{(n)}(L_xL_y^\dagger + L_yL_x^\dagger)\right)\\ =&1 + \left(2\frac{\lambda_{1,1}^{(n)}}{3} + 2\frac{o(0,1)}{3o(0,0)}\lambda_{1,5}^{(n)} + \lambda_{2,1}^{(n)}\right)(L_x + L_y) + \left(2\frac{\lambda_{1,2}^{(n)}}{3} + 2\frac{o(1,0)}{3o(0,0)}\lambda_{1,5}^{(n)} + \lambda_{2,2}^{(n)}\right)(L_x^\dagger + L_y^\dagger)\\ &+ \left(2\frac{o(1,1)}{o(0,0)}\lambda_{1,5}^{(n)2} + \lambda_{2,5}^{(n)}\right)(L_xL_y^\dagger + L_yL_x^\dagger) + \mathcal{O}(u_f^{vN_\tau}\kappa^{wN_\tau}) \quad \text{with} \quad v+w=3\end{aligned} \tag{6.20}$$

Analogously to section 6.1, the interactions at distance $\sqrt{2}a$ become the new nearest neighbor couplings, whereas the ones at distance $2a$ become the new next to nearest neighbor interactions by rotating the lattice by $\pi/4$ [15].

Thus, the running couplings are given by

$$\lambda_{1,1}^{(n+1)} = 2\frac{\lambda_{1,1}^{(n)}}{3} + 2\frac{o(0,1)}{3o(0,0)}\lambda_{1,5}^{(n)} + \lambda_{2,1}^{(n)} \tag{6.21}$$

$$\lambda_{1,2}^{(n+1)} = 2\frac{\lambda_{1,2}^{(n)}}{3} + 2\frac{o(1,0)}{3o(0,0)}\lambda_{1,5}^{(n)} + \lambda_{2,2}^{(n)} \tag{6.22}$$

$$\lambda_{1,5}^{(n+1)} = 2\frac{o(1,1)}{o(0,0)}\lambda_{1,5}^{(n)2} + \lambda_{2,5}^{(n)} \tag{6.23}$$

$$\lambda_{2,1}^{(n+1)} = \frac{\lambda_{1,1}^{(n)}}{3} + \frac{o(0,1)}{3o(0,0)}\lambda_{1,5}^{(n)} \tag{6.24}$$

$$\lambda_{2,2}^{(n+1)} = \frac{\lambda_{1,2}^{(n)}}{3} + \frac{o(1,0)}{3o(0,0)}\lambda_{1,5}^{(n)} \tag{6.25}$$

$$\lambda_{2,5}^{(n+1)} = \frac{o(1,1)}{o(0,0)}\lambda_{1,5}^{(n)2} \tag{6.26}$$

Note that the previous assumption of all couplings except for $\lambda_{1,5}^{(n)}$ being at least of order $\mathcal{O}(u_f^{vN_\tau}\kappa^{wN_\tau})$ with $v+w=2$ is fulfilled self-consistently for all $n \geq 0$. Additionally, the gauge integrals $o(0,0)$, $o(1,0)$, $o(0,1)$ and $o(1,1)$ can be obtained with the solution to the 1+1D static quark gauge integral (5.31).
In the last step, we check whether our recursion relations recover the pure gauge limit correctly. As one finds quickly from (6.13), we have $o(1,0) = 0 = o(0,1)$ and $o(1,1) = 1 = o(0,0)$, if $\kappa = 0$. Then we have the implications

$$\text{Equation (6.21):} \quad \lambda_{1,1}^{(n)} = 0 = \lambda_{2,1}^{(n)} \qquad \Rightarrow \lambda_{1,1}^{(n+1)} = 0 \tag{6.27}$$

$$\text{Equation (6.22):} \quad \lambda_{1,2}^{(n)} = 0 = \lambda_{2,2}^{(n)} \qquad \Rightarrow \lambda_{1,2}^{(n+1)} = 0 \tag{6.28}$$

$$\text{Equation (6.24):} \quad \lambda_{1,1}^{(n)} = 0 \qquad \Rightarrow \lambda_{2,1}^{(n+1)} = 0 \tag{6.29}$$

$$\text{Equation (6.25):} \quad \lambda_{1,2}^{(n)} = 0 \qquad \Rightarrow \lambda_{2,2}^{(n+1)} = 0 \tag{6.30}$$

By combining (6.27) with (6.29) as well as (6.28) with (6.30) one obtains $\lambda_{1,1}^{(n)} = 0 = \lambda_{2,1}^{(n)} \Rightarrow \lambda_{1,1}^{(n+1)} = 0 = \lambda_{2,1}^{(n+1)}$ and $\lambda_{1,2}^{(n)} = 0 = \lambda_{2,2}^{(n)} \Rightarrow \lambda_{1,2}^{(n+1)} = 0 = \lambda_{2,2}^{(n+1)}$. Because of the boundary conditions (6.12) these couplings will always vanish in the pure gauge limit. Thus, the only relevant couplings follow the relations

$$\lambda_{1,5}^{(n+1)} = 2\lambda_{1,5}^{(n)2} + \lambda_{2,5}^{(n)} \tag{6.31}$$

$$\lambda_{2,5}^{(n+1)} = \lambda_{1,5}^{(n)2} \tag{6.32}$$

which are equivalent to the pure gauge running couplings (6.8) and (6.9).

Chapter 7

1+1D: Evaluation of the Renormalization Scheme

It is shown that all expressions for the running couplings in 1+1D can be written as matrix recursion relations. An analytical solution to them is found leading to the transfer matrix if the number of spatial sites is given by $N_x = N_\kappa 2^{n_x}$. This allows us to calculate intensive observables in terms of an eigenvalue problem in the thermodynamic limit. This procedure is applied to the pressure as well as the baryon density. The continuum limit is performed numerically. Finally, results for both observables are discussed at varying parameters of the theory and compared at different orders of the hopping parameter expansion [15].

7.1 Transforming Running Couplings into Matrix Recursion Relations

The expressions for running couplings found for the 1+1D effective theory have a common structure. Any of them is expressed by a quadratic recursion relation and when considering only a finite amount of representations of the gauge action all sums are finite[1]. Further, it is possible to split the indices of the running couplings into two groups: the ones that are added up and the ones that are not. Each of them can then be indexed by a natural number. For our previously discussed cases this leads to the bijections

1. Heavy quarks:

$$r \leftrightarrow i_r \in \mathbb{N} \tag{7.1}$$

2. Leading order corrections:

$$(\alpha, r) \leftrightarrow i_{(\alpha,r)} \in \mathbb{N} \tag{7.2}$$

3. Next to leading order corrections

$$(a_1, a_2, r_1, r_2, r_3) \leftrightarrow i_{(a_1,a_2,r_1,r_2,r_3)} \in \mathbb{N} \text{ and } (a_3, a_4, r_4) \leftrightarrow j_{(a_3,a_4,r_4)} \in \mathbb{N} \tag{7.3}$$

The explicit choice of the mapping is arbitrary and one can expect physical observables to not depend on it. Using these mappings all sums in the recursion relations (5.19), (5.37) and (5.54) can be transformed to sums over these natural numbers and can be identified as quadratic recursion relations of matrix elements. Further, these relations exhibit the form

$$\boldsymbol{h}^{(n+1)} = \boldsymbol{h}^{(n)} \boldsymbol{g} \boldsymbol{h}^{(n)} \tag{7.4}$$

The elements of the matrices are determined by the boundary conditions of the recursion relations and the gauge integrals appearing in the transformations

[1] For calculations in practice it is necessary to abort the sums at a finite order of β

1. Heavy quarks:

$$h_{ij}^{(0)} = \lambda_{r_i}\delta_{r_i r_j} \text{ and } g_{ij} = \int \mathrm{d}U \det Q_{\text{stat}}^{\text{loc}}(U)\chi_{r_i}(U^\dagger)\chi_{r_j}(U) \tag{7.5}$$

2. Leading order corrections:

$$h_{ij}^{(0)} = \frac{(-h_2)^{\alpha_i}}{\alpha_i!}\lambda_{r_i}\delta_{r_i r_j}\delta_{\alpha_i\alpha_j} \text{ and } g_{ij} = \int \mathrm{d}U \det Q_{\text{stat}}^{\text{loc}}(U)\chi_{r_i}(U^\dagger)\chi_{r_j}(U)W_{1111}^{-,\alpha_i+\alpha_j} \tag{7.6}$$

3. Next to leading order corrections:

$$h_{ij}^{(0)} = h_{v_{1,i}v_{2,i}v_{3,j}v_{4,j}}\lambda_{r_{1,i}}\delta_{r_{1,i}r_{2,i}}\lambda_{r_{3,i}}\delta_{r_{3,i}r_{4,j}} \tag{7.7}$$

$$\begin{aligned} g_{ij} = &\left(\int \mathrm{d}U \det Q_{\text{stat}}^{\text{loc}}(U)W_{v_{1,j}}(U)W_{v_{3,i}}(U)\chi_{r_{4,i}}(U^\dagger)\chi_{r_{1,j}}(U)\right) \\ &\left(\int \mathrm{d}U \det Q_{\text{stat}}^{\text{loc}}(U)W_{v_{2,j}}(U)W_{v_{4,i}}(U)\chi_{r_{2,j}}(U^\dagger)\chi_{r_{3,j}}(U)\right) \end{aligned} \tag{7.8}$$

Equation (7.4) is quickly solved by the approach

$$\boldsymbol{h}^{(n)} = \left(\boldsymbol{h}^{(0)}\boldsymbol{g}\right)^{2^n-1}\boldsymbol{h}^{(0)} \tag{7.9}$$

Note that the matrix $\boldsymbol{h}^{(0)}\boldsymbol{g}$ is not necessarily symmetric, so complex eigenvalues might occur depending on the parameters of the theory. Additionally, when considering the $\mathcal{O}(\kappa^4)$-effective action both $\boldsymbol{h}^{(0)}$ and $\boldsymbol{g}$ are not quadratic, but their product is [10–12].

7.2 The Partition Function for Periodic Boundary Conditions

The partition function is of major interest when evaluating a theory as it can be used to obtain many aggregate observables of the system. Here we calculate the partition function for heavy quarks with periodic boundary conditions in both dimensions. However, the steps can be performed including corrections in κ analogously and the more general result is discussed.

A single iteration of coarse graining halves the amount of sites in the lattice, so $N_x^{(n)}$ needs to be divisible by two. Assuming that the size of the lattice is a power of two $N_x^{(0)} = 2^{n_x}$ the renormalization group transformation can be applied n_x times. This reduces the lattice to a single site interacting with itself due to the periodic boundary conditions [16]

$$Z = c_0^{N_x N_\tau}\int [\mathrm{d}U]^{(n_x)} \det Q_{\text{stat}}^{(n_x)} \prod_{x=1}^{N_x^{(n_x)}} \sum_{r_1,r_2} \lambda_{r_1 r_2}^{(n_x)}\chi_{r_1}(U_x)\chi_{r_2}(U_{x+1}^\dagger) \tag{7.10}$$

$$= c_0^{N_x N_\tau}\sum_{r_1,r_2}\lambda_{r_1 r_2}^{(n_x)}\int \mathrm{d}U \det Q_{x,\,\text{stat}}(U)\chi_{r_1}(U)\chi_{r_2}(U^\dagger) \tag{7.11}$$

After reusing the previously introduced bijections the constituents of (7.11) can be identified as the matrix elements in (7.5)[2]

$$Z = c_0^{N_x N_\tau}\sum_{ij} h_{ij}^{(n_x)} g_{ji} = c_0^{N_x N_\tau}\,\mathrm{Tr}\,\boldsymbol{h}^{(n_x)}\boldsymbol{g} = c_0^{N_x N_\tau}\,\mathrm{Tr}\left[\left(\boldsymbol{h}^{(0)}\boldsymbol{g}\right)^{N_x}\right] = c_0^{N_x N_\tau}\,\mathrm{Tr}\left[\left(\boldsymbol{g}\boldsymbol{h}^{(0)}\right)^{N_x}\right] \tag{7.12}$$

Because different choices of the bijective mapping correspond to choosing different bases of the matrices $\boldsymbol{h}^{(n_x)}$ and $\boldsymbol{g}$, the partition function (7.12) does not depend on its explicit choice. Thus, neither do physical observables, as it was expected.

Performing the steps including corrections in κ leads to the same expression (7.12). Only the matrices $\boldsymbol{h}^{(0)}$

[2] This is analogous to combinations of renormalization group transformations and the transfer matrix in the 1D Ising model [15]

and $\boldsymbol{g}$ have to be chosen according to section 7.1 and the exponent inside the trace has to be shifted from $N_x \to N_x/N_\kappa$.
Because of the cyclicity of the trace the last equality sign holds, even though the matrices neither commute nor are quadratic in general. Further, when considering the $\mathcal{O}(\kappa^4)$ effective action using the last equality sign in (7.12) decreases the dimension of the matrix and thus reduces computational costs.
Another observation in (7.12) is its structure being similar to those usually obtained from transfer matrix approaches [15]. This is in agreement with the usual interpretation of irreducible characters as wave functions and the respective representation as a quantum number [18].
Further, this suggests the interpretation of compound node functions in a similar manner. For each tuple from the bijections (7.1)-(7.3) the dimension of the transfer matrix is increased by one. Thus, for any of those there exists a many body wave function in the Hilbert space of a lattice site. They therefore serve as quantum numbers, while the strong coupling and heavy quark expansions act as a truncation of the Hilbert space [15].

7.3 Accuracy of the Strong Coupling Expansion

The fact, that the heavy quark recurrence scheme is accurate to arbitrary order in β, is used to obtain insight in the accuracy of the strong coupling expansion. Figure 7.1 shows the relative error of the heavy quark partition function up to high values of β.

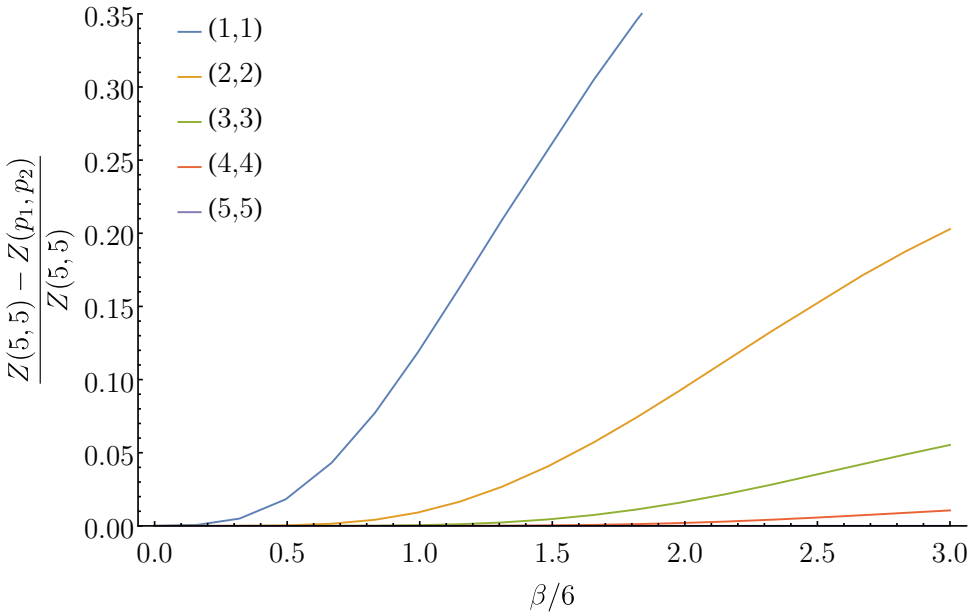

Figure 7.1: The relative error of the heavy quark partition function for different amount of representations. Here $h_1 = 1$, $\bar{h}_1 = 0$, $N_f = 1$ and $N_c = 3$ have been chosen.

The numbers in the brackets represent the highest values of p_1 and p_2 respectively, i.e. $(4, 4)$ means all irreducible representations with $p_1, p_2 \leq 4$ are included in the gauge action. The error is calculated relative to the partition function with the most representations, $p_1, p_2 \leq 5$ corresponding to the first $(5 + 1)(5 + 1) = 36$ irreducible representations.
The line $(1, 1)$ includes the trivial, fundamental, anti-fundamental and adjoint representation, which corresponds to the ones used in the currently known effective theories in 3+1D. Its curve shows a relative error of $\approx 12\%$ at $\beta \approx 6$, which is in agreement with earlier discussions of the accuracy of the 3+1D effective theory [29]. Especially at larger values of the inverse coupling representations of higher dimensions than those previously mentioned are necessary to obtain accurate results in the continuum limit $\beta \to \infty$.
Note that taking the absolute value in the relative error is not necessary. Therefore, aborting the strong coupling expansion typically leads to underestimating the exact partition function.

7.4 Observables

7.4.1 Observables to Be Discussed

In this section using the partition function (7.12) the pressure p, (anti) quark density n_q ($n_{\bar{q}}$) and baryon number density $n_B = (n_q - n_{\bar{q}})/3$ at temperature T and spatial volume V are discussed. They are related to the partition function via the relations [15, 16]

$$p = T \left.\frac{\partial}{\partial V} \log Z\right|_T = \frac{T}{V} \log Z \tag{7.13}$$

$$n_q = \frac{h_1}{V} \left.\frac{\partial}{\partial h_1} \log Z\right|_{T,V} = \frac{h_1}{V} \frac{1}{Z} \left.\frac{\partial}{\partial h_1} Z\right|_{T,V} \tag{7.14}$$

The anti quark density is obtained by replacing h_1 with $\bar{h}_1$ in (7.14). The last equality sign in (7.13) holds only in the thermodynamic limit. To render the (anti) quark density the derivative has to be taken. Using the cyclicity of the trace one quickly obtains from (7.12) [15]

$$n_q = \frac{h_1}{V} \frac{c_0^{N_x N_\tau} 2^{n_x}}{Z} \operatorname{Tr}\left[\left(\boldsymbol{h}^{(0)} \boldsymbol{g}\right)^{2^{n_x}-1} \boldsymbol{h}^{(0)} \left.\frac{\partial}{\partial h_1} \boldsymbol{g}\right|_{T,V} \right] \tag{7.15}$$

Again the anti quark density is obtained by replacing h_1 with $\bar{h}_1$.
It is common to normalize the baryon chemical potential $\mu_B = 3\mu$ with respect to the baryon mass m_B. It has been calculated up to order $\mathcal{O}(\kappa^n u_f^m)$ where $n + m \leq 7$ [9]

$$am_B = -3 \log 2\kappa - 6\kappa^2 \frac{u_f}{1 - u_f} + 24\kappa^4 u_f - 54\kappa^4 u_f^2 - 60\kappa^4 u_f^3 \tag{7.16}$$

When performing calculations in the heavy quark limit corrections of order $\mathcal{O}(\kappa^2)$ and higher are to be neglected.

7.4.2 The Thermodynamic Limit

Naturally, one is interested in physical systems with large spatial extend. This corresponds to taking the limit $V \to \infty$ in the continuum or $N_x \to \infty$ in lattices while keeping the lattice spacing $a(\beta)$ finite [7]. Here we exemplify how to perform this limit for intensive observables using the quark density (7.14). However, the procedure can be applied to other quantities analogously.
In our framework the limit of many lattice sites can be taken by iterating the recursion scheme infinitely many times, e.g. $n_x \to \infty$ [12]. In fact, the only dependence of n_x in (7.14) appears in the exponents of the transfer matrix. By performing the trace in its eigenbasis we can gain further insight in the behavior of the observable. Let $d_1, \ldots, d_t$ be the eigenvalues of $\boldsymbol{h}^{(0)}\boldsymbol{g}$ and $E_{d_1}, \ldots, E_{d_t}$ their respective sets of (orthonormal) eigenvectors. Using these quantities the quark density reads [15]

$$n_q = \frac{h_1}{aN_\kappa} \frac{1}{\sum_{i=1}^t |E_{d_i}| d_i^{2^{n_x}}} \sum_{i=1}^t d_i^{2^{n_x}-1} \sum_{\boldsymbol{v} \in E_{d_i}} \boldsymbol{v}^\dagger \left(\boldsymbol{h}^{(0)} \left.\frac{\partial}{\partial h_1} \boldsymbol{g}\right|_{T,V} \right) \boldsymbol{v} \tag{7.17}$$

As it was already stated in section 7.1 the eigenvalues are complex valued in general. This results in oscillations in both sums of (7.17), which have to disappear in the thermodynamic limit. Because we only have a finite amount of eigenvalues, this is only possible, if the eigenvalues with largest modulus are real valued. We choose d_1 to denote one of them. For brevity we assume $-d_1$ to not be an eigenvalue of the transfer matrix. This is indicated by (7.12), because expressions using the transfer matrix usually hold for arbitrary N_x. However, no proof to this is given in this thesis, but this has been checked numerically for every evaluation [15, 16].
In the limit $n_x \to \infty$ both the numerator and denominator are dominated by terms $\propto d_1$ and all other contributions are neglected [15, 16]

$$n_q = \frac{h_1}{aN_\kappa d_1 |E_{d_1}|} \sum_{v \in E_{d_1}} \boldsymbol{v}^\dagger \left(\boldsymbol{h}^{(0)} \left.\frac{\partial}{\partial h_1} \boldsymbol{g}\right|_{T,V} \right) \boldsymbol{v} \tag{7.18}$$

Performing an analogous calculation for the pressure (7.13) one obtains [15, 16]

$$p = \frac{1}{a^2} \log c_0 + \frac{T}{aN_\kappa} \log |d_1| \tag{7.19}$$

In the pure gauge limit the density matrix is already in diagonal form and its eigenvalues are the couplings λ_r with $\lambda_0 = 1$ the largest. Thus, in (7.19) only the first term persists and our result is reduced to the expression well known from literature [30].
A physical pressure is only obtained after subtraction of vacuum divergences [16], e.g.

$$p \to p - \lim_{T \to 0} p \Big|_{\mu=0} \tag{7.20}$$

On the lattice the zero temperature limit corresponds to taking the limit $N_\tau \to \infty$ while keeping the lattice spacing finite. At zero chemical potential it implies h_1, $\bar{h}_1$ and λ_r for $r \neq 0$ to vanish. Thus, none of the terms in the action proportional to node functions or characters contribute except for the trivial character contribution. Subtracting it from (7.19) yields the physical pressure [7, 15, 16]

$$p = \frac{T}{aN_\kappa} \log |d_1| \tag{7.21}$$

In pure gauge theory the pressure always vanishes and no dynamics take place. This agrees with the typical notion of the "two [dimensional] gauge field [having] no physical degrees of freedom" [16].

7.4.3 Setting the Scale and Continuum Extrapolation

In contrast to our effective theory QCD does not lie on a lattice but rather in a continuous space time. Thus, in order for our theoretical description to describe actual physics the limit of decreasing lattice spacing a or conversely increasing β has to be taken. This, however, is to be performed with the caveat of keeping physical parameters, i.e. temperature T and volume V, fixed. As we already performed the thermodynamic limit in section 7.4.2 the latter example does not apply to this discussion [7].
Another obstacle is determining the correct scaling behavior of our theory to reproduce physical observables, e.g. determine the lattice spacing as function of the coupling $a(\beta)$. In general, $a(\beta)$ depends on the hopping parameter κ as well. However, in discussions of the 3+1D theory this dependence was argued to be negligible for heavy quarks. In this thesis the same assumption is made and we determine the scaling behavior based on pure gauge theory [10, 11].
To actually determine $a(\beta)$ an observable has to be computed on the lattice and has to be related to its continuum value. Then, $a(\beta)$ can be chosen in a way,, that the lattice observable reproduces its continuum counterpart for all values of the inverse coupling. In this thesis we use the approach of Huang, et al., where the string tension σ was chosen to obtain a simple expression for the lattice spacing. The lattice string tension σ_L was already given in (3.9) [31].
In the continuum limit the area law of the Wilson loop is known to persist and the string tension assumes a value independent on the temperature and volume of the system, e.g. [15, 16, 30]

$$W(C) = e^{-N_x N_\tau \sigma_L} \to e^{-A\sigma} \quad \text{with} \quad A = \lim_{\beta \to \infty} a^2 N_x N_\tau \quad \text{and} \quad \sigma = \lim_{\beta \to \infty} \frac{\sigma_L}{a^2} \tag{7.22}$$

Now the lattice spacing can be chosen in a way allowing σ_L / a^2 to reproduce the continuum string tension for all values of β [31]

$$a(\beta) = \sqrt{-\frac{1}{\sigma} \log u_f} \tag{7.23}$$

All observables and parameters of the theory will then be given as dimensionless ratios to the continuum string tension, i.e. $T \to T/\sqrt{\sigma}$. In Figure 7.2 the dimensionless lattice spacing $\sqrt{\sigma} a$ is shown as a function of β and it shows its expected limiting behavior for increasing values of the inverse coupling [31].
The last step necessary before taking the continuum limit is altering N_τ and κ in a way, that leaves the temperature and particle mass constant. Here we approach this in the same way as in the 3+1D theory by inverting the relation $T = (aN_\tau)^{-1}$ and fixing the baryon mass $m_B/\sqrt{\sigma}$. For N_τ one immediately finds [10]

$$N_\tau = \frac{\sqrt{\sigma}}{T} \frac{1}{\sqrt{-\log u_f}} \tag{7.24}$$

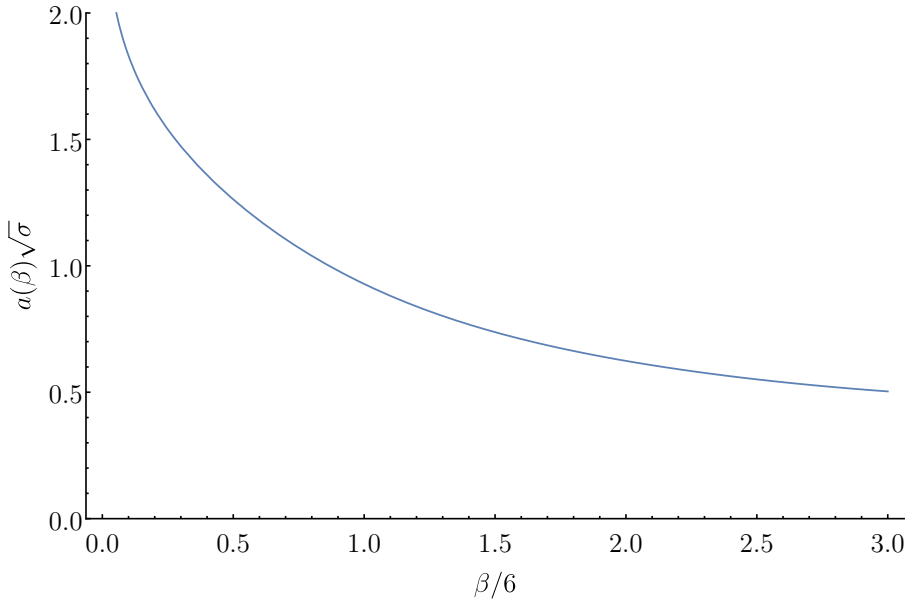

Figure 7.2: The lattice spacing $\sqrt{\sigma}a$ as a function of the inverse coupling β obtained following the approach of Huang et al. [31]

By fixing the baryon mass in the heavy quark limit we obtain with (7.23)

$$\kappa(\beta) = \frac{1}{2}\exp\left(-\frac{1}{3}\frac{m_B}{\sqrt{\sigma}}\sqrt{-\log u_f}\right) \tag{7.25}$$

From (7.25) larger values of β are found to correspond to increasing values of κ, so the hopping parameter expansion further limits the range of β, where our theory is accurate. This is in agreement with previous discussions of 3+1D effective theories. Inverting the baryon mass including corrections to $\mathcal{O}(\kappa^2)$ and beyond require numerical inversion [10].
Because our theory is only applicable in a finite range of β, observables have to be extrapolated to the continuum limit. Here, we follow the procedure of the discussion of the 3+1D effective theory. A (dimensionless) observable, i.e. $n_B/\sqrt{\sigma}$, is calculated for different values of $\sqrt{\sigma}a(\beta)$ and fitted to a second degree polynomial [7, 10]

$$\frac{n_B}{\sqrt{\sigma}} = \frac{n_{B,\text{cont}}}{\sqrt{\sigma}} + A_1\sqrt{\sigma}a + A_2(\sqrt{\sigma}a)^2 + \mathcal{O}\left((\sqrt{\sigma}a)^3\right) \tag{7.26}$$

The constant term in (7.26) then corresponds to the continuum value of our observable. The coefficients A_1 and A_2 are also dimensionless [10].

7.4.4 Results for Observables

In this section the results for the baryon density and the pressure in dependence on μ_B/m_B are discussed. Both the lattice spacing and the temperature after continuum extrapolation are varied.

Observables in the Heavy Quark Limit

In the heavy quark case the hopping parameter κ is chosen to satisfy $\kappa(\beta) < 10^{-2}$ for all values of beta, in which we expect our theory to be accurate, e.g. $\beta/6 \in [0, 3]$. Thus, we set $\frac{m_B}{\sqrt{\sigma}} = 25$. The smallest reachable lattice spacing is given by $\sqrt{\sigma}a(\beta/6 = 3) \approx 1/2$. For the continuum extrapolation 11 equidistant points in the interval $\sqrt{\sigma}a \in [1/2, 1]$ are used.
The baryon density for heavy quarks with varying lattice spacing is shown in figure 7.3a and its continuum extrapolation at varying temperatures is shown in figure 7.3b. The corresponding plots of the pressure are shown in figure 7.3c and figure 7.3d, respectively.
All plots in figure 7.3 show the same qualitative behavior as found in discussions of the 3+1D effective theory.

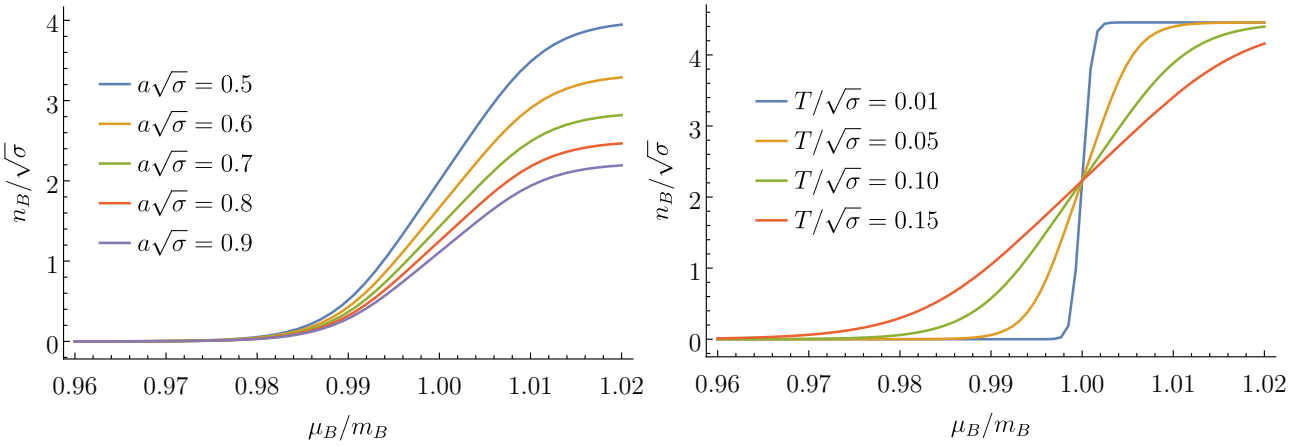

(a) The baryon density for varying lattice spacing and $T/\sqrt{\sigma} = 0.1$

(b) The continuum extrapolated baryon density for varying temperatures

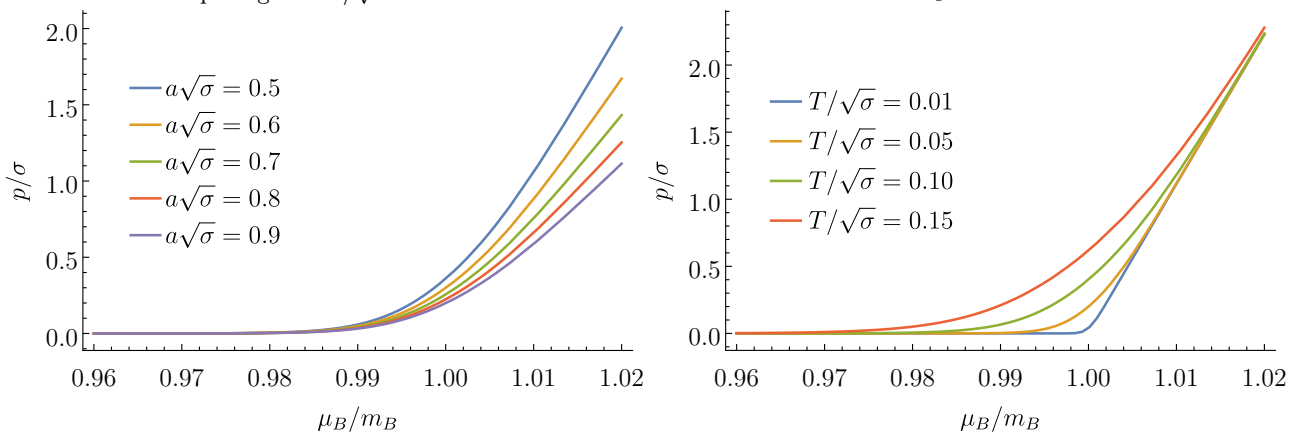

(c) The pressure for varying lattice spacing and $T/\sqrt{\sigma} = 0.1$

(d) The continuum extrapolated pressure for varying temperatures

Figure 7.3: Observables vs. the baryon chemical potential in the static quark limit for $N_f = 1$, $N_c = 3$ and $m_B/\sqrt{\sigma} = 25$

Even though the lattice action is explicitly dependent on the chemical potential, observables do not change when the chemical potential is small compared to the baryon mass m_B. If $\mu_B \approx m_B$, the onset region is reached and the system starts filling up with baryons. Here a dependence on the chemical potential becomes apparent. This feature is known as the silver blaze property [10, 32, 33].
At increasing values of μ_B the system reaches an unphysical saturation resulting from the discretization of space time and the Pauli-principle. Every lattice site can hold at most $2N_cN_f$ quarks or equivalently $2N_f$ baryons. In the continuum this effect does not occur, which resembles itself in the diverging behavior for decreasing lattice spacing in figure 7.3a. Thus, our results become inaccurate for $\mu_B > m_B$ and reducing the lattice spacing is mandatory to obtain accurate results [5].
Figure 7.3b shows the behavior of the liquid-gas transition to nuclear matter for varying temperatures. While at low temperatures the transition is of first order, increasing the temperature removes this discontinuous character and replaces it with a crossover [5].

Observables Beyond Heavy Quarks

As already mentioned in 5.3, higher order gauge corrections to the quark couplings h_1, $\bar{h}_1$, h_2, h_{3_1} and h_{3_2} are implied by higher representations beyond the heavy quark limit. Thus, the gauge action is included only up to the adjoint representation. In comparison to the the heavy quark case this leads to a more restricted range of lattice spacing available for continuum extrapolation. Here, 11 equidistant points in the interval $\sqrt{\sigma}a \in [9/10, 14/10]$ are used. The results are compared for baryon masses down to $\frac{m_B}{\sqrt{\sigma}} = 5$ - satisfying $\kappa < 0.1$

in the lattice spacing interval.
Going beyond the heavy quark limit no new qualitative behavior of the observables is found. Thus, only a comparison between the different orders in the heavy quark expansion for varying baryon masses is shown in figure 7.4.

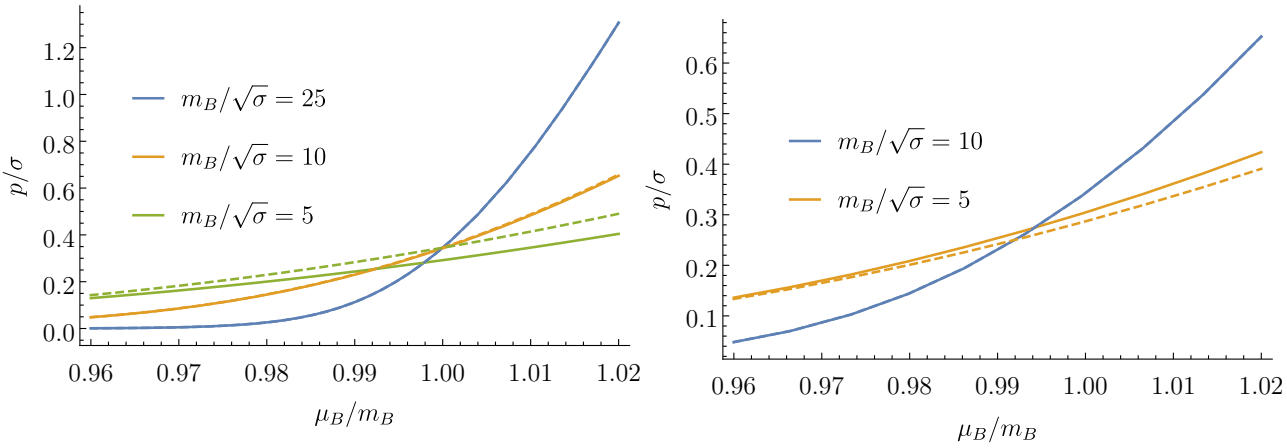

(a) Comparison of the pressure in the heavy quark limit (dashed lines) and to $\mathcal{O}(\kappa^2)$ (solid lines) for different baryon masses

(b) Comparison of the pressure to $\mathcal{O}(\kappa^2)$ (dashes lines) and $\mathcal{O}(\kappa^4)$ (solid lines) for different baryon masses

Figure 7.4: Comparison of the pressure vs. the baryon chemical potential for different orders in the heavy quark expansion at $N_f = 1$, $T/\sqrt{\sigma} = 0.15$ and $N_c = 3$ and varying baryon masses

Figure 7.4a shows the pressure for $m_B/\sqrt{\sigma} = 25$, 10 and 5 in both the heavy quark limit (dashed lines) and to leading order (solid lines), whereas figure 7.4b compares the pressure to leading (dashed lines) and next to leading order (solid lines) for $m_B/\sqrt{\sigma} = 10$ and 5.
As shown in figure 7.4a, at high baryon masses ($m_B/\sqrt{\sigma} = 25$) leading order corrections are negligible because both curves agree well with each other. Approaching lower masses ($m_B/\sqrt{\sigma} = 10$) first disagreements become apparent, which further increase when going to even smaller baryon masses ($m_B/\sqrt{\sigma} = 5$). Typically, the pressure in the heavy quark limit overshoots its leading order counterpart.
In figure 7.4b at $m_B/\sqrt{\sigma} = 10$, in contrast to the previous case, both pressures agree well. At lower baryon masses ($m_B/\sqrt{\sigma} = 5$) differences are small, but noticeable. Both observations show the convergence of the heavy quark expansion. The pressure to $\mathcal{O}(\kappa^4)$ is typically undershot by its leading order analogue.
Comparing figure 7.4a to 7.3d the pressure can be observed to be significantly smaller in this part of the discussion. For $m_B/\sqrt{\sigma} = 25$ and $T/\sqrt{\sigma} = 0.15$ the $\mathcal{O}(\kappa^2)$-pressure assumes values up to $p/\sqrt{\sigma} \approx 1.3$, whereas the respective pressure in the heavy quark limit in figure 7.3d assumes values up to $p/\sqrt{\sigma} \approx 2.4$. As observed in section 7.3, this can be ascribed to neglecting higher representations, causing the partition function to be estimated from below.

Chapter 8

2+1D: The Confinement-Deconfinement Transition

In this chapter the renormalization group transformations from 2+1D pure gauge theory and the static quark limit (chapter 6) are used to determine the critical inverse coupling β_c of the confinement-deconfinement transition. The results of this discussion are compared to simulation values from previous analysis in the literature.

8.1 Determining the Fixed Point

In this section properties of the fixed point of the renormalization group transformations from chapter 6 are discussed. This is done by determining the values of the critical couplings for static quarks and taking the pure gauge limit afterwards.
As discussed in chapter 2 the couplings show invariance under renormalization group transformations, if the system has been driven to a fixed point. For our static quark running couplings this relates directly to solving [12]

$$\lambda_{1,1}^{(n)} = \lambda_{1,1}^{(n+1)} = 2\frac{\lambda_{1,1}^{(n)}}{3} + 2\frac{o(0,1)}{3o(0,0)}\lambda_{1,5}^{(n)} + \lambda_{2,1}^{(n)} \tag{8.1}$$

$$\lambda_{1,2}^{(n)} = \lambda_{1,2}^{(n+1)} = 2\frac{\lambda_{1,2}^{(n)}}{3} + 2\frac{o(1,0)}{3o(0,0)}\lambda_{1,5}^{(n)} + \lambda_{2,2}^{(n)} \tag{8.2}$$

$$\lambda_{1,5}^{(n)} = \lambda_{1,5}^{(n+1)} = 2\frac{o(1,1)}{o(0,0)}\lambda_{1,5}^{(n)2} + \lambda_{2,5}^{(n)} \tag{8.3}$$

$$\lambda_{2,1}^{(n)} = \lambda_{2,1}^{(n+1)} = \frac{\lambda_{1,1}^{(n)}}{3} + \frac{o(0,1)}{3o(0,0)}\lambda_{1,5}^{(n)} \tag{8.4}$$

$$\lambda_{2,2}^{(n)} = \lambda_{2,2}^{(n+1)} = \frac{\lambda_{1,2}^{(n)}}{3} + \frac{o(1,0)}{3o(0,0)}\lambda_{1,5}^{(n)} \tag{8.5}$$

$$\lambda_{2,5}^{(n)} = \lambda_{2,5}^{(n+1)} = \frac{o(1,1)}{o(0,0)}\lambda_{1,5}^{(n)2} \tag{8.6}$$

The equations (8.3) and (8.6) can be used directly to obtain

$$\left(\lambda_{1,5}^{(n)}, \lambda_{2,5}^{(n)}\right) = \left(0,0\right) \text{ or } \left(\lambda_{1,5}^{(n)}, \lambda_{2,5}^{(n)}\right) = \left(\frac{o(0,0)}{3o(1,1)}, \frac{o(0,0)}{9o(1,1)}\right) \tag{8.7}$$

The first solution corresponds to the trivial fixed point at $\beta = 0$ and is therefore disregarded. The second solution represents a fixed point at finite β and is therefore the physically relevant case [12].
Simply using the latter case of (8.7) to determine the remaining running couplings gives

$$o(0,1)\lambda_{1,5}^{(n)} = 0 = o(1,0)\lambda_{1,5}^{(n)} \tag{8.8}$$

which is seemingly inconsistent with the non-trivial fixed point away from the pure gauge limit $\kappa \to 0$. However, this can be solved by investigating the orders of the running couplings.

Because all terms involving $\lambda_{1,1}^{(n)}$ and $\lambda_{1,2}^{(n)}$ in (6.21), (6.22), (6.24) and (6.25) are neither proportional to any other coupling nor to an κ^{N_τ}, their order always stays at $\mathcal{O}(u_f^{vN_\tau}\kappa^{wN_\tau})$ with $v+w=2$. On the other hand, at $n=1$ the two-point coupling is of $\mathcal{O}(u_f^{2N_\tau})$. Due to the fact that the orders of the couplings cannot decrease for increasing n, all terms in (8.1), (8.2), (8.4) and (8.5) involving $\lambda_{1,5}^{(n)}$ are at least of order $\mathcal{O}(u_f^{vN_\tau}\kappa^{wN_\tau})$ with $v+w=3$ for $n>0$. As the system can only be driven to criticality for $n>0$, neglecting all those contributions is consistent with the derivation of the running couplings. Thus, the only relevant relation to the deconfinement transition is given by the non-trivial solution in (8.7) [12].
In the pure gauge limit the critical couplings are given by

$$\left(\lambda_{1,5}^{(n)}, \lambda_{2,5}^{(n)}\right) = \left(\lambda_f^{(n)}, \lambda_{2,f}^{(n)}\right) = \left(\frac{1}{3}, \frac{1}{9}\right) \tag{8.9}$$

8.2 The Critical Inverse Coupling in Pure Gauge Theory

To drive the analytical evaluation further another approximation is introduced. We replace the initial next to nearest neighbor coupling $\lambda_{2,f}$ by λ_f^2. This step is analogous to the approximation of next to nearest neighbor interactions in the 2D Ising model and leads to the boundary conditions [15]

$$\lambda_f^{(0)} = \lambda_f \quad \text{and} \quad \lambda_{2,f}^{(0)} = \lambda_f^2 \tag{8.10}$$

This reduces the accuracy of our discussion and corrections appear already at order $\mathcal{O}(u_f^{2N_\tau})$ instead of $\mathcal{O}(u_f^{2N_\tau+6})$.
To determine the critical value of λ_f the renormalization scheme is iterated once

$$\lambda_f^{(1)} = 3\lambda_f^2 \quad \text{and} \quad \lambda_{2,f}^{(1)} = \lambda_f^2 \tag{8.11}$$

By using (8.9) it is found that the running couplings are driven to criticality, if

$$\lambda_f = \frac{1}{3} \tag{8.12}$$

This relation can be inverted to determine the critical inverse coupling β_c of the deconfinement transition in dependence on N_τ and N_c.
To compare our results to literature values we consider $N_c = 2, \ldots, 5$ and $N_\tau = 2, \ldots, 5$. In the tables 8.1 to 8.4 the solutions to (8.12) are listed with their respective literature values $\beta_{c,\text{lit}}$, which are taken from [34], and the absolute relative deviations $|\Delta\beta_c|/\beta_{c,\text{lit}} = |\beta_c - \beta_{c,\text{lit}}|/\beta_{c,\text{lit}}$.

N_τ	β_c	$\beta_{c,\text{lit}}$	$\lvert\Delta\beta_c\rvert/\beta_{c,\text{lit}}$ in %
2	3.0876	3.4475	10.4394
3	4.5309	4.9430	8.3369
4	5.9226	6.4830	8.6448
5	7.2994	8.1430	10.3600

Table 8.1: Critical inverse coupling β_c for SU(2)

N_τ	β_c	$\beta_{c,\text{lit}}$	$\lvert\Delta\beta_c\rvert/\beta_{c,\text{lit}}$ in %
2	8.9267	8.1489	9.5449
3	12.6488	11.3711	11.2365
4	16.3067	14.7170	10.8021
5	19.9532	18.1310	10.0501

Table 8.2: Critical inverse coupling β_c for SU(3)

N_τ	β_c	$\beta_{c,\text{lit}}$	$\lvert\Delta\beta_c\rvert/\beta_{c,\text{lit}}$ in %
2	17.1586	14.8403	15.6219
3	24.0450	20.3770	18.0007
4	30.8689	26.2280	17.6945
5	37.6884	32.1540	17.2123

Table 8.3: Critical inverse coupling β_c for SU(4)

N_τ	β_c	$\beta_{c,\text{lit}}$	$\lvert\Delta\beta_c\rvert/\beta_{c,\text{lit}}$ in %
2	27.7731	23.5315	18.0254
3	38.7103	32.0650	20.7246
4	49.6003	41.0570	20.8085
5	60.4972	50.6700	19.3946

Table 8.4: Critical inverse coupling β_c for SU(5)

Our results for $N_c = 2$ and $N_c = 3$ reproduce the literature values with an accuracy of around 10%, whereas the accuracy for $N_c = 4$ and $N_c = 5$ are around 20%.

Note that most values of β_c are outside of the region where the effective theory can be expected to be accurate. Still, our renormalization scheme reproduces the critical values qualitatively. Due to the large critical values high order corrections to the couplings λ_f and $\lambda_{2,f}$ can be expected to be necessary to increase the accuracy of the theory. Deriving these corrections is, however, beyond the scope of this thesis [10, 11].

8.3 Deconfinement of Static Quarks at Finite Density

In the following the same approximation as in section 8.2 is applied. Therefore the relevant boundary conditions to this discussion read

$$\lambda_{1,5}^{(0)} = \lambda_f, \quad \lambda_{2,5}^{(0)} = \lambda_f^2 \tag{8.13}$$

Analogous to the previous section the renormalization group transformation is applied once

$$\lambda_{1,5}^{(1)} = 3\frac{o(1,1)}{o(0,0)}\lambda_f^2 \quad \text{and} \quad \lambda_{2,5}^{(1)} = \frac{o(1,1)}{o(0,0)}\lambda_f^2 \tag{8.14}$$

Similar to the previous section the running couplings are at their critical value, if

$$\lambda_f = \frac{o(0,0)}{3o(1,1)} \tag{8.15}$$

This equation can be used to determine the critical inverse coupling β_c in dependence on N_c, N_τ as well as the heavy quark couplings h_1 and $\bar{h}_1$.
Because the derivation of the renormalization scheme assumed $N_c \geq 3$ and due to the high inaccuracies found in the previous section for $N_c = 4, 5$, only SU(3) is considered in this section. For this gauge group the critical inverse coupling β_c is shown in figure 8.1 for $N_\tau = 2, \ldots, 5$ and $\kappa = 0.01$.

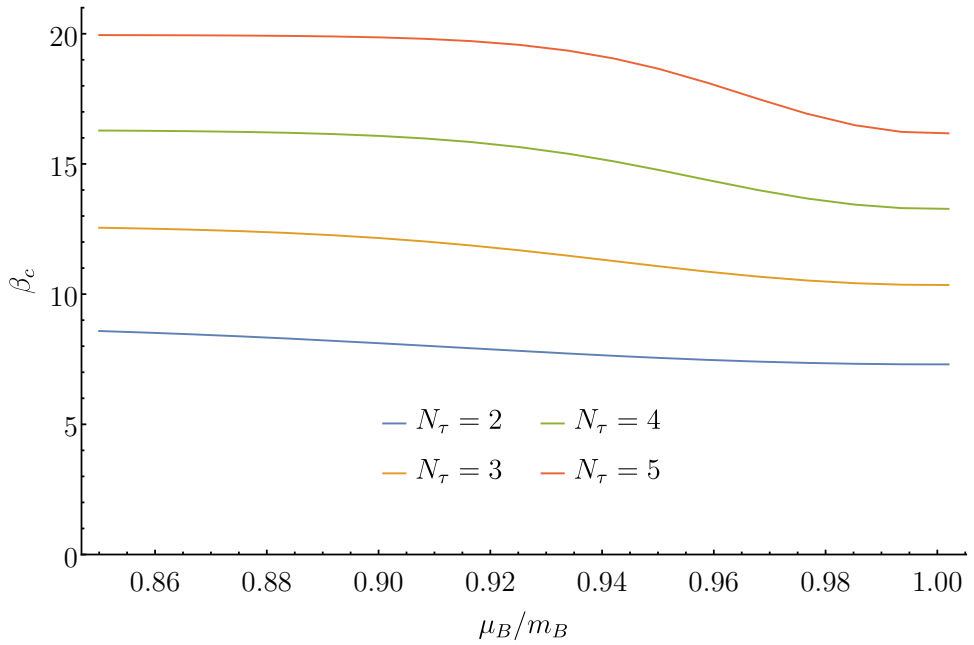

Figure 8.1: The critical inverse coupling β_c in the static quark limit for $N_c = 3$ and $\kappa = 0.01$ vs. the baryon chemical potential μ_B/m_B for $N_\tau = 2, \ldots, 5$

In figure 8.1 it can be observed that the presence of the static determinant reduces the value of β_c. This may be explained by the static determinant explicitly breaking center symmetry. As the influence of the symmetry breaking fields is mediated by h_1 and $\bar{h}_1$ increasing the chemical potential leads to decreasing β_c [16].

Another feature is the silver blaze property that was already discussed in the context of 1+1D in section 7.4.4. The values of β_c are for low chemical potentials independent on this parameter, even though μ_B/m_B explicitly appears in the action. Only if $\mu_B/m_B \approx 1$, the critical inverse coupling shows a dependence on the chemical potential. The lower the temperature (or equivalently the higher N_τ) is, the more this effect is pronounced [32, 33].
It is important to note that the renormalization scheme becomes less accurate at $\mu_B/m_B \approx 1$ as the order of accuracy of the transformation can be rewritten as $\mathcal{O}(u_f^{vN_\tau}\kappa^{wN_\tau}) = \mathcal{O}(u_f^{vN_\tau}h_1^{w_1}\bar{h}_1^{w_2})$ with $v+w = 2 = v+w_1+w_2$ [11].

Chapter 9

Conclusion

In this work renormalization group techniques were applied to an effective theory of LQCD in 1+1 and 2+1 dimensions. The theory was derived in previous works by expanding around the strong coupling and heavy quark limit. There, it was also found that the model can be interpreted as a spin model [8–11]. This suggested the use of coarse graining renormalization. It describes the process of successively reducing the spacial degrees of freedom of a discretized theory. The technique determines recursion relations for the couplings of the model in dependence of its typical length scale [12, 15].
In 1+1 dimensions the coarse graining technique was tested first in the pure gauge limit. The running couplings reproduced the analytic solution of the system, which is well known from literature [15, 20]. Afterwards, the static quark determinant was included in the description of the model. Subsequently, the running couplings were determined while additionally considering parts of the kinetic quark determinant. All recursion relations were observed to maintain a common form. Written as matrix recursion relations they were solved analytically. This lead to the transfer matrix of the theory, which allowed us to take the thermodynamic limit [15, 16]. The pressure and baryon density were discussed both on the lattice and after continuum extrapolation.
In 2+1 dimensions the renormalization transformation was applied to pure gauge theory and the static quark limit. To implement that, results from the discussion in 1+1 dimensions were taken into consideration. The fixed point was determined and the critical inverse coupling of the confinement-deconfinement transition was obtained both in the pure gauge limit and at finite chemical potential. The results were discussed and compared to the literature. The literature values were reproduced qualitatively.
All in all, coarse graining renormalization proved itself as a viable tool in the treatment of the effective theory. Therefore, further research in the application of renormalization group transformations on the model, especially in 3+1 dimensions, would be of great interest. In 2+1D the accuracy of the deconfinement transition might be improved by considering corrections to the nearest and next to nearest neighbor couplings. Additionally, a generalization of the 2+1D renormalization group transformation to capture parts of the kinetic quark determinant might lead to important insights.

Appendix A

The Gauge Node Matrix Elements

The calculation of the node gauge integral for SU(N_c) in section 5.4.3 gives

$$
\begin{aligned}
M_{4,l'_j-l_i+k} = \sum_{m_1=0}^{\alpha_1} \cdots \sum_{m_N=0}^{\alpha_N} \frac{1}{m_1! \ldots m_N!} \exp\left(2\pi i \sum_{n=1}^{N} m_n u_n / K_n\right) h_1^{\sum_{n=1}^{N}(a_n-b_n)m_n+2} \bar{h}_1^{\sum_{n=1}^{N}\bar{a}_n m_n} \Bigg[\\
B\left(l_i - l'_j - k + 1 + 2N_f - \sum_{n=1}^{N}(a_n - \bar{a}_n + \bar{b}_n)m_n > 0\right) \\
\frac{1}{\left(l_i - l'_j - k + 2N_f - \sum_{n=1}^{N}(a_n - \bar{a}_n + \bar{b}_n)m_n\right)!} \sum_{t=0}^{l_i - l'_j - k + 2N_f - \sum_{n=1}^{N}(a_n - \bar{a}_n + \bar{b}_n)m_n} \\
\binom{l_i - l'_j - k + 2N_f - \sum_{n=1}^{N}(a_n - \bar{a}_n + \bar{b}_n)m_n}{t} \left(-\sum_{n=1}^{N} b_n m_n + 2N_f\right)_t h_1^{-\sum_{n=1}^{N} b_n m_n + 2N_f - t} \\
\left(-\sum_{n=1}^{N} \bar{b}_n m_n + 2N_f\right)_{l_i - l'_j - k + 2N_f - \sum_{n=1}^{N}(a_n - \bar{a}_n + \bar{b}_n)m_n - t} \bar{h}_1^{l'_j - l_i + k + \sum_{n=1}^{N}(a_n - \bar{a}_n)m_n + t} \\
+ B\left(\sum_{n=1}^{N} \bar{b}_n m_n > 2N_f \wedge \bar{h}_1 < 1\right) \frac{1}{\left(\sum_{n=1}^{N} \bar{b}_n m_n - 2N_f - 1\right)!} \sum_{t=0}^{\sum_{n=1}^{N} \bar{b}_n m_n - 2N_f - 1} \binom{\sum_{n=1}^{N} \bar{b}_n m_n - 2N_f - 1}{t} \\
\left(l'_j - l_i + k - 2N_f - 1 + \sum_{n=1}^{N}(a_n - \bar{a}_n + \bar{b}_n)m_n\right)_t \left(-\bar{h}_1\right)^{l'_j - l_i + k - 2N_f - 1 + \sum_{n=1}^{N}(a_n - \bar{a}_n + \bar{b}_n)m_n - t} \\
\left(-\sum_{n=1}^{N} b_n m + 2N_f\right)_{\sum_{n=1}^{N} \bar{b}_n m_n - 2N_f - 1 - t} \left(\frac{1}{h_1} - \bar{h}_1\right)^{-\sum_{n=1}^{N}(b_n - \bar{b}_n)m_n + 4N_f + 1 + t} \\
+ B\left(\sum_{n=1}^{N} b_n m_n > 2N_f \wedge h_1 > 1\right) \frac{1}{\left(\sum_{n=1}^{N} b_n m_n - 2N_f - 1\right)!} \sum_{t=0}^{\sum_{n=1}^{N} b_n m_n - 2N_f - 1} \binom{\sum_{n=1}^{N} b_n m_n - 2N_f - 1}{t} \\
\left(l'_j - l_i + k - 2N_f - 1 + \sum_{n=1}^{N}(a_n - \bar{a}_n + \bar{b}_n)m_n\right)_t \left(-\frac{1}{h_1}\right)^{l'_j - l_i + k - 2N_f - 1 + \sum_{n=1}^{N}(a_n - \bar{a}_n + \bar{b}_n)m_n - t} \\
\left(-\sum_{n=1}^{N} \bar{b}_n m + 2N_f\right)_{\sum_{n=1}^{N} b_n m_n - 2N_f - 1 - t} \left(\bar{h}_1 - \frac{1}{h_1}\right)^{-\sum_{n=1}^{N}(\bar{b}_n - b_n)m_n + 4N_f + 1 + t} \Bigg]
\end{aligned}
\tag{A.1}
$$

The first block inside the square brackets corresponds to the residue at $z = 0$, whereas the second and third block correspond to the residues at $z = -\bar{h}_1$ and $z = -\frac{1}{h_1}$, respectively.

Appendix B

List of Compound Node Functions

i	$\prod_{(ab\bar{a}\bar{b},\alpha)\in v_i} W^{\alpha}_{ab\bar{a}\bar{b}}$	v_1	v_2	v_3	v_4
1	1	✓	✓	✓	✓
2	W_{0101}	✓	✓	✓	
3	W^2_{0101}		✓		
4	W_{1200}	✓	✓	✓	
5	$W_{1200}W_{0101}$		✓		
6	W^2_{1200}		✓		
7	W_{0012}	✓	✓	✓	
8	$W_{0012}W_{0101}$		✓		
9	$W_{0012}W_{1200}$		✓		
10	W^2_{0012}		✓		
11	W_{1111}	✓	✓	✓	
12	$W_{1111}W_{0101}$		✓		
13	$W_{1111}W_{1200}$		✓		
14	$W_{1111}W_{0012}$		✓		
15	W^2_{1111}		✓		
16	W_{0022}	✓	✓	✓	
17	$W_{0022}W_{0101}$		✓		
18	$W_{0022}W_{1200}$		✓		
19	$W_{0022}W_{0012}$		✓		
20	$W_{0022}W_{1111}$		✓		
21	W^2_{0022}		✓		
22	W_{2200}	✓	✓	✓	
23	$W_{2200}W_{0101}$		✓		
24	$W_{2200}W_{1200}$		✓		
25	$W_{2200}W_{0012}$		✓		
26	$W_{2200}W_{1111}$		✓		
27	$W_{2200}W_{0022}$		✓		
28	W^2_{2200}		✓		
29	W_{0011}	✓	✓	✓	✓
30	$W_{0011}W_{0101}$		✓	✓	
31	$W_{0011}W_{1200}$		✓	✓	
32	$W_{0011}W_{0012}$		✓	✓	
33	$W_{0011}W_{1111}$		✓	✓	
34	$W_{0011}W_{0022}$		✓	✓	
35	$W_{0011}W_{2200}$		✓	✓	
36	W^2_{0011}	✓	✓	✓	

i	$\prod_{(ab\bar{a}\bar{b},\alpha)\in v_i} W^{\alpha}_{ab\bar{a}\bar{b}}$	v_1	v_2	v_3	v_4
37	$W^2_{0011}W_{0101}$		✓		
38	$W^2_{0011}W_{1200}$		✓		
39	$W^2_{0011}W_{0012}$		✓		
40	$W^2_{0011}W_{1111}$		✓		
41	$W^2_{0011}W_{0022}$		✓		
42	$W^2_{0011}W_{2200}$		✓		
43	W^3_{0011}		✓	✓	
44	W^4_{0011}		✓		
45	W_{1100}	✓	✓	✓	✓
46	$W_{1100}W_{0101}$		✓	✓	
47	$W_{1100}W_{1200}$		✓	✓	
48	$W_{1100}W_{0012}$		✓	✓	
49	$W_{1100}W_{1111}$		✓	✓	
50	$W_{1100}W_{0022}$		✓	✓	
51	$W_{1100}W_{2200}$		✓	✓	
52	$W_{1100}W_{0011}$	✓	✓	✓	✓
53	$W_{1100}W_{0011}W_{0101}$		✓		
54	$W_{1100}W_{0011}W_{1200}$		✓		
55	$W_{1100}W_{0011}W_{0012}$		✓		
56	$W_{1100}W_{0011}W_{1111}$		✓		
57	$W_{1100}W_{0011}W_{0022}$		✓		
58	$W_{1100}W_{0011}W_{2200}$		✓		
59	$W_{1100}W^2_{0011}$		✓	✓	
60	$W_{1100}W^3_{0011}$		✓		
61	W^2_{1100}	✓	✓	✓	
62	$W^2_{1100}W_{0101}$		✓		
63	$W^2_{1100}W_{1200}$		✓		
64	$W^2_{1100}W_{0012}$		✓		
65	$W^2_{1100}W_{1111}$		✓		
66	$W^2_{1100}W_{0022}$		✓		
67	$W^2_{1100}W_{2200}$		✓		
68	$W^2_{1100}W_{0011}$		✓	✓	
69	$W^2_{1100}W^2_{0011}$		✓		
70	W^3_{1100}		✓	✓	
71	$W^3_{1100}W_{0011}$		✓		
72	W^4_{1100}		✓		

In total there are 12 compound node functions for v_1, 72 for v_2, 28 for v_3 and 4 for v_4 found in section 5.4.

Bibliography

[1] Owe Philipsen. *Quantenfeldtheorie und das Standardmodell der Teilchenphysik*. Springer Berlin Heidelberg, Berlin, Heidelberg, 2018.

[2] N. Cabibbo and G. Parisi. Exponential hadronic spectrum and quark liberation. *Phys. Lett. B*, 59(1):67–69, oct 1975.

[3] Mark G. Alford, Andreas Schmitt, Krishna Rajagopal, and Thomas Schäfer. Color superconductivity in dense quark matter. *Rev. Mod. Phys.*, 80(4):1455–1515, nov 2008.

[4] Tillmann Boeckel and Jürgen Schaffner-Bielich. Little inflation at the cosmological QCD phase transition. *Phys. Rev. D*, 85(10):103506, may 2012.

[5] Owe Philipsen. A 3d effective lattice theory for phase transitions in Yang-Mills and heavy dense QCD. *J. Phys. Conf. Ser.*, 631(1), 2015.

[6] M. Fromm, J. Langelage, S. Lottini, M. Neuman, and O. Philipsen. Onset Transition to Cold Nuclear Matter from Lattice QCD with Heavy Quarks. *Phys. Rev. Lett.*, 110(12):122001, mar 2013.

[7] Christof Gattringer and Christian B. Lang. *Quantum chromodynamics on the lattice: An introductory presentation*, volume 788 of *Lecture Notes in Physics*. Springer Berlin Heidelberg, Berlin, Heidelberg, 2010.

[8] Jens Langelage, Stefano Lottini, and Owe Philipsen. Centre symmetric 3d effective actions for thermal SU(N) Yang-Mills from strong coupling series. *J. High Energy Phys.*, 2011(2):57, feb 2011.

[9] Alena Schoen. *Effective heavy quark theory of strong coupling lattice QCD in 1 + 1 dimensions*. Master thesis, Goethe Universität Frankfurt am Main, 2018.

[10] Mathias Neuman. *Effective Theory for Heavy Quark QCD at Finite Temperature and Density with Stochastic Quantization*. Phd thesis, Goethe Universität Frankfurt am Main, 2015.

[11] Jonas Rylund Glesaaen. *Heavy Quark QCD at Finite Temperature and Density Using an Effective Theory*. Phd thesis, Goethe Universität Frankfurt am Main, 2016.

[12] Nigel Coldenfeld. *Lectures on phase transitions and the renormalization group*. CRC Press, mar 2018.

[13] Michael E Fisher. Renormalization group theory: Its basis and formulation in statistical physics. *Rev. Mod. Phys.*, 70(2):653–681, apr 1998.

[14] Istvan Montvay and Gernot Münster. *Quantum Fields on a Lattice*, volume 1. Cambridge University Press, Cambridge, UK, jul 1994.

[15] Andreas Wipf. *Statistical approach to quantum field theory: An introduction*, volume 864 of *Lecture Notes in Physics*. Springer Berlin Heidelberg, Berlin, Heidelberg, 2013.

[16] Jean Zinn-Justin. *Quantum Field Theory and Critical Phenomena*. Oxford University Press, jun 2002.

[17] William Fulton and Joe Harris. *Representation Theory*, volume 129 of *Graduate Texts in Mathematics*. Springer New York, New York, NY, 2004.

[18] Walter Greiner and Berndt Müller. *Quantum Mechanics: Symmetries*. Springer Berlin Heidelberg, Berlin, Heidelberg, 1994.

[19] A. A. Migdal. Recursion equations in gauge field theories. 42(3):114–119, 1996.

[20] Jean Michel Drouffe and Jean Bernard Zuber. Strong coupling and mean field methods in lattice gauge theories. *Phys. Rep.*, 102(1-2):1–119, 1983.

[21] Jens Langelage, Mathias Neuman, and Owe Philipsen. Heavy dense QCD and nuclear matter from an effective lattice theory. *J. High Energy Phys.*, 2014(9), 2014.

[22] Christian Wozar, Tobias Kaestner, Andreas Wipf, and Thomas Heinzl. Inverse Monte Carlo determination of effective lattice models for SU(3) Yang-Mills theory at finite temperature. *Phys. Rev. D*, 76(8):085004, oct 2007.

[23] G. Bergner, J. Langelage, and O. Philipsen. Effective lattice Polyakov loop theory vs. full SU(3) Yang-Mills at finite temperature. *J. High Energy Phys.*, 2014(3):39, mar 2014.

[24] Owe Philipsen and Jonas Scheunert. QCD in the heavy dense regime for general Nc: on the existence of quarkyonic matter. *J. High Energy Phys.*, 2019(11), 2019.

[25] Yusuke Nishida. Phase structures of strong coupling lattice QCD with finite baryon and isospin density. *Phys. Rev. D - Part. Fields, Gravit. Cosmol.*, 69(9):15, 2004.

[26] Owe Philipsen and Jonas Scheunert. Baryonic or quarkyonic matter? *Proc. Sci.*, 336(August):0–11, 2018.

[27] Joseph Bak and Donald J. Newman. *Complex Analysis*. Undergraduate Texts in Mathematics. Springer New York, New York, NY, 2010.

[28] O. Borisenko, S. Voloshyn, and V. Chelnokov. Su(N) Polynomial Integrals and Some Applications. *Reports Math. Phys.*, 85(1):129–145, 2020.

[29] Michael Fromm, Jens Langelage, Stefano Lottini, and Owe Philipsen. The QCD deconfinement transition for heavy quarks and all baryon chemical potentials. *J. High Energy Phys.*, 2012(1):42, jan 2012.

[30] H. G. Dosch and V. F. Müller. Lattice Gauge Theory in Two Spacetime Dimensions. *Fortschritte der Phys.*, 27(11-12):547–559, 1979.

[31] S. Huang, J.W. Negele, and J. Polonyi. Meson structure in QCD2. *Nucl. Phys. B*, 307(4):669–704, oct 1988.

[32] Thomas D. Cohen. Functional Integrals for QCD at Nonzero Chemical Potential and Zero Density. *Phys. Rev. Lett.*, 91(22):222001, nov 2003.

[33] J. R. Ipsen and K. Splittorff. Baryon number Dirac spectrum in QCD. *Phys. Rev. D*, 86(1):014508, jul 2012.

[34] Jack Liddle and Michael Teper. The deconfining phase transition in D=2+1 SU(N) gauge theories. mar 2008.

Selbstständigkeitserklärung

Erklärung nach §30 (12) Ordnung für den Bachelor - und dem Masterstudiengang. Hiermit erkläre ich, dass ich die Arbeit selbstständig und ohne Benutzung anderer als der angegebenen Quellen und Hilfsmittel verfasst habe. Alle Stellen der Arbeit, die wörtlich oder sinngemäß aus Veröffentlichungen oder aus anderen fremden Texten entnommen wurden, sind von mir als solche kenntlich gemacht worden. Ferner erkläre ich, dass die Arbeit nicht - auch nicht auszugsweise - für eine andere Prüfung verwendet wurde.

Frankfurt, den